DIAMOND CHEMICAL VAPOR DEPOSITION AND PRACTICAL APPLICATIONS

Except where reference is made to the work of others, the work described in this dissertation is my own or was done in collaboration with my advisory committee. This dissertation does not include proprietary or classified information.

_____

Yu-Chun Chen

Certificate of Approval:

_____	_____
Bogdan M. Wilamowski, Co-Chair Professor Electrical and Computer Engineering	Yonhua Tzeng, Co-Chair Professor Emeritus Electrical and Computer Engineering
_____	_____
Minseo Park Associate Professor Physics	Chwan-Hwa Wu Professor Electrical and Computer Engineering

_____

George T. Flowers
Dean
Graduate School

DIAMOND CHEMICAL VAPOR DEPOSITION AND PRACTICAL APPLICATIONS

Yu-Chun Chen

A Dissertation

Submitted to

the Graduate Faculty of

Auburn University

in Partial Fulfillment of the

Requirements for the

Degree of

Doctor of Philosophy

Auburn, Alabama

August 10, 2009

DIAMOND CHEMICAL VAPOR DEPOSITION AND PRACTICAL APPLICATIONS

Yu-Chun Chen

_____

Signature of Author

_____

Date of Graduation

VITA

Yu-Chun Chen, son of Chia-Hsiung Chen and Lan-Feng Shih, was born on December 15, 1974 in Changhua, Taiwan. He entered Feng-Chia University in Taiwan and graduated from the Department of Electronic Engineering with a Bachelor of Science in 1998. He attended the graduate program in the Department of Electrical and Computer Engineering in Auburn University in 2001 and graduated with the degree of Master of Science in August, 2003. He then entered the doctoral program in the same, Yonhua Tzeng, research group and received Auburn University Graduate Research Fellowship in January, 2004. He is married to Mei-Chun Lin.

DISSERTATION ABSTRACT

DIAMOND CHEMICAL VAPOR DEPOSITION AND PRACTICAL APPLICATIONS

Yu-Chun Chen

Doctor of Philosophy, August 10, 2009
(M.S., Auburn University, 2003)
(B.S., Feng-Chia University, Taiwan, 1998)

118 Typed Pages

Directed by Yonhua Tzeng and Bogdan M. Wilamowski

Diamond chemical vapor deposition (CVD) technique has been studied intensively and has overcome some of the constraints of traditional high-pressure high-temperature (HPHT) diamond synthesis methods in the last decades. In this work, microwave plasma enhanced chemical vapor deposition (MPCVD) technique has been employed to synthesize three different kinds of crystallites of diamonds, including single crystal, polycrystalline and nanocrystalline diamonds, and to study their practical applications.

Large diamond single crystals and clean diamond windows can be produced at very high growth rates, and the mechanical, chemical, optical and electronic properties of the material are extraordinary and can be tuned over a wide range. The goal is to produce large diamond single crystals for diamond anvils to make a new generation of

high-pressure-temperature experimentation to study Earth and planetary materials possible.

Composite thin films of nanodiamond and silica nanotubes were synthesized on silica nanotube matrix that was seeded with nanodiamond particles. Scanning electron microscopy (SEM), Raman spectroscopy, and energy-dispersive x-ray spectroscopy (EDX) were used to analyze the composite. Wet chemical etching was applied to selectively remove exposed silica from the composites for further revealing the nanostructure of the composites. When appropriately selected sizes of nanodiamond particles were used as diamond seeds, silica nanotubes capped with CVD-grown diamond crystals were also obtained. Potential applications and implication of composites of nanodiamond and 1-D nanostructures are discussed.

Fabrication of patterned diamond structures in an inexpensive way is desirable for many electrical and heat-dissipation applications. In this study, nanodiamond suspensions in ethylene glycol were used as inks for inkjet printing. By utilizing inks with optimized nanodiamond suspensions, high number density of diamond nanoparticles were laid down directly by inkjet printing to form almost continuous nanodiamond films of designed patterns on a substrate. A brief CVD process was adequate for the further growth of nanodiamond seeds to form a continuous nanocrystalline diamond film. This process allows inexpensive seeding of diamond in selected areas as well as possible formation of 1-D, 2-D, and 3-D nanodiamond structures. Details of the inkjet printing process and its potential applications will be reported.

ACKNOWLEDGEMENTS

The author would like to extend his deepest thanks to Dr. Yonhua Tzeng for his being a great academic advisor and supervising all the work described in this dissertation during the author's graduate study at Auburn University.

The author would like to express his great appreciation to Dr. Bogdan M. Wilamowski for being the co-chair and his encouragement and assistance for the completion of this dissertation.

The author would like to express his appreciation to Dr. Russell J. Hemley, Dr. Ho-Kwang Mao, and Dr. Chih-Shiue Yan at Carnegie Institution of Washington for their professional supervision and assistance on the single crystal diamond synthesis project.

The author would like to thank his committee members, Dr. Minseo Park and Dr. Chwan-Hwa Wu, for their professional advices on this dissertation.

The author would also express his appreciation to Mr. Charles Ellis, Dr. An-Jen Cheng, Mr. Calvin Cutshaw, Dr. Chao Liu, and Mr. William Baugh for their assistance and professional advises.

The author would like to thank his family and wife for their love, encouragement, dedication, and support over the years.

Style manual or journal used: Bibliography conforms to those of the transactions of the Institute of Electrical and Electronics Engineers

Computer software used: Microsoft Word 2003 for Windows

TABLE OF CONTENTS

LIST OF FIGURES

LIST OF TABLES

CHAPTER 1

INTRODUCTION

Diamond is valued not only as a gem, but also technologically as an extraordinary material with unique physical, chemical, and optical properties. Due to its well-known high hardness, singular strength, high thermal conductivity, low coefficient of thermal expansion, chemical inertness, excellent optical transparency, and semiconductor properties, it has attracted intensive scientific studies and technological interests worldwide.

The available supply of natural diamonds is, though, very limited and could not fulfill the high demand of industry from drills in oil mining to optical windows in aerospace technology. Furthermore, the broad varieties of impurities and defects found in natural diamonds generally complicate the applications of these crystals for their research and industry uses.

In order to overcome the availability and crystal quality issues, scientists have developed techniques to synthesize diamonds in the laboratory. There are currently two ways to create man-made diamond, High Pressure High Temperature (HPHT) and Chemical Vapor Deposition (CVD) methods. The first successful uses of the HPHT technique to create diamond from graphite with a seed crystal and suitable for jewelry occurred during the last decades [1 - 5]. The diamond crystals produced with this technique have high purities but have been of limited size, typically up to 3 carats raw

available commercially, due to the tremendous size of equipment, namely the hydraulic presses. The basic concept of the HPHT method is demonstrated in Figure 1.1 [6]. In order to increase the sizes of crystals created by this method, the size of the presses will have to be several stories high. After being polished to get rid of defects and being faceted, HPHT diamonds are rarely larger than 1 carat. For many potential electronic and optical applications, diamond crystals made by this technique are not suitable because various shapes and thicknesses from nanometers to a much larger size are usually desired.

One of most important developments in diamond synthesis is the CVD method. A typical bell jar microwave CVD reactor for diamond deposition is shown in Figure 1.2. The microwave power in introduced through a waveguide located at the top of the chamber, and a pump is attached to maintain a constant working pressure while gases being fed. The first attempt at creating diamond using CVD process was reported in 1949 [7]. Since then, diamond CVD process for bulk and thin film diamonds has been studied intensively. [8 - 12]. The Industrial Diamond Division of De Beers had first started mass production of polycrystalline diamond for industrial applications. General Electric (GE) also demonstrated the technology for producing thick and transparent polycrystalline CVD diamond films in 1995 [13]. High quality polycrystalline diamond products become available commercially including windows for various optical applications and diamond blades for cutting instruments. Well-polished polycrystalline diamond wafers can also be purchased for research purposes.

Nanocrystalline diamond also attracted a large number of interests due to its unique electrical and mechanical properties different from those of single crystal and polycrystalline diamonds [14, 15]. The smooth surface of nanocrystalline diamond

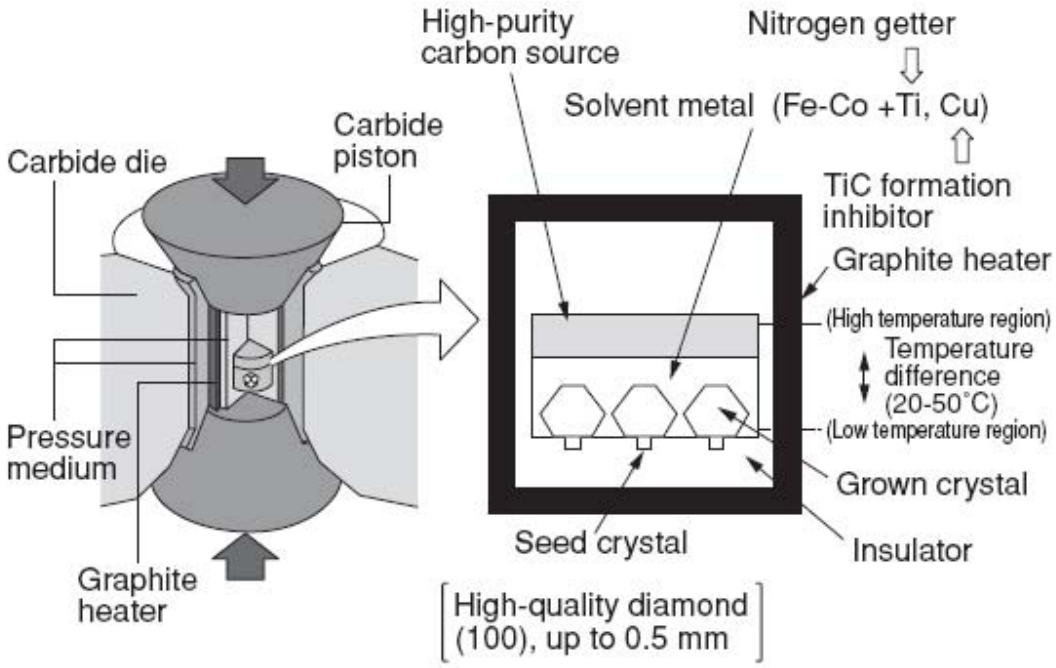

Figure 1.1: A schematic example of a Belt type HPHT press: Diamond seeds are placed at the bottom of the press. The internal part of press is heated by a graphite heater that generates temperatures above 1400°C and melts the solvent metal. The molten metal dissolves the high purity carbon source, which is then transported to the diamond seeds and precipitates. If nitrogen is removed by mixing small quantities of Ti with the metal, a colorless diamond is synthesized [6].

makes a good candidate for patterning other external structures onto as substrates, including surface acoustic wave (SAW) devices [16], and for protective coatings [17].

During the current decade, the developments of this advanced CVD technique have overcome some of the constraints of HPHT methods. The technique can be applied to produce crystals with much larger sizes, introduce diamond coatings on various materials, and control the doping of "impurities" in the deposits, and so on. Hence, more applications for electronics and optics can be achieved. It has also been employed as sensors with sensitive detection abilities [18 - 20]. Recently, the CVD technique that produces nanocrystalline diamond samples in this dissertation was also used to create specimens for developing the process using nanodiamond films to shuttle drugs to cells without producing the negative effects of modern delivery agents.

Three different kinds of crystallites of diamonds are studied in this dissertation, including single crystal, polycrystalline, and nanocrystalline diamonds. The growth techniques have been modified and further made more suitable for desired applications. Practical applications are made to demonstrate the research potential of this excellent material. While all types of CVD diamond techniques become mature, a new era of CVD diamond research and applications with significant properties has just begun.

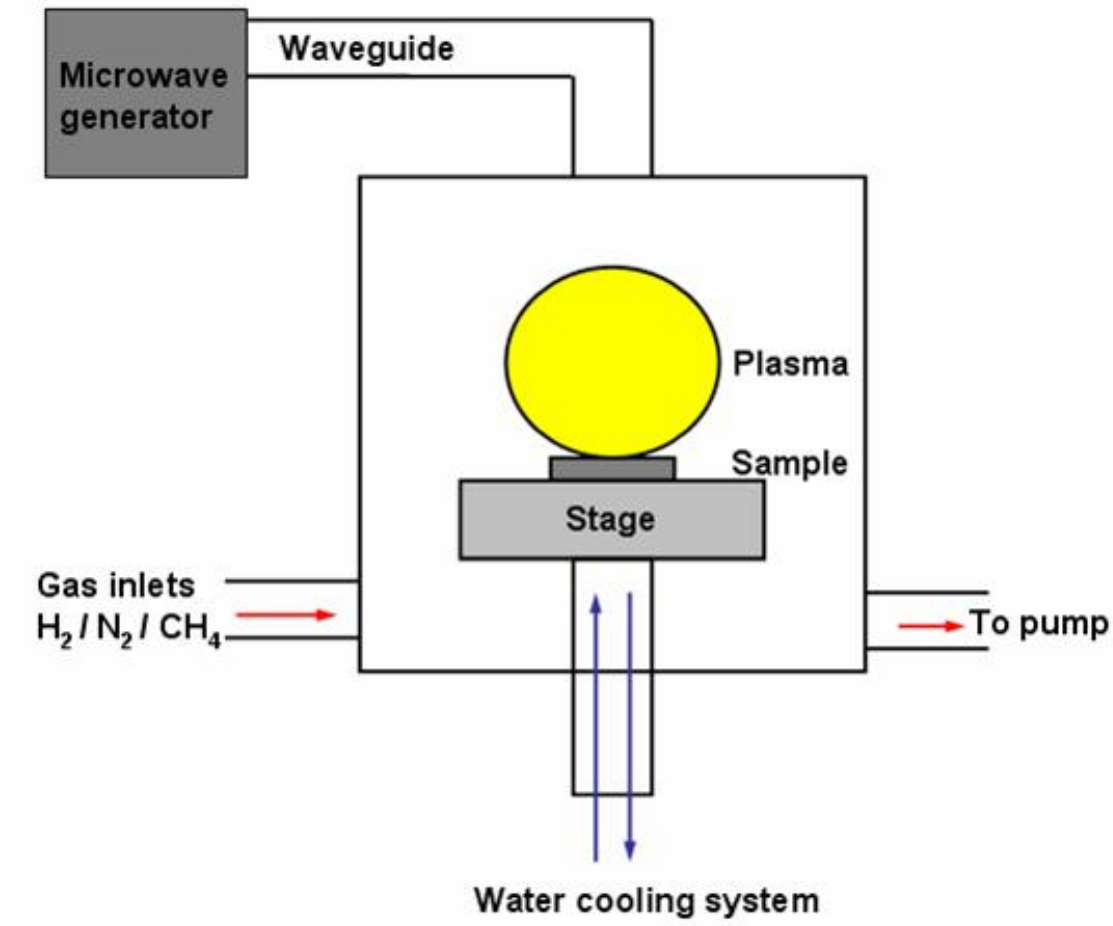

Figure 1.2: A typical microwave CVD reactor.

CHAPTER 2

LITERATURE REVIEW

Diamond is one of the most unique materials with excellent physical and chemical properties which have ever been discovered. Whether it comes from nature or it is man-made, it all shares the similar advantages on material properties over others, while the synthetic diamond materials usually suppress the defects that are commonly seen in the natural diamonds. Among the diamond synthesis methods, chemical vapor deposition of diamond has received a great deal of attention in the material sciences because it made happen many new applications of diamond that had previously been either too expensive to implement or too difficult to make economically.

2.1 Structures and Material Properties of Diamond

The outstanding properties of diamond are shown in Table 2.1 [21]. It demonstrates the suitability of being a potential candidate to be an excellent engineered research material for many applications. It is well-known that diamond is the hardest substance found in nature, and it is realized that diamond is actually four times harder than the next hardest natural mineral, corundum (sapphire and ruby) [22]. In terms of diamond's physical properties, diamond is the ultimate material in several ways including the extreme hardness, a scale of 10 on Mohs scale of mineral hardness, at the top of the hardness scale; wide-range optical properties; excellent thermal conductivity; low

Property	***Value***	***Units***
Hardness	1.0×10^{4}	kg/mm^2
Strength, tensile	>1.2	GPa
Friction Coefficient	0.03	Dimensionless
Sound velocity	1.8×10^{4}	m/sec
Density	3.52	g/cm^3
Young's modulus	1.22	GPa
Thermal expansion coefficient	1.1×10^{-6}	K^{-1}
Thermal conductivity	900 - 2320	W/m·K
Debye temperature	2000	K
Optical transmissivity (from nm to far IR)	225	Dimensionless
Loss tangent at 40 Hz	6.0×10^{-4}	Dimensionless
Dielectric constant	5.7	Dimensionless
Dielectric strength	1.0×10^{7}	V/cm
Electron mobility	1800 - 2200	cm^2/V-sec
Hole mobility	1200 - 1600	cm^2/V-sec
Electron saturation velocity	2.7×10^{7}	cm/s
Hole saturation velocity	1.0×10^{7}	cm/s
Work function on (111) surface	Negative	eV
Bandgap	5.45 – 5.50	eV
Resistivity	10^{13} - 10^{16}	Ω-cm

Table 2.1: Principle properties of diamond. (modified from ref. [21])

coefficient of thermal expansion; highest melting point; and remarkable semiconductor properties [23, 24].

Diamond and graphite are two allotropes of carbon: pure forms of the same element but different in structure. Diamond is a transparent crystal of tetrahedrally bonded carbon atoms and crystallizes into the face-centered cubic diamond lattice structure. In the diamond lattice structure, each carbon atom is linked to four neighboring atoms with hybrid sp^3 atomic orbitals (Figure 2.1). Each of the bond length is only 0.154nm, which

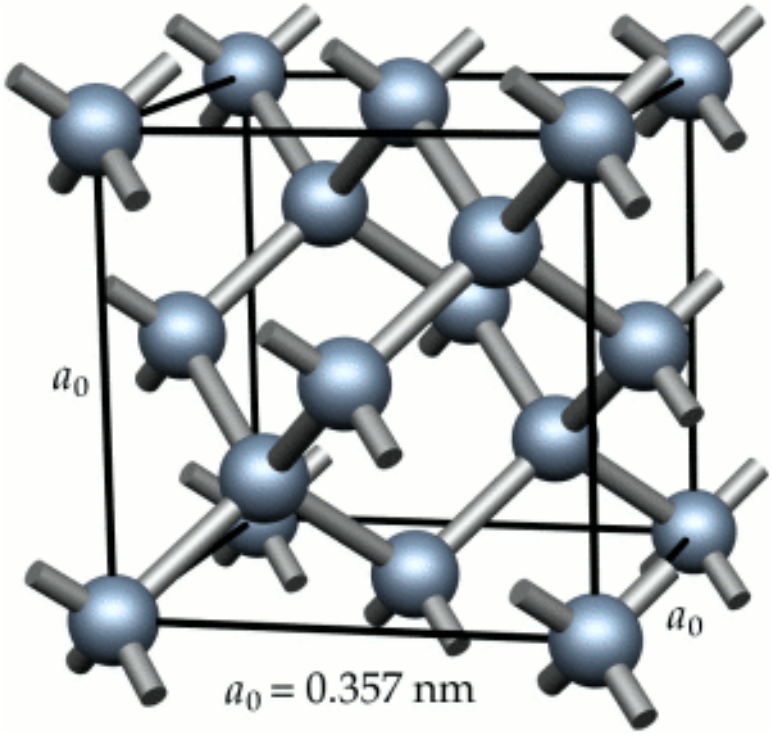

Figure 2.1: Face-centered cubic structure of a diamond crystal [25].

makes the diamond with a tightly packed structure and a high bond energy of 711 kJ/mol, while in graphite lattice structure, each carbon atom combines with its three neighbors using hybrid sp^2 bonds, with a short bond length of 0.141 nm and a high strength of 524 kJ/mol, forming a series of continuous hexagonal structures (Figure 2.2). The fourth orbital is located perpendicularly to the planes and paired with another electron of the adjacent plane by a much weaker van der Waals bond (π bond) whose strength is only 7 kJ/mol [7, 26].

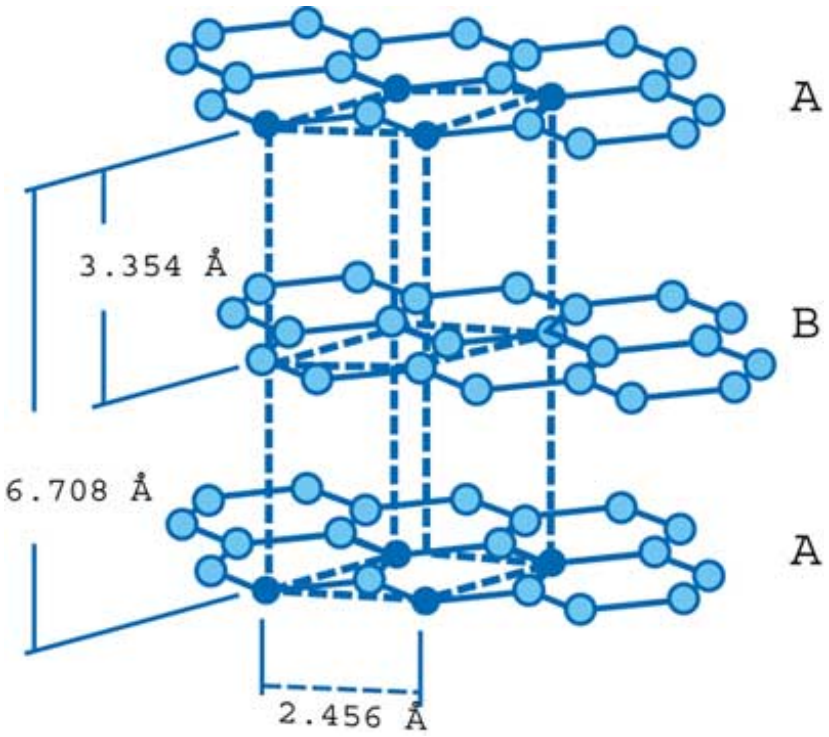

Figure 2.2: Structure of graphite crystal. [26]

Diamonds have been adapted for many uses because of its exceptional physical characteristics. The most notable is its highest hardness (5700 - 10400 kg/mm^2) and largest Young's modulus (1.22 GPa) [27], its high dispersion index, the highest melting point (3820K), lowest dynamic friction coefficient (0.03 - 0.05) [28], and extremely high thermal conductivity (900 - 2320 W/m·K) [27]. At a temperature above 1700 °C (1973K/3583°F), diamond could be converted to graphite [29]. Light-weight diamonds have a density ranging from 3.15 to 3.53 g/cm^3 and extremely close to 3.52 g/cm^3 when it comes to very pure diamonds [30].

Recently, the high thermal conductivity of diamond has been employed for high-power laser diode substrates to improve the performance and increase the output power of the diodes. Also, diamond in the form of thick films has been used as heat spreaders to increase the packaging density of very large scale integrated circuit (VLSI) and multiple-chip module compacts [31].

Furthermore, diamond is transparent over a larger range of wavelengths, from the deep ultraviolet through the visible into the far infrared, than any other solid or liquid substance [22, 32, 33]. So it has been frequently made into windows for optical instruments. The most important optical properties of diamond are the optical absorption and reflection index for certain wavelength and temperature. That is because diamond has a small absorption coefficient of light and an appropriate refraction index from infrared to ultraviolet region [27].

Diamond is chemically inert and does not react with common acids even at elevated temperatures. A large number of industrial applications take advantage of diamond's excellent properties coupled with extreme strength and chemical inertness

over other materials for harsh conditions [34].

Diamond is a semiconductor with a wide band gap of 5.45 - 5.50eV [35 - 39]. Especially when the diamond surface is terminated by hydrogen, it has a negative electron affinity (or work function), so that its conduction band bottom edge lies above the vacuum level. Electrons in its conduction band could pass into the vacuum without an energy barrier.

In addition, the Hall mobility of electrons, 1800 - 2200 cm^2/V-sec, and the Hall mobility of holes, 1200 - 1600 cm^2/V-sec, of diamond at room temperature as well as the high field electron velocity and the electrical breakdown field outperform those of widely used silicon in the semiconductor industries [27].

With all these advantages of high carrier mobility, high saturation velocity, high thermal conductivity, good chemical resistance, and wide band gap, diamond thus becomes an excellent candidate for realizing high-power and high-frequency electronic applications in extreme environmental and radiation conditions [40].

2.2 Synthesis Method - Chemical Vapor Deposition

As the name CVD implies, this deposition method involves a series of gas-phase and surface chemical reactions and the deposition of reaction products, i.e., diamond, on a solid substrate surface. Figure 2.3 shows main processes inside a CVD chamber [41].

For diamond deposition, a carbon-containing precursor is required in order to provide carbon for diamond nucleation and growth. Many gas-phase carbon sources can be used, including methane, alcohol, acetylene, and carbon monoxide, while methane is most commonly used [27, 42 - 44]. The gas mixtures usually contain not only the carbon

source but also a very high molar ratio of very active atomic hydrogen for stabilizing the growing metastable diamond surface, promoting abstraction of hydrogen from molecules in the gas phase as well as on the diamond growing surface, and preferential etching of non-diamond carbon deposits. Oxygen and fluorine are sometimes also employed for similar purposes.

CVD techniques are generally applied using various methods to activate (decompose) the gases for the generation of radicals responsible for the material deposition, including electrical discharge (e.g., microwave CVD [45], radio frequency CVD [46], direct

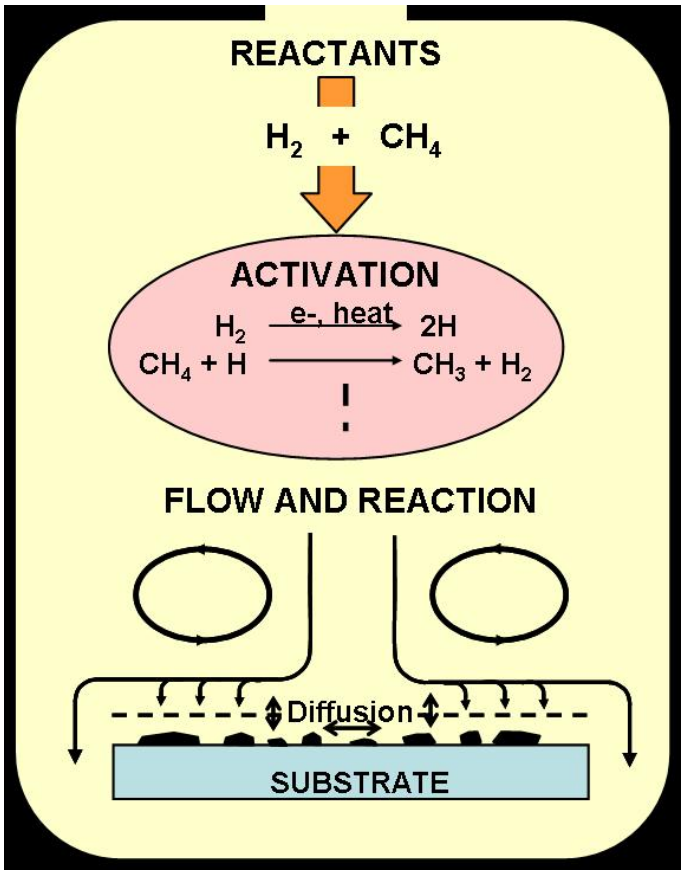

Figure 2.3: Inside CVD chamber, a simplified view [41].

current CVD [47]), thermal methods (e.g., hot filament CVD [11]), and combustion flame (e.g., oxyacetylene torch [48]).

The reactor setup employing an electrical discharge uses a vacuum chamber with a rotary pump that runs continuously during the process. The pressure inside the chamber is kept constant, by a throttle value, while all gases are fed into the chamber with desired and steady flow rates. Unlike HPHT synthesis, which is typically carried out at pressures in excess of 5 GPa (~50,000 atmospheres), diamond CVD is usually carried out at a fraction of one atmosphere mainly for the sake of safety concerning the use of explosive gas mixtures and because of the limits for plasma generation. The conditions of low pressure (sub-atmospheric pressures) and low temperature for diamond CVD are actually in favor of growth of graphite instead of diamond according the phase diagram of carbon (Figure 2.4) [49], due to the fact that graphite is thermodynamically stable while diamond is kinetically stable or so-called metastable.

Silicon, molybdenum, or other materials can be used as substrates for heterogenerous growth [50] while natural or synthetic diamond plates for homoepitaxy [51, 52]. Microwave, radio frequency, or direct current power is introduced into the chamber to generate a discharge. A schematic diagram for such an electrical discharge method is shown in Figure 2.5 [46, 53, 54]. The gas molecules are dissociated to generate carbon atoms for deposition onto the substrate surface, although details of the process are still not fully understood. Electrical discharge CVD, especially microwave plasma CVD (MPCVD), is currently the most widely used technique for diamond deposition. Microwave plasma CVD does not require any electrode, which reduces the chances of contaminations in the film caused by electrode erosion. The substrate is heated by the

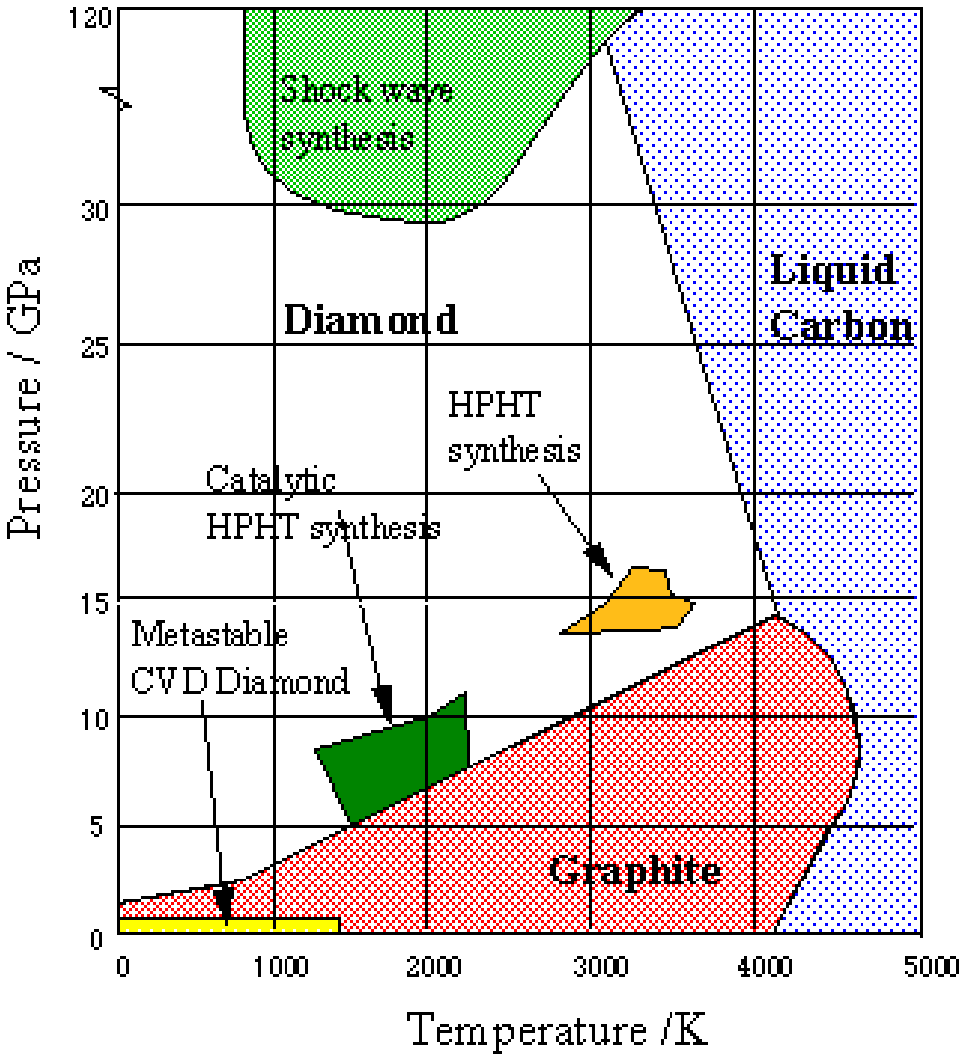

Figure 2.4: Phase diagram of Carbon. The conditions of low pressure and low temperature for diamond CVD are actually in favor of growth of graphite instead of diamond according the phase diagram [49].

absorption of microwave, the bombardment by energetic plasma species, and the exothermic recombination of radicals, such as atomic hydrogen, on the diamond growing surface. Comparing to radio frequency discharges, which commonly operate at 13.5 MHz, microwave discharges operate at a much higher frequency (*e.g.,* at a frequency of 2.45 GHz). This creates a higher concentration of electrons that produce a higher density of radicals for diamond growth. High ionization fractions are generated as electrons collide with gas atoms and molecules. The plasma formed typically has a ball shape and sits on top the substrate, which increases the efficiency of mass transport of diamond growing radicals to the diamond surface for deposition and reduces the coating on the chamber walls. Nowadays with the most advanced CVD chambers, a plasma sheet can be formed right on top of the substrate and is of a large coverage area. The technique therefore is reproducible and requires low maintenance costs.

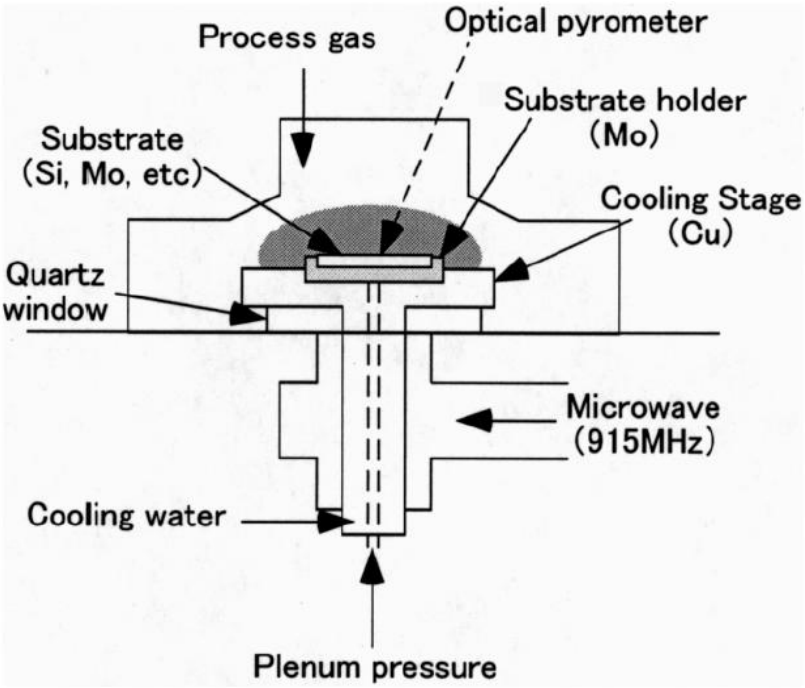

(a)

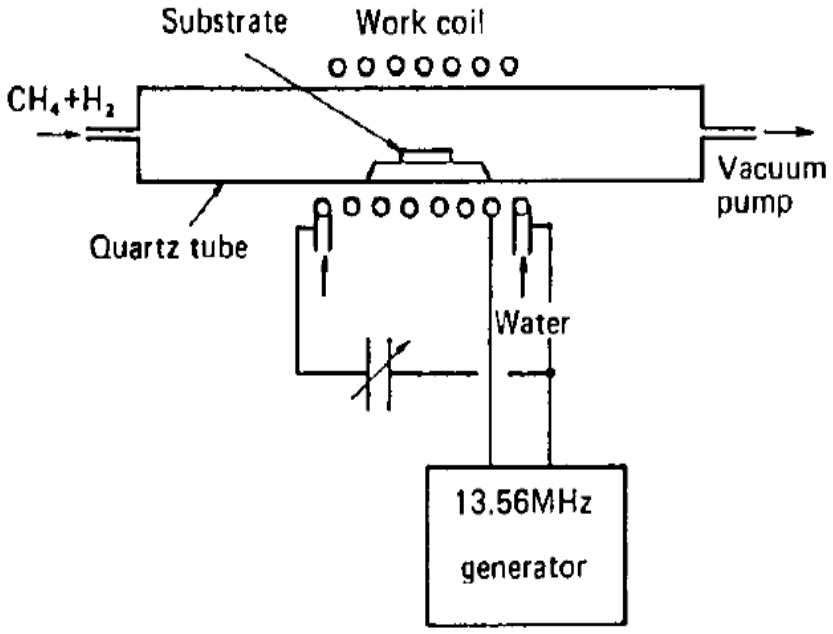

(b)

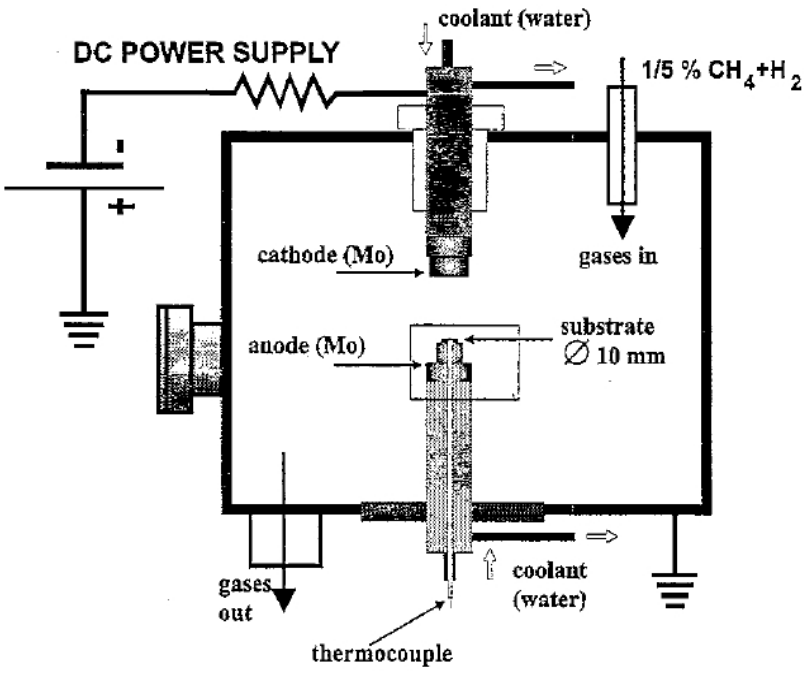

(c)

Figure 2.5: Apparatus of a typical electrical discharge CVD system: (a) Microwave plasma CVD [53]; (b) Radio frequency plasma CVD [46]; (c) Direct current plasma CVD [54]

More importantly, the diamond produced by this method is usually of better quality.

Hot filament CVD (HFCVD) was first developed by Matsumoto and co-workers at NIRIM of Japan [10, 11]. They were able to reach growth rates of more than 1 μm hr^{-1} with this method. The method has a very similar setup to electrical discharge methods. A vacuum chamber, a pump, sub-atmospheric working pressure, and gas feed-ins are also needed (Figure 2.6(a)). Diamond grains are deposited on a heated substrate from a gas mixture, which is activated by a hot filament placed near the substrate. This thermal method involves a piece of metal filament such as tungsten and tantalum that can generate high temperatures exceeding 2000°C by applying electrical current but also could react with carbon-containing gas to form carbides. The substrate can as well be heated by the hot filament alone. A separate heater or cooling mechanism could be employed to adjust the substrate temperature more precisely during the deposition process. A bias voltage can be applied between the filament and the substrate to produce an electrical discharge that subsequently promotes the deposition rate and enhances the nucleation density when the substrate is biased negatively. This method was the first to achieve nucleation and continuous growth of diamond on various substrates at a low cost and is the simplest method for applications that do not require ultrahigh quality of diamond films. Hot filaments take time for metal filaments to be converted to carbides before the rapid depletion of carbon in the gas phase stops. This delay causes an induction time before diamond grows at a reasonable rate, and a used filament must be replaced with a new one. Problems can occur in the reproducibility and the operation that takes a long period of time due to the limited life of filaments. With the latest developments on the HFCVD technology, uniform films, such as 12 inch in diameter, can

be produced with this method and are commercially available.

Combustion flame CVD, such as that produced with an oxyacetylene torch shown in Figure 2.6(b), uses relatively higher gas flow rates in comparison to the other two methods [57]. A combustion method that works under atmospheric pressure flame was first reported by Akatsuka and co-workers with a growth rate up to 250 μm hr^{-1} in 1988 [58] and triggered new diamond deposition activities due to the simple set-up and yet a high growth rate of this approach. Gas mixtures of oxygen and ethylene were also studied by the group at US Naval Research Laboratory [59]. A high growth rate of 880 μm hr^{-1} using RF thermal plasma torch was reported [60]. When the gases flow through a high-power electrical discharge, they form a jet containing high concentrations of neutral gas particles and radicals as well as ionized particles. High concentration of radicals result in a high diamond growth rate. However, because of the extreme heat generated by the thermal plasma jet, the process is more difficult to control and requires high gas flow rates. All species are directly deposited onto a water-cooled substrate surface. This method can make diamond films over smaller deposition areas; however, the stability and the uniformity of the deposited film are not easy to be achieved. Different working environments for combustion flame CVD, either in an open atmosphere or in an enclosed chamber, have been tested in order to increase the film quality [61]. The deposition can be carried out in both argon-controlled and oxygen-controlled chambers in order to minimize impurities from diffusion into the flame from the ambient atmosphere. However, unlike the diamond films produced in the open and oxygen-controlled atmospheres, the films produced with argon show features of amorphous carbon (i.e., in Raman spectra). Thus, the best quality diamond films have been obtained when the

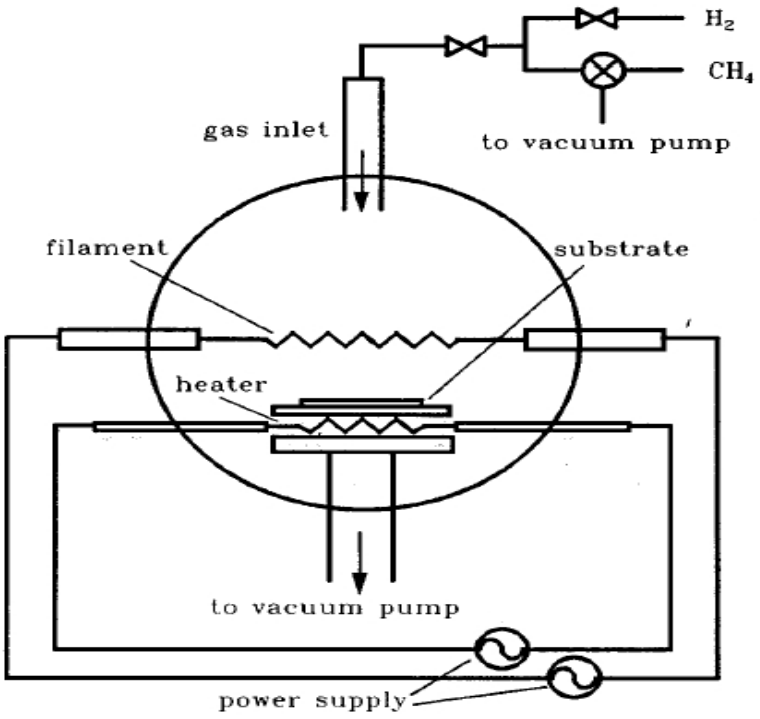

(a)

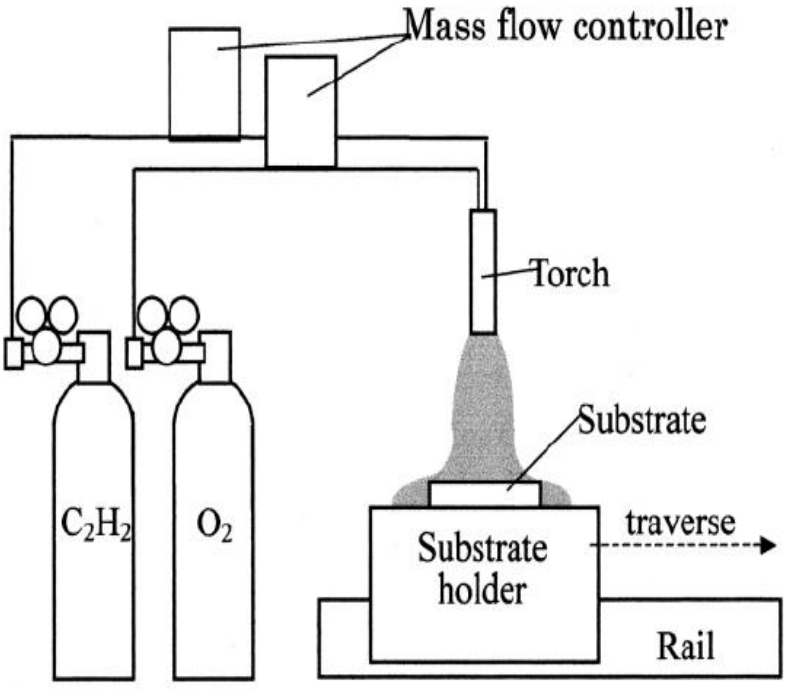

(b)

Figure 2.6: Apparatus of the CVD systems using (a) Hot filament [55]; (b) Combustion flame [56]

chamber is oxygen-controlled, most likely due to the in-situ etching of non-diamond features.

A C/H/O phase diagram is shown in Figure 2.7 [62]. It was introduced by Bachmann et al. providing a common scheme for a number of major diamond chemical vapor deposition (CVD) methods used to date, including thermal CVD, hot filament CVD, various plasma deposition techniques and combustion flames. Based on experimental conditions for results summarized by this diagram, low pressure CVD diamond synthesis is feasible within a well-defined field, so-called diamond domain, located at the center of the ternary diagram and defined by two thick dashed lines. This domain allows general predictions of gas phase compositions and starting materials suitable for diamond synthesis. On the oxygen-rich side of this diagram, the diamond domain is adjacent to the region where no deposition occurs at all. On the carbon-rich side of the diagram, non-diamond carbon growth occurred when the gas composition gets beyond the diamond region. It truly gives an explanation for the quality variations of diamonds deposited from different gas mixtures. Their analysis also shows that the large deposition rate differences between the various methods correlate well with the corresponding gas temperatures, which indicates that high temperature in the gas phase fosters high rate diamond growth.

In this dissertation, microwave plasma enhanced chemical vapor deposition (MPCVD) was used. Different concentrations of hydrocarbons, mainly CH_4, diluted in other gases, including argon and/or hydrogen for diamond growth are examined and are subjected to change according to the desired crystallites and morphology and material properties of diamond specimen. Different seeding/nucleation methods were also tested.

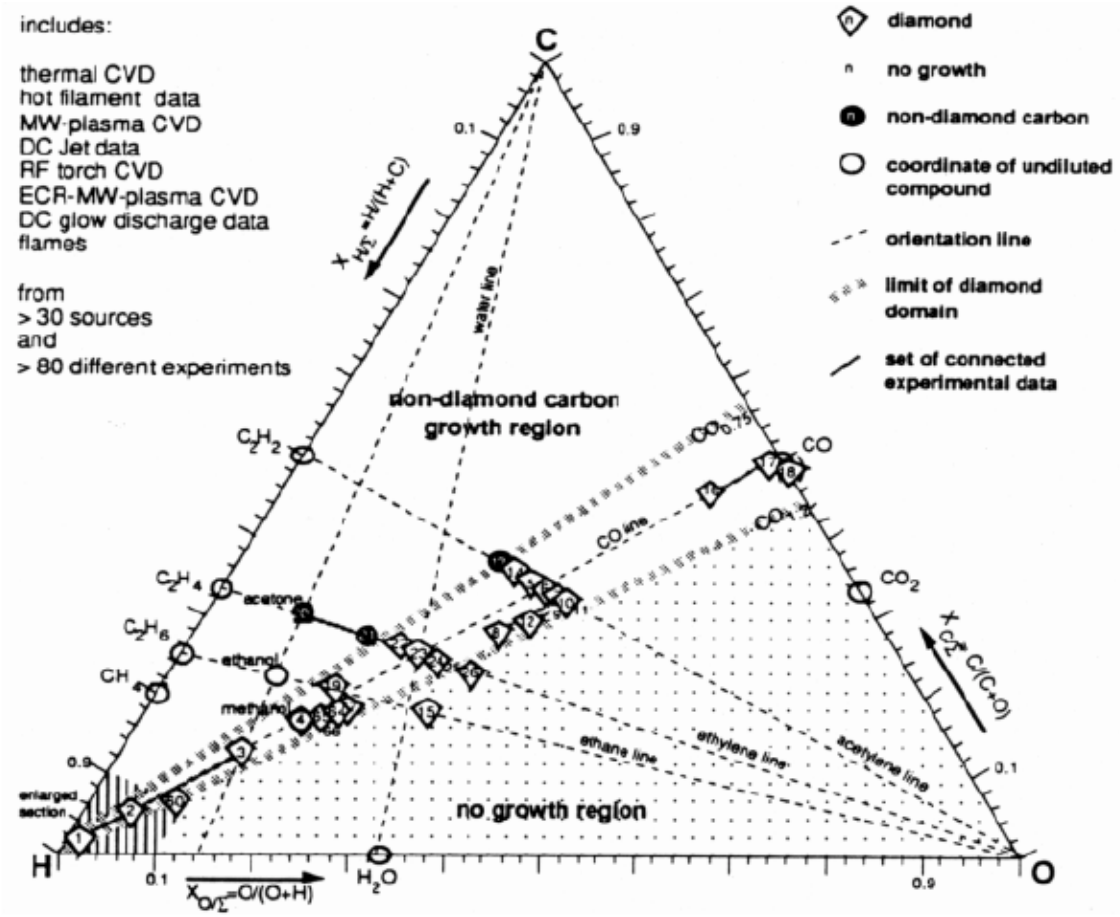

Figure 2.7: C/H/O phase diagram for diamond CVD process showing the narrow diamond growth region along the C-O line. [62]

Pre- and post-treatments on samples, including heat and plasma treatments, were studied in order to refine and modify the properties.

2.3 Single Crystal Diamond (SCD)

Although small natural diamond of less than 0.3 carat costs less than CVD diamond of the same size, CVD diamond has the cost-effective advantage when it comes to larger sizes as illustrated in Figure 2.8.

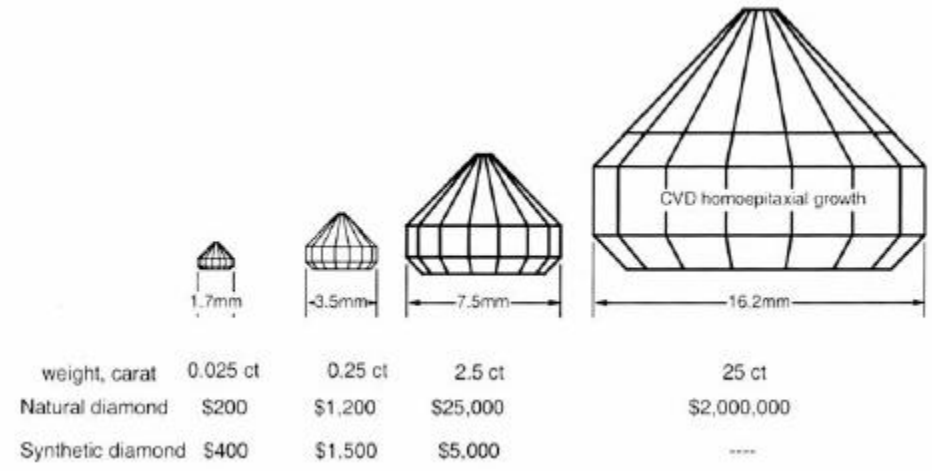

Figure 2.8: Dimension and cost comparison between natural and CVD diamonds.

Homoepitaxial growth of diamond single crystals has been demonstrated by several research groups [18, 42, 63-65]. Back in the early 1990s, CVD diamond single crystal deposited on single crystal HPHT synthetic substrates was performed by plasma torch CVD [57] at growth rates of 100 - 200 μm/hr. But the use of this method was limited due to the difficulty of precise temperature control and high cost of gas consumption. Plus,

the problem of local point defects was present. Diamond single crystal CVD growth by hot filament [52] and microwave plasma [52, 66] exhibits stable growth conditions, but for years the growth rates were low, less than 10 μm/hr [17, 67], and most plates produced had a thicknesses of less than 1 mm.

Commercial products of single crystal CVD diamond have been explored by Element Six and Sumitomo for electronics [64, 68], and by Apollo Diamond Inc. for gems [69]. The major drawbacks of single crystal CVD diamond in industrial applications have been the slow growth process and small area (maximum around 10 × 10 mm^2), and also the formation of defects, such as formations of twins and polycrystalline diamond limiting its future as a large-volume material [70, 71]. However, these problems have been overcome with recent developments. Among all the works, the Carnegie group developed relatively high-temperature and high-pressure CVD processes that led to a very high growth rates for single crystal diamonds [72 - 74], and these crystals can be tuned to exhibit extraordinary mechanical properties by an annealing process [75]. Their purpose was to enhance the growth of large single crystal CVD diamonds for its use as diamond anvils in high pressure research. In order to produce large and durable CVD diamond, high growth rates, high strength, twin-free material, and optical transparency are the primary goals and challenges.

In order to enhance growth rates and produce a smooth, twin-free diamond surface, a small amount of nitrogen was added in the reacting gas mixture to promote the growth of the {100} facet [76, 77]. Following the report of high-rate plasma enhanced CVD of diamond at higher gas pressure, temperature, and methane concentration by Tzeng's group in 1994 [78, 79] with a follow-up publication in Diamond and Related Materials

[80]. Some groups have enhanced the single crystalline diamond growth rates to 50 - 150 μm/hr with a high density plasma at higher pressures over 150 Torr and a higher methane concentration up to 20% on the CH_4 / H_2 gas mixture,, which was up to 100 times faster than the typical growth rate of 1 μm/hr for conventional CVD diamond growth processes [74]. It has been reported that with a refined microwave plasma CVD process, scientists are capable of producing one 3mm-thick twin-free gem-quality diamond per day.

Generally, laser dicing and mechanical polishing are required to separate the CVD layer from the seed substrate to obtain free-standing crystals after CVD growth. The technique of producing free-standing large-area single crystal diamond film by CVD technique without any required mechanical polishing procedure was demonstrated by Tzeng's group in 1993 [66]. MeV ion implantation was done on the natural diamond substrate by oxygen ion beam prior to the CVD growth. After the growth, the as-grown film along with the substrate were loaded into an oxygen environment and were heated up for separation. The separated CVD film was transparent and flat with a thickness of 15 μm. Another free-standing single crystal diamond films were obtained also without post-polishing [44]. The whole crystal was annealed to graphitize a buried region of ^{12}C that was implanted before the CVD growth, and then the buried graphite layer was etched away. Both groups successfully separated the CVD film from the natural diamond substrates.

A demonstration of boron doped CVD diamond as a p-type semiconductor for electronics is in progress but the n-type is still elusive [81]. In addition to the challenge of controlling the variety of impurities/dopants for electronic applications, challenges for single-crystal CVD diamond growth include producing large area plates ($> 10 \times 10$ mm^2),

and three-dimensional crystals (> 10 mm^3 cubes, > 20 carats), and improving diamond crystalline quality (*i.e.*, reducing stress) [69]. With commercially available HPHT synthetic diamond seeds with maximum sizes of around 3 carats and a maximum area around 10×10 mm^2 while microwave plasma CVD limiting growth to the top area of the diamond substrate (one-dimensional diamond growth), potential solutions to producing large-area CVD diamonds include as the mosaic or tile arrangement of several {100} pieces of diamond seeds [82], or three-dimensional growth on all {100} faces at proper growth condition [74].

Heteroepitaxial growth of single crystalline diamond has also been reported [83 - 85]. Heteroepitaxial growth of diamond depends critically on the development of a suitable lattice-matched substrate system. Oxide substrates, notably MgO and $SrTiO_3$, on which thin epitaxial films of iridium serve as a nucleation layer for diamond have already shown considerable promises [86]. Other materials which served as nucleation layers, such as platinum, have also been demonstrated. However, heteroepitaxial growth of diamond often generates diamond films in the range of micrometers in thickness. As for bulk single crystal diamond deposition, single crystalline diamond substrates are the most desired and widely used, since the quality of the diamond films is strongly affected by the quality of the substrates.

2.4 Polycrystalline Diamond (PCD)

The deposition of diamond by CVD is controlled by strongly coupled parameters, of which each has impacts on the final product. In general, the substrate temperature, the concentration of plasma species, and the substrate materials determine the crystallinity of

the obtained film. Polycrystalline diamond is composed of many small crystals oriented in different crystallographic directions. Numerous CVD techniques have been used to produce polycrystalline diamond for research and industrial applications. The polycrystalline diamond is usually grown at low growth rates, up to a few micrometers per hour, at substrate temperatures below 1000°C in a low concentration of methane (typically 0.1 - 2%) gas mixtures that were highly diluted by hydrogen. A major advance was reported by going well beyond the traditionally low methane concentration and low substrate temperatures, achieving growth of well-faceted diamond crystals by microwave plasma CVD at substrate temperature as high as 1500°C with methane concentration approaching 100%. Polycrystalline diamond was grown at a rate exceeding 50 μm hr^{-1} [78, 80].

Addition of nitrogen during the growth process resulted in an increased single crystal diamond growth rate, and that is consistent with observations for PCD films [73]. Deposition of polycrystalline diamond films can be done on non-diamond substrates, such as silicon and molybdenum, with silicon substrates being the most commonly used for deposition of PCD. However, diamond thin films deposited on non-diamond substrates using CVD techniques usually exhibit a polycrystalline-like morphology, which contains both randomly oriented crystals and non-diamond carbon defects [87]. The grain boundaries of polycrystalline diamonds possess non-diamond carbon phases such as graphite, which limits wide applications in electronics and reduces its durability in abrasives. The misorientation of diamond grains can be corrected, to some extent, by means of, for example, ion bombardment assisted diamond nucleation processes, and highly oriented polycrystalline diamond films can be deposited on a variety of substrates.

A typical micrograph of a PCD sample is shown in Figure 2.9. Commercial PCD wafers can have a diameter larger than 12 inch across the planar surface, uniform quality, and a thickness of several millimeters. When the deposition process is completed, the substrates are removed by plasma dry etching or dissolving in chemicals. Furthermore, these PCD techniques are also capable of coating polycrystalline diamond onto subjects with irregular shapes for a variety of applications.

The types of defects often observed in SCD and PCD films grown by CVD techniques include the followings [7, 88 - 92]: (1) Point lattice defects, including neutral vacancies, interstitials, and substitutional elements; (2) line lattice defects, such as dislocations; (3) planar lattice defects, such as twinning, stacking faults, and grain boundaries; and (4) volume lattice defects, such as graphite sp^2 inclusions and voids.

When diamond nucleates, it is frequently observed to have twinning defects. Twinning commonly occurs during CVD growth on the (111) surfaces, and an impurity atom (e.g., hydrogen) is incorporated at the top of a tetrahedron, causing the tetrahedron in the next layer to be reversed [97]. Stacking faults usually occur at the crystal surface and can relatively easily be observed. Nitrogen can be added into the gas mixtures for the CVD process to lower the growth rate in the (111) direction, avoid growth defects and increase the growth rate in the (100) direction [72, 73]. It also results in smoother growth surfaces, where the stacking faults occur. Voids in homoepitaxial diamond films produce stresses in the films. These stresses can be lowered by reducing the substrate temperature during the growth [8]. If the stresses exceed a certain level, lattice discontinuity, micro-twinning, and even cracks can form in the deposited films.

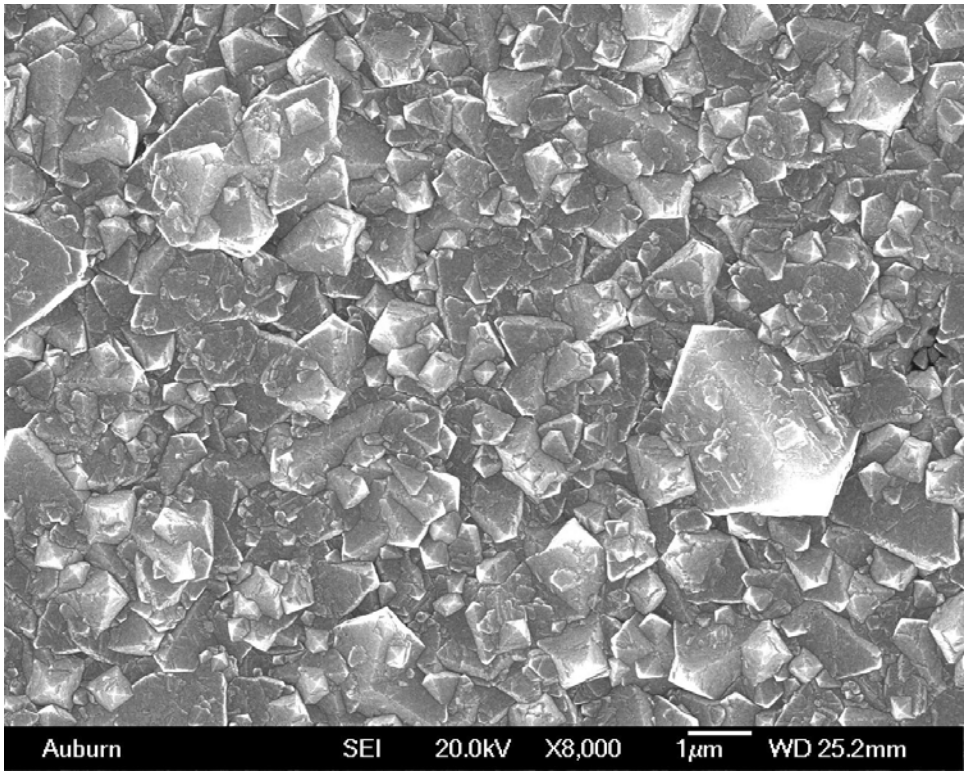

Figure 2.9: SEM image of a typical polycrystalline diamond substrate surface.

2.5 Nanocrystalline Diamond (NCD)

The synthesis of nanocrystalline diamond films has become a mature CVD technique in the past decade. By adding noble gas, typically argon, into traditional CH_4 / H_2 gas mixtures, the nanocrystalline diamond thin films composed of 3 - 15 nm crystallites have been deposited. An SEM image taken from a nanocrystalline diamond sample surface is shown in Figure 2.10. High concentration of C_2 dimers were found in the carbon-containing noble gas plasmas, leading to a new growth and nucleation mechanism for diamond deposition, which involves the insertion of those dimers into carbon-carbon and carbon-hydrogen bonds. As a result, a secondary nucleation rate on the order of 10^{10} $cm^{-2}s^{-1}$ was achieved and resulted in nanometer sized diamond crystals in the films. The grain size can also be controlled continuously and reproducibly over this range by changing the gas-phase chemistry of the plasma-enhanced chemical vapor deposition process [28, 93].

Nanocrystalline diamond films have properties much different from those of single crystalline and polycrystalline diamond films and are suitable for diverse applications. For example, there can be up to 10% of the total carbon in the nanocrystalline films being located at 2 to 4 atom-wide grain boundaries. Due to the fact that the grain boundary carbon is π-bonded, the mechanical, electrical, and optical properties of nanocrystalline diamond are unique. The grain boundaries of nanocrystalline diamond were found to be conductive, which causes the entire film to become electrically conductive and suitable to function as, for example, an excellent cold cathode material [94]. Furthermore, because of the very small crystallite size, the surfaces of nanocrystalline diamond films are very smooth and desirable for applications such as low friction coatings, surface

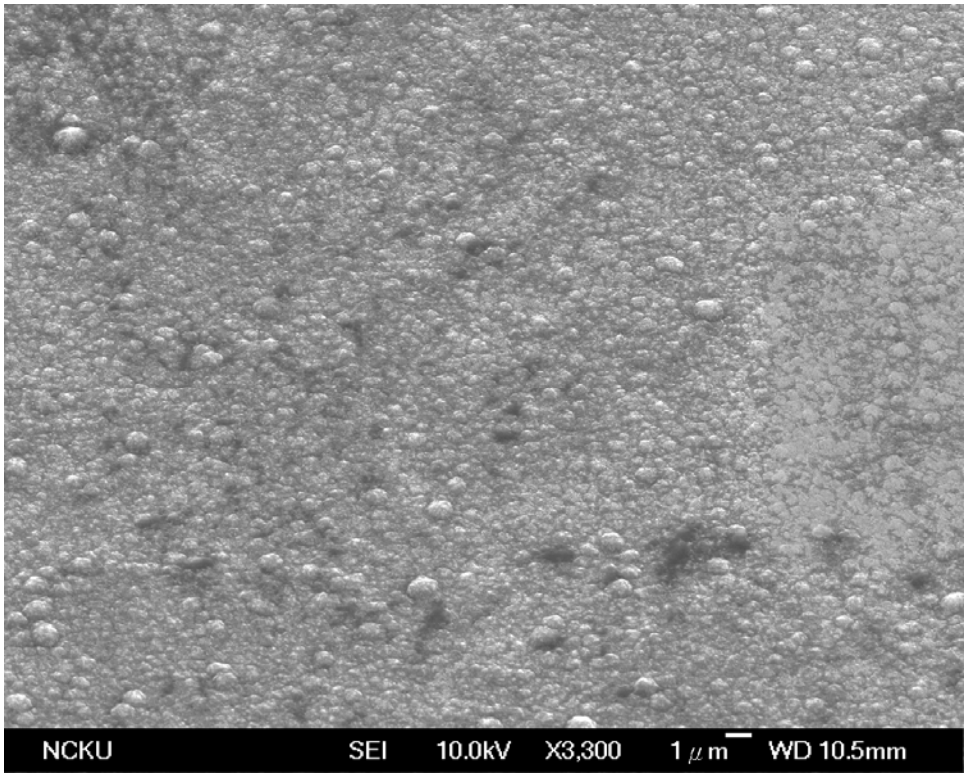

Figure 2.10: SEM image taken from a nanocrystalline diamond sample surface.

acoustic wave (SAW) devices, and micro-electro-mechanical systems (MEMs) on top of their chemical resistance performance. An example of application which employed nanocrystalline diamond film as a protective coating is shown in the Figure 2.11. MEMs gears made of silicon fabricated in Auburn University were coated with nanocrystalline diamond to increase the durability and chemical resistance. In this particular case, seeding was done by ultrasonication with nanocrystalline diamond seeding solution, and the gears were subjected to diamond deposition for 20 minutes on each side. Continuous films covering the whole surfaces of the gears were obtained. The color difference on the film indicating a slight difference of the film thickness was caused by the different plasma density with respect to the position of each local point on the gears.

2.6 Nucleation Mechanism

Surface nucleation is the primary reaction responsible for CVD diamond growth. During early development of CVD diamond deposition, single crystal diamonds were used as substrates. Unlike homoepitaxial diamond growth, diamond deposition on non-diamond substrates could be efficient and successful only with proper nucleation process. It is essential for optimizing the desired properties of the diamond films, such as grain size, orientation, transparency, adhesion, and roughness [95]. In 1982, Matsumoto made a breakthrough in depositing diamond on non-diamond substrates without diamond seeds present, but the film was not continuous [10, 11]. Five years later, scientists found that scratching the substrate surface with diamond powder could greatly enhance nucleation density [96], and the effect of scratching has been studied extensively ever

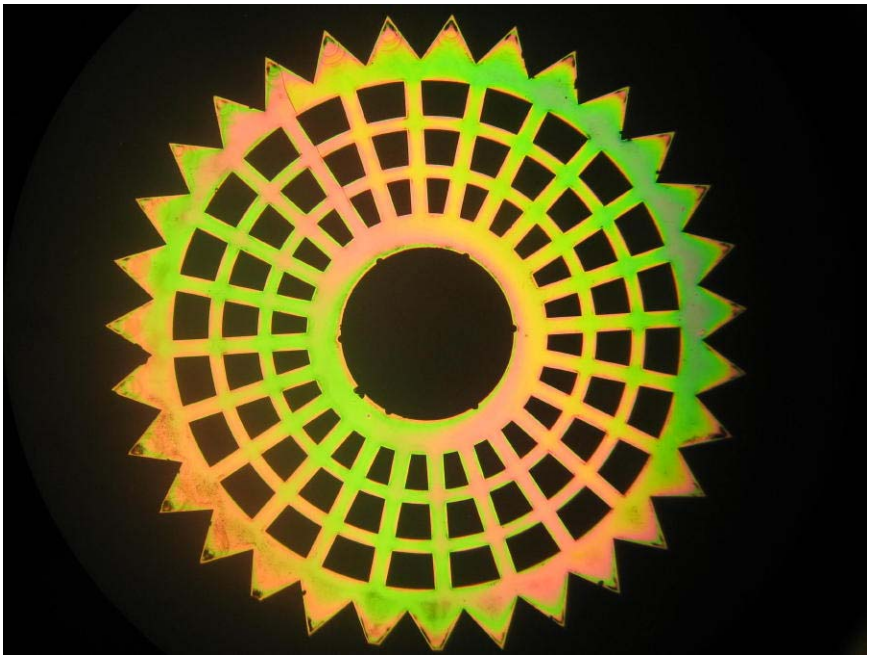

(a)

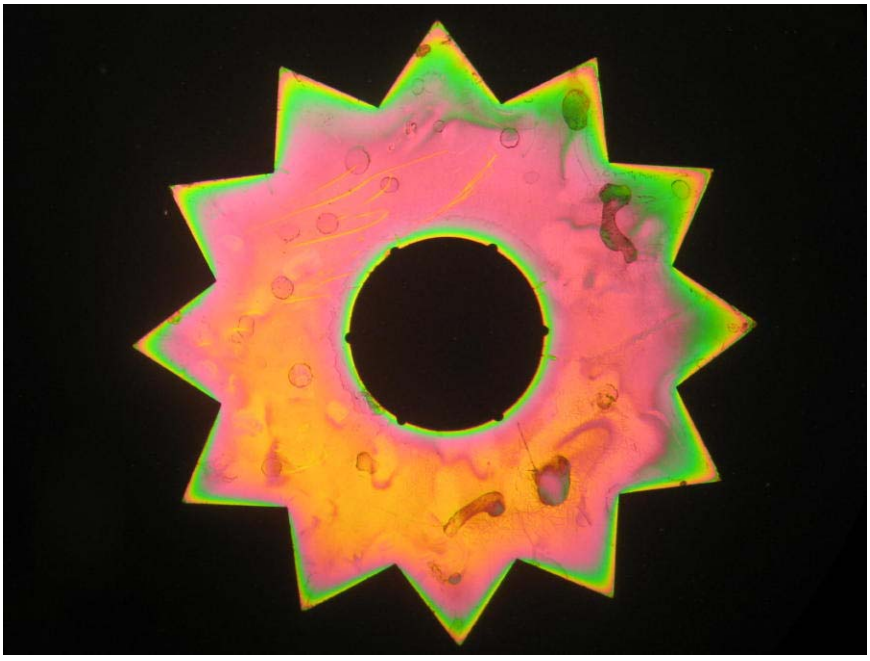

(b)

Figure 2.11: (a) MEMs gear coated with nanocrystalline diamond to improve the durability and chemical resistance. (b) Critical point dryer could be employed to further improve the uniformity of diamond coatings.

since. Diamond abrasion could reduce the induction time for nucleation and increases the nucleation density [97]. The nucleation density enhanced by scratching or abrading with diamond grits of a silicon substrate can reach roughly three orders of magnitude, up to 10^7 cm^{-2}, higher than that of a non-scratched silicon substrate. The nucleation density increases proportionally to the scratching time, and the surface morphology changes from isolated diamond crystals for a short scratching time to smaller in size, higher number density crystals with an increasing scratching time [98]. To date, the understanding of the nucleation is still very limited. Also, there are studies and experimental evidences on the gas phase (homogeneous) nucleation of diamond for growth on non-diamond surfaces. From the earlier state, the density of diamond particles obtained from gas phase at atmospheric and sub-atmospheric pressure [99] was still relatively low compared to the typical surface (heterogeneous) nucleation done by scratch or other mechanical approaches to a later improvement, a high density of diamond nucleation (10^9 - 10^{11} cm^{-2}) was claimed at low pressures (0.1 - 1 Torr) using either hot filament CVD or ECR microwave CVD [100]. The effect of homogeneous nucleation from gas phase during the deposition is very small and could be neglect.

Surface pre-treatments are necessary in order to facilitate the nucleation and the initial growth of NCD films deposited from the C_2 precursors [101]. High surface carbon concentration also has a promoting effect [102]. Furthermore, it is believed that nucleation sites could be either grooves of scratching lines or protrusions produced by etching-redeposition [103].

Figure 2.12 is a SEM image of surface of a silicon substrate after a conventional ultrasonication seeding process [104]. The substrate was placed in the nanodiamond

seeding solution during the ultrasonication. The fine distribution of diamond nano-crystals over the surface significantly reduces the required growth time for a continuous film to form and also increases the uniformity of the deposit.

2.7 Growth Mechanism

The growth of diamond from chemical vapor phase is basically chemical reactions with a competition between the formation of diamond structures and non-diamond (including graphitic) structures.

The homoepitaxial growth, by which diamonds grow from diamond crystal seeds, has been intensively studied since the 1960's. Atomic hydrogen, which promotes reactions, is among key ingredients in the chemical vapor deposition process [105, 106]. During a deposition process, the structures of deposit are strongly determined by the surface temperature that is partially contributed by the thermal deposition of hydrogen and recombination leading to surface reconstruction [105, 107, 108]. Active carbon containing species including acetylene molecules, methyl radicals and carbon atoms contribute to diamond deposition. It is believed that hydrogen, fluorine or oxygen could help the growth of diamond. For growing diamond on non-diamond substrates, nucleation is necessary. Studies showed that hydrogen or fluorine can contribute to nucleation while oxygen could not, because the halogen species, fluorine and hydrogen, are able to sustain the sp^3 structural configuration of the surface carbon atoms. Furthermore, the adsorption energies are relatively large for the H and F species, indicating that these species would help stabilize the diamond in the (111) orientation. The adsorption of CH_3 or CF_3 to a radical carbon on a H- or F-terminated diamond (111)

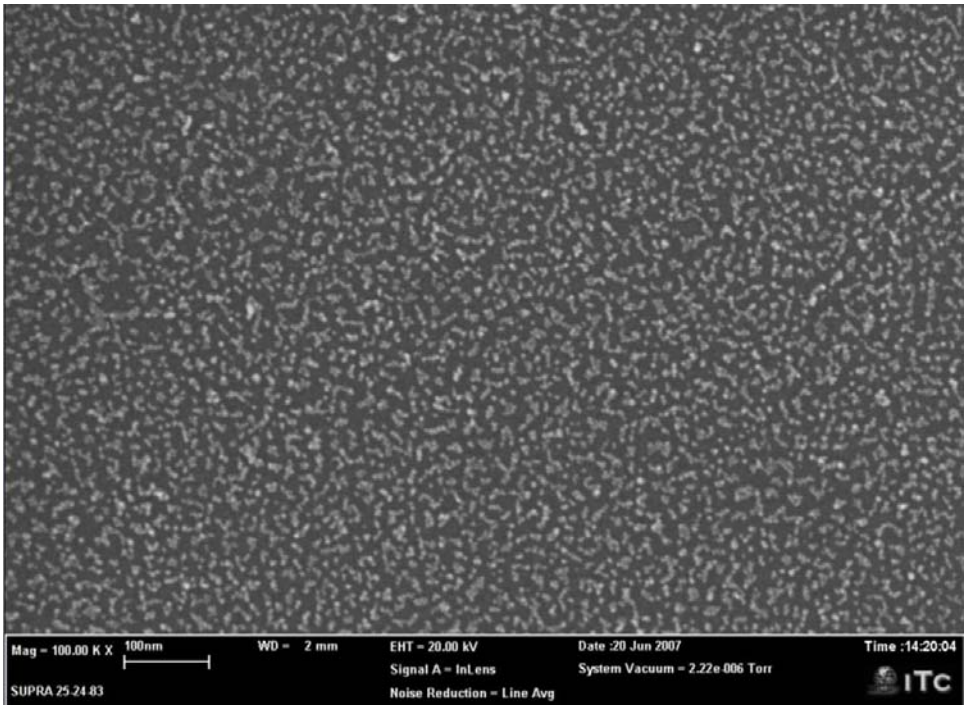

Figure 2.12: SEM image of a seeded silicon substrate after an ultrasonication process. Uniform distribution of nanodiamond seeds was obtained. [104]

surface also stabilizes the sp^3 structural configuration of the radical carbon atom [109].

Atomic hydrogen which is dissociated from the hydrogen-containing gas or from hydrogen that serves as a diluting gas is a crucial species in diamond deposition. Atomic hydrogen plays several important roles including etching graphite, stabilizing diamondsurface, creating radicals, and abstracting hydrogen from the diamond growing surfaces.

Atomic hydrogen converts hydrocarbons into radicals, which is a necessary precursor for diamond formation, and abstracts hydrogen from the hydrocarbons which are attached on the surface [110] and thus creates reactive surface radical sites for further adsorption of diamond precursors. One atomic hydrogen from the gas phase, when combining with another hydrogen atom on the diamond surface leaves one dangling bond with the carbon atom on the surface. The diamond surfaces then become hydrogen-terminated. The hydrocarbon species, such as CH_3 radicals, come to the growth surface and form sp^3 covalence bonds with two adjacent surface carbon atoms, of which each contains a dangling bond [111]. With such process being repeated, more carbon atoms join the diamond lattice and thus diamond grows. A schematic diagram for the mechanism stated above is shown in Figure 2.13 [112].

However, too much atomic hydrogen present during the CVD process would possibly cause unnecessarily strong abstraction and also increase the formation of monohydrogenated (H-C-C-H) dimers that cause the graphite phase to readily appear. It further results in the deterioration of diamond film quality. So the concentration of hydrogen in terms of numbers of atomic hydrogen per unit volume presented in the growth process should be closely monitored to ensure the quality of the deposit [28].

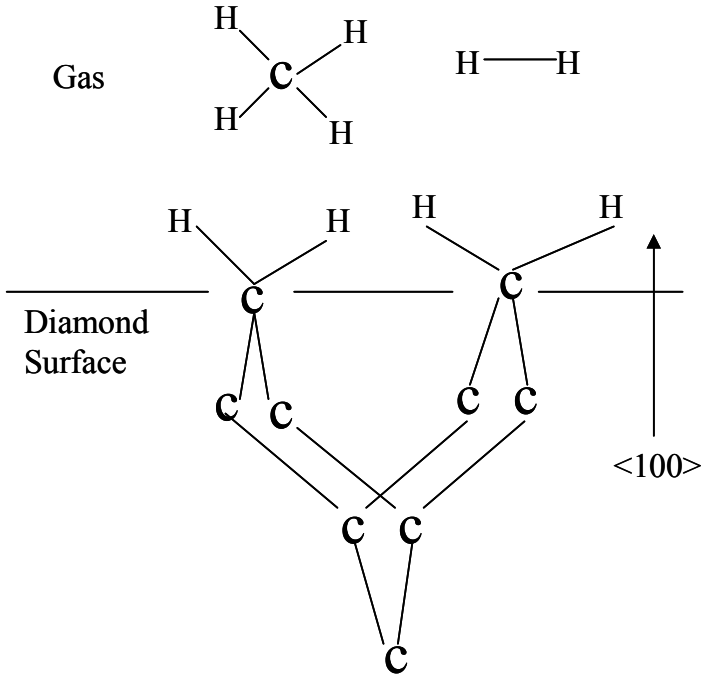
Gas
H
H
C
H
H
H—H
H
H
H
H
C
C
Diamond
Surface
C
C
C
C
C
C
<100>

(a)

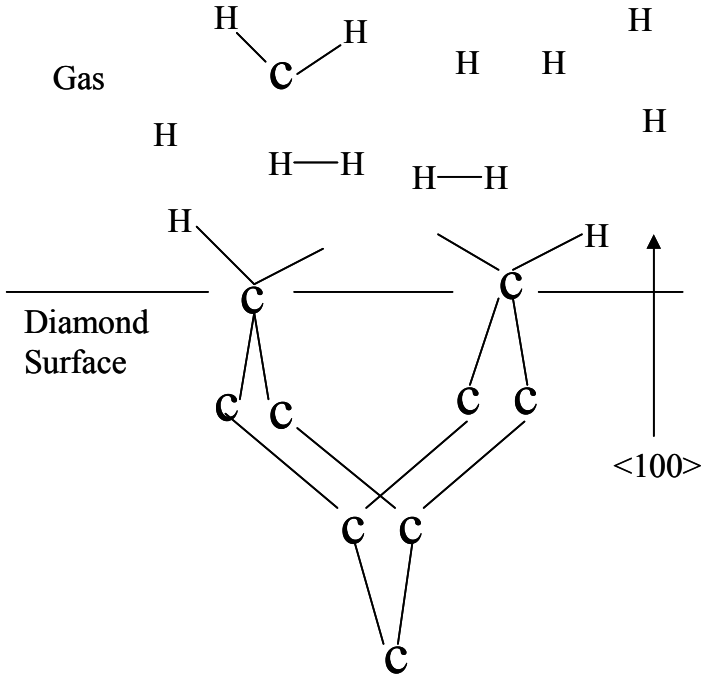
Gas
H
H
C
H
H
H
H
H
H—H
H—H
H
H
C
C
Diamond
Surface
C
C
C
C
C
C
<100>

(b)

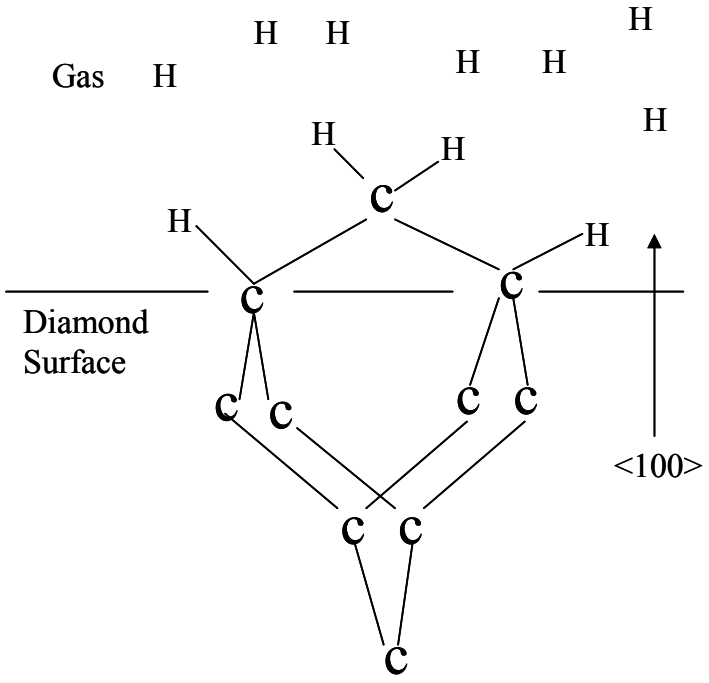

(c)

Figure 2.13: Schematic diagram of growth of diamond involving atomic hydrogen on the (100) plane. (a) Hydrogen-terminated diamond surface and the gas mixture are shown; (b) Ionization of methane and hydrogen gases: atomic hydrogen and CH_2 radicals are generated. The abstraction of surface hydrogen atoms results in two dangling bonds at the diamond surface; (c) Incorporation of a CH_2 radical into the diamond lattice is demonstrated. [112]

During CVD growth process, H^+ ions also etch graphite and other non-diamond species along with atomic hydrogen and etch even more rapidly [113, 114]. Atomic hydrogen etches, or preferentially reacts with, graphite more than 20 times faster than it etches diamond. It serves as a purification agent and removes graphite and other non-diamond species that could possibly form efficiently from the deposition sites [115]. It also stabilizes the diamond surface and maintains the sp^3 hybridization configuration [116]. The H^+ ion bombardment is usually enhanced by applying a negative bias to the substrate. Other than the presence of atomic and ionic hydrogen which contributes to the diamond growth, some scientists also employed oxygen as one of gases during diamond growth. Atomic oxygen and OH radicals are formed and perform selective etching of graphite as well as other non-diamond structures [28, 117].

2.8 Electron Field Emission of Diamond

Diamond is a wide band gap semiconductor with a gap of 5.5 eV. Electron field emission from high quality single crystal diamond is quite difficult, mainly because of its high resistivity. Electron field emission could occur more easily when it comes to polycrystalline diamond. It was reported that the emission performance varies inversely with the grain sizes [118]. The lowest turn-on electric field was found for nanocrystalline diamond films compared with other diamond films of larger grain sizes [119].

The Electron Affinity (EA) is a measure of the energy change when an electron is added to a neutral atom to form a negative ion. In the diagram shown in Figure 2.14, the electron affinity is illustrated as the energy difference from the lower edge of the conduction band in the semiconductor to the vacuum level.

A negative electron affinity (NEA) was reported for the first time in 1979 on the hydrogen terminated type IIb natural diamond (111) plane surface [35]. Since then, it was commonly recognized that hydrogenated diamond (111) surface exhibits NEA. When NEA occurs, the vacuum level is lower than the lower edge of the conduction band. In this case, the electrons injected into the conduction band of the semiconductor material are emitted to vacuum without restriction caused by any surface barrier (see Figure 2.15). Hence, a material with such a characteristic is expected to be a cold cathode material that could be driven by a low voltage.

The bare surface of diamond has an electron affinity of 0.37 eV, while the hydrogenated diamond (111) surface has an EA of -1.27 eV according to recent accurate measurements [39]. Thus the valence band lies between 5.9 and 4.2 eV below the vacuum level. The presence of other atoms, such as oxygen, could also have an effect on the electron affinity. The oxygen terminated surface has a large positive EA, about 2.6 eV, according to calculations. The changes in electron affinity arise because the C–H and C–O bonds possess dipoles which cause a surface dipole layer and a voltage step at the surface [121, 122]. The C–H bond has a positive H site and lowers the affinity, while the C–O bond has a negative O and raises the affinity [120].

Scientists have made many efforts during diamond specimens' synthesis to obtain a diamond material with low turn-on electric fields and high emission current densities. Among those attempts, the followings are the most effective: (a) Post treatment, such as plasma, could greatly increase the surface conductivity of diamond [123], and further more, surface modification of diamond films was done to achieve a negative electron affinity, or at least a low positive electron affinity [124]. (b) Local electric field can be

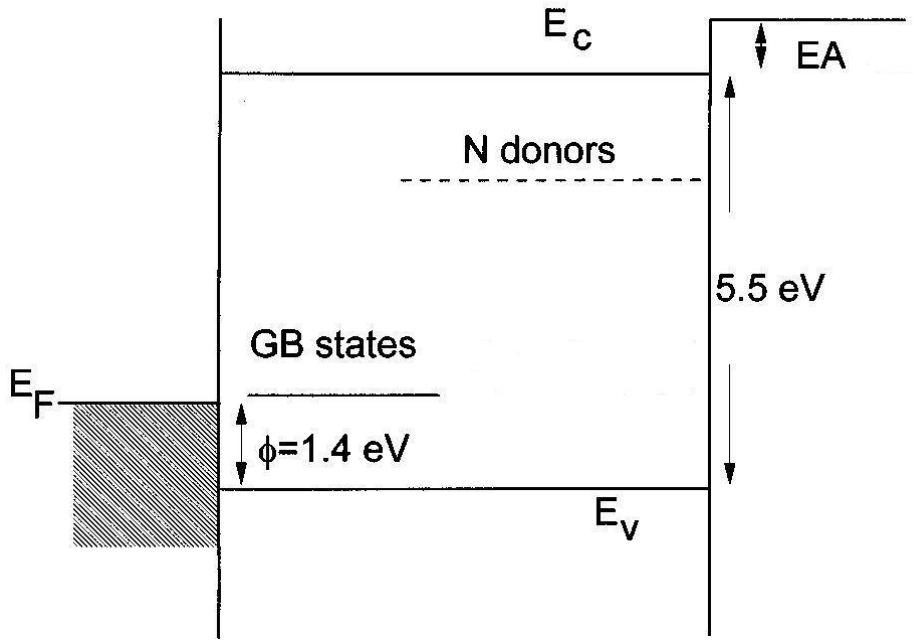

Figure 2.14: Schematic band diagram of diamond, and its defect levels (modified from [120]).

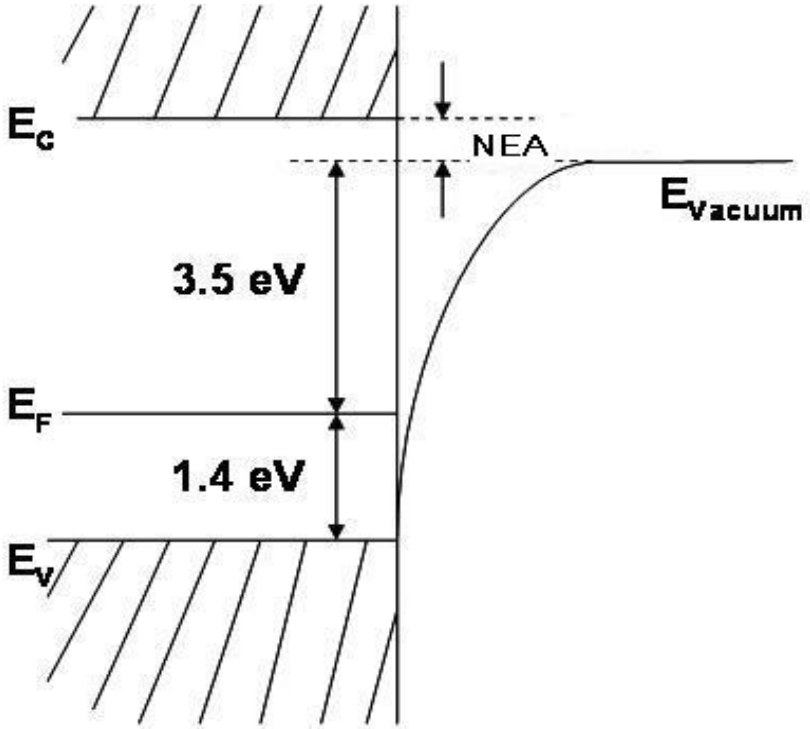

Figure 2.15: Diamond band diagram w.r.t. vacuum level without external electric field demonstrating NEA (Modified from [112]).

enhanced by fabricating diamond films with certain morphology or shapes. Thus, lower electric field could achieve a higher current density [125, 126]. (c) Defects could be induced into the diamond bulks or onto the surface of diamond films to help with electron injection through the diamond film and from the surface of diamond into vacuum [118, 127, 128]. (d) Some scientists believe that the field emission from polycrystalline and nanocrystalline diamond is dominated by the sp^2 bonding at the grain boundaries instead of the diamond sp^3 bonding. The sp^2 bonding has a work function close to graphite, 4.7 eV. The carbon dangling bonds within grains have a energy of 1.4 eV above the valence band as seen in Figure 2.14. By varying the content of sp^2 in the diamond film, a conductive path for electrons or an internal field enhancement in the diamond film is generated [129, 130].

Turning to doping of diamond, the conductivity of diamond, either the bulk or the film surface, could be significantly increased, while a higher conductivity usually suggests a better electron field emission capability. Boron is a shallow acceptor and serves as a p-type dopant while nitrogen is a deep donor and recently-found phosphorous acts as a shallow donor for n-type doping. In Figure 2.16, a comparison of threshold fields of diamonds with different dopants is shown. Among those, boron-doped diamond has a relatively high threshold field, and the field emission characteristic can be improved by phosphorous doping [131]. The figure also shows the striking result of nitrogen-doped diamond having a threshold field as low as 0.5 V/μm [132].

2.9 Diamond Classification

The following classification mainly applies to single crystal diamonds. There are

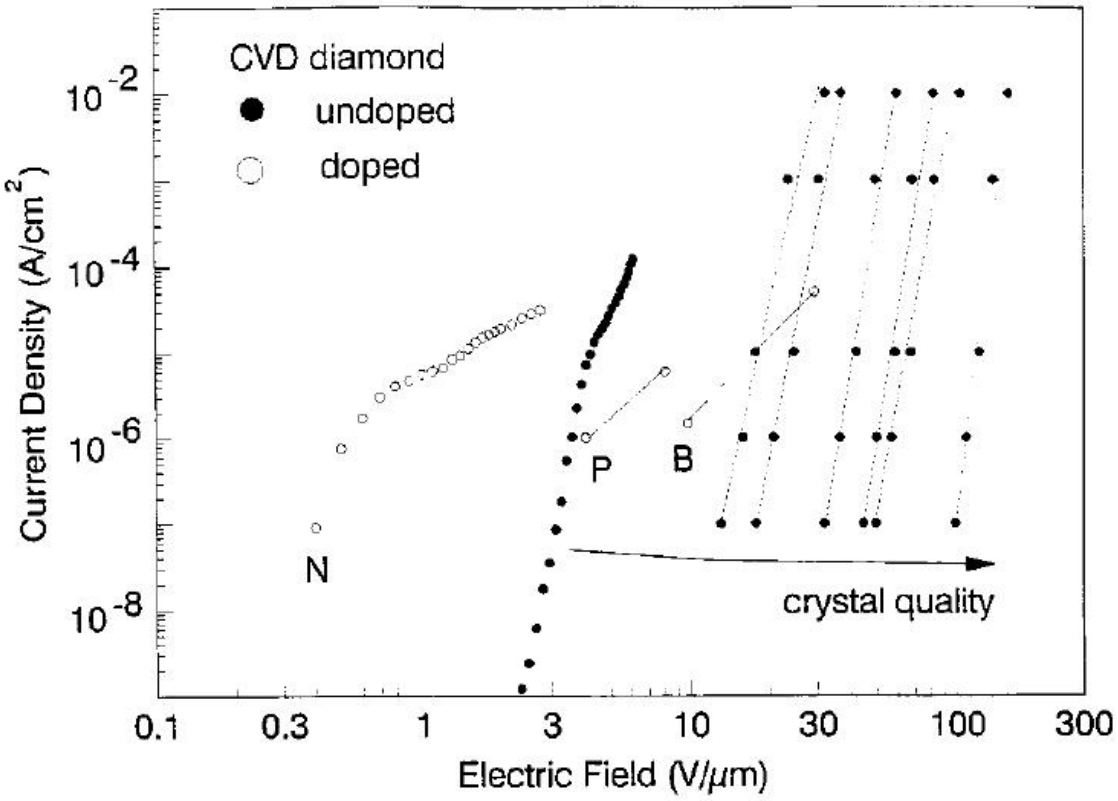

Figure 2.16: Field emission from diamonds with different dopants including boron, phosphorous, and nitrogen [120]

four known types of diamonds (Ia, Ib, IIa, IIb), classified according to the presence of nitrogen in the crystal and certain other properties. Synthetic diamonds, by HPHT or CVD methods, can also be categorized according to this scheme. However there can still be a wide variation in some properties between diamonds of the same type [3, 133, 134].

2.9.1 Type Ia Diamond

Most natural diamonds, ~99.9%, are of this type. They contain nitrogen as an impurity in a fairly substantial amount, of the order of 0.3%. The nitrogen concentrated in various aggregates in the crystal. The nitrogen gives rise to strong absorption in the ultraviolet region. This type of diamond would be colorless or have a slight tint of yellow.

2.9.2 Type Ib Diamond

This type of diamond is very rare in nature, ~1.0%. However, all synthetic diamonds are of this type. They contain nitrogen on isolated substitutional lattice sites at the concentrations up to 500 ppm. Nitrogen produces paramagnetic resonance in this form.

The highest hydrogen concentration was recorded by a type Ib crystal among type Ia, Ib, and IIa specimens, and those all have ~1 at. % of hydrogen contrary to the infrared evidence [135]. The initially type Ib diamonds are considered to have changed to type Ia after many years in a HPHT environment, in which the nitrogen diffused and coalesced into aggregates.

These diamonds absorb green light as well as blue light, and have a darker color than type 1a diamonds. Depending on the precise concentration and spread of the nitrogen atoms, these diamonds can appear deep yellow, orange, brown, or greenish.

2.9.3 Type IIa Diamond

This type is also very rare in nature. This type of diamond has insufficient nitrogen to be easily detected by infrared or ultraviolet absorption measurements. This type of diamond could be synthesized for industrial purposes.

An imperfect carbon lattice will make the diamond absorb some light, which will give it a yellow, brown, even pink or red color.

2.9.4 Type IIb Diamond

Extremely rare in nature as these diamonds contains even lower concentration of nitrogen than type IIa crystals that some of the boron acceptors are not compensated causing the crystals to act as a p-type semiconductor. This type of diamond would appear gray or blue in color. Synthetic diamond can be purposely manufactured by incorporating boron and excluding nitrogen for desired applications.

2.9.5 Mixed

Some diamonds consisting of several different types in one stone are sometimes seen.

CHAPTER 3

SINGLE CRYSTAL CVD DIAMOND GROWTH

3.1 Introduction

Since the discovery of the synthetic diamond using chemical vapor deposition (CVD) methods, the new technique has been studied extensively and created a large number of potential applications [9]. A variety of CVD techniques have been developed and studied due to the high demand of industry while microwave plasma enhance CVD being the most common method currently used due to its easiness for precise control during the deposition process. One of the advantages of CVD diamonds over HPHT diamonds is that diamond single crystals created by CVD techniques could be much larger in size than that created by traditional HPHT process, and the properties of which can also be in-situ controlled by varying the combinations of gas compositions and working pressures and introduction of desired impurities, or further modified by post-deposition treatments, such as plasma treatments, in order to meet the requirements of desired applications.

Large diamond single crystals not only can be applied as fine jewelry, but also can make more applications possible both in scientific research and industry. It was reported that CVD techniques for homoepitaxially growth of high-quality single crystals of diamond could be achieved at a very high growth rate [74] and significantly reduced the deposition time needed. The following cutting and polishing processes revealed that these single crystals had very high fracture toughness in some cases. After annealing, this

material was ultrahard having Vickers hardness values beyond those of annealed and unannealed natural diamonds [75] and suitable for being the material used for next generation high-pressure devices, cutting tools, and optical windows in harsh environments..

This study is to produce large diamond single crystals with a good quality and high growth rate as diamond anvils for geophysical high pressure research. Schematic of a current “panoramic” cell is shown in Figure 3.1 [136] while large crystals could enhance the sample volume at the diamond tips, and the work was presented in Joint Applied Diamond Conference and Nano Carbons 2005 [137, 138].

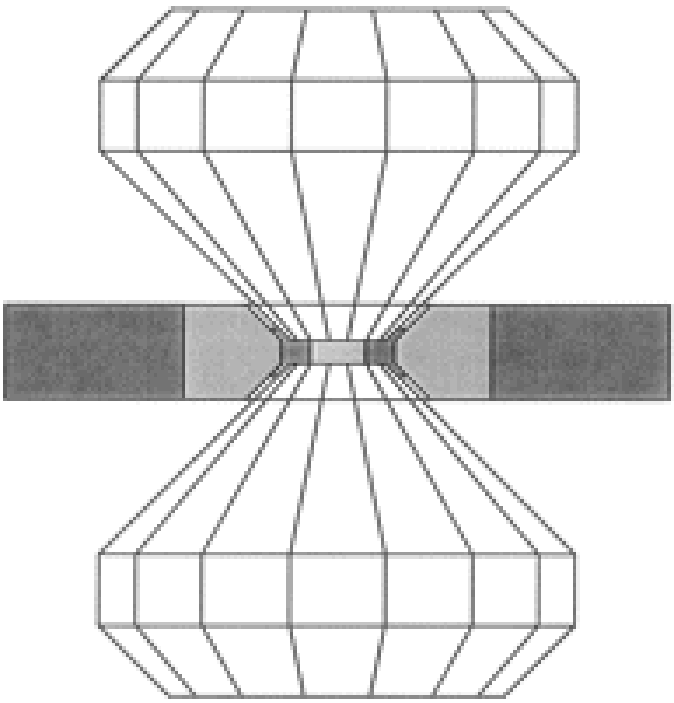

Figure 3.1: Schematic of a “panoramic” cell for high pressure research [136].

3.2 Experimental Details

Commercially available HPHT diamond single crystal plates, type Ib {100}, with a typical size of 4 × 4 × 1.5 mm^3 were used as seed substrates for homoepitaxial growth of CVD diamond single crystals. The seed crystal was first cleaned by merging into acetone and methanol sequentially during the ultrasonication treatment for 30 min to remove possible fluid residue from factory polishing and then fixed onto a custom-designed substrate holder made of molybdenum with cooling water flowing inside in order to maintain a constant temperature within the desired temperature range during deposition process. SEKI chamber, AX5400, was employed for this microwave plasma enhanced chemical vapor deposition process. The system was designed to have waveguides introducing microwave power into the chamber from the top. Two customized windows on two different sides of the chamber allowed the dual-infrared pyrometer to monitor the temperature of the substrate surface in real time and also granted the users the ability to visually observe the surface morphology of the deposit while the growth process was being carried out. The deposition process would be stopped immediately when a defect, such as formation of twinning defect or polycrystalline diamond, was visually observed to prevent defective structures from further spreading. Mechanical polishing sometimes was required to remove defects, and the specimen will be subjected to further growth after carefully inspections after a cleaning process was performed.

The percentage of each gas in the gas mixture was to be as follows: N_2 / CH_4 = 0.2% - 5.0% and CH_4 / H_2 = 12% - 20%. The hydrogen remained as a high portion of the gas mixture, while nitrogen was added to enhance the {100} face growth. The working pressure was varied between 120 Torr and 220 Torr, a relatively higher working pressure

compared to other groups to promote higher growth rate. The substrate temperature was carefully kept at 900°C - 1500°C [138]. When the working pressure increased, the growth rate also increased but with a potential increasing possibility of occurrence of defects. Temperature is one of the most critical factors during the growth process. When the temperature fell outside of the optimal range, either graphite or polycrystalline diamond would be deposited.

3.3 As-Grown Crystal

The growth was done on the {100} face surface of the seed substrate where the highest growth rate could be achieved with the addition of nitrogen. Although the addition of nitrogen promotes a higher growth rate, the crystals grown with nitrogen present usually have a yellowish color. The color of a crystal could become more colorless when the percentage of nitrogen decreases. A small amount of oxygen helps refine the diamond quality by removing non-diamond structures. One of the as-grown diamond single crystals with the seed crystal still remaining at the bottom is shown in Figure 3.2(a). Before any mechanical polishing was applied, the surfaces were smooth and showed typical morphology of step flow, which is commonly seen on CVD diamond single crystal surface. The crystal was measured to have a size of approximately $5 \times 5 \times 2.7$ mm^3 with the original seed substrate, $4 \times 4 \times 1.5$ mm^3, underneath after 12 hours of continuous growth. The growth rate was suggested to be 100μm/hr. Figure 3.2(b) shows the side view of the crystal. Some polycrystalline diamond deposit was observed on the sidewall of the as-grown crystal. The polycrystalline diamond deposit occurred due to the non-uniform distribution of plasma that causes the temperature differences among the

regions while the CVD layer grew thicker. The growth was the most rapid in the <100> direction, and the deposit actually had a larger surface area than the seed substrate itself, extended out in all four <100> sides horizontally. The crystal appeared clear, near colorless, and still transparent without any visible defects. This result indicates that while all the growth parameters are carefully controlled, quality diamond single crystals grown by CVD could be obtained.

3.4 SEM and Rocking Curve Measurement

Image by Scanning Electron Microscope (SEM) is shown in Figure 3.3. Typical stacking morphology, step flow, of single crystal CVD diamond was observed with a uniform distribution all across the surface, which indicated a preciously controlled growth condition. No surface defects, such as twinning or polycrystalline diamond formation, were detected.

Rocking curve measurements were applied on both the HPHT seed and the CVD crystal after the CVD growth process to inspect the deposit quality. One of {100} faces of each of HPHT and CVD crystals was carefully mapped.

The HPHT seed substrate exhibited an excellent and uniform crystalline quality across the crystal surface, which was expected, and had a full width at half maximum (FWHM) of 0.005 (Figure 3.4). Although the mapping of CVD crystal revealed the existence of local point defects, which was not visually noticeable, the crystal still showed a FWHM of 0.006 (Figure 3.5). The results suggested that the quality of CVD diamond was very similar to that of the HPHT diamond seed even it was grown rapidly.

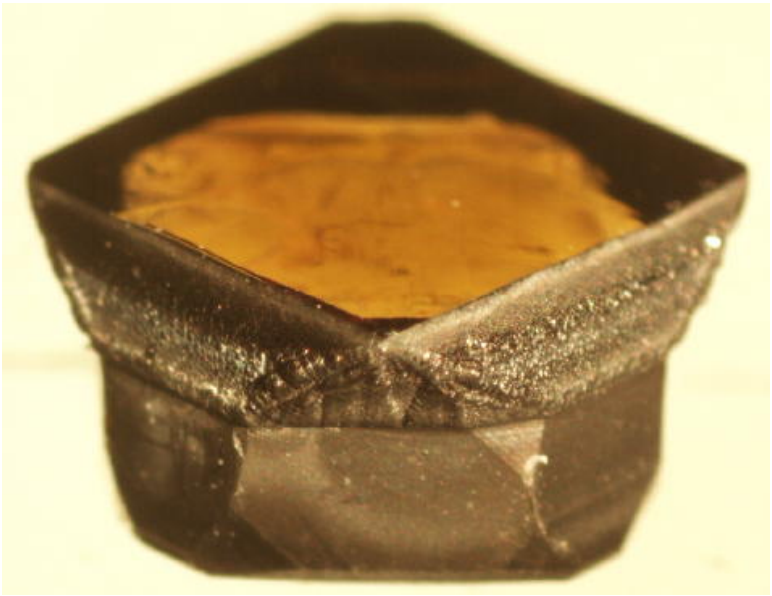

(a)

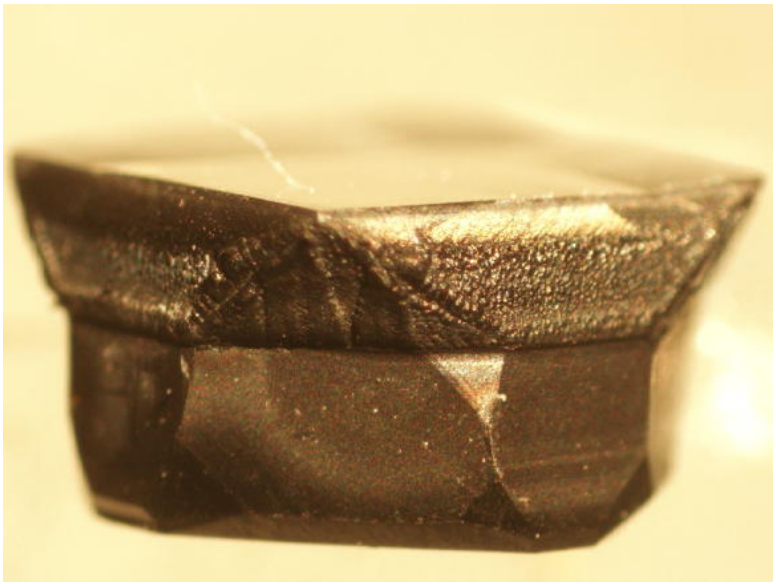

(b)

Figure 3.2: (a) As-grown diamond single crystal with the HPHT synthetic diamond seed still attached. The crystal was measured to have a size of approximately $5 \times 5 \times 2.7$ mm^3 with the original seed substrate, $4 \times 4 \times 1.5$ mm^3, underneath; (b) Side view of the crystal. Some polycrystalline diamond deposit with small grain size was observed.

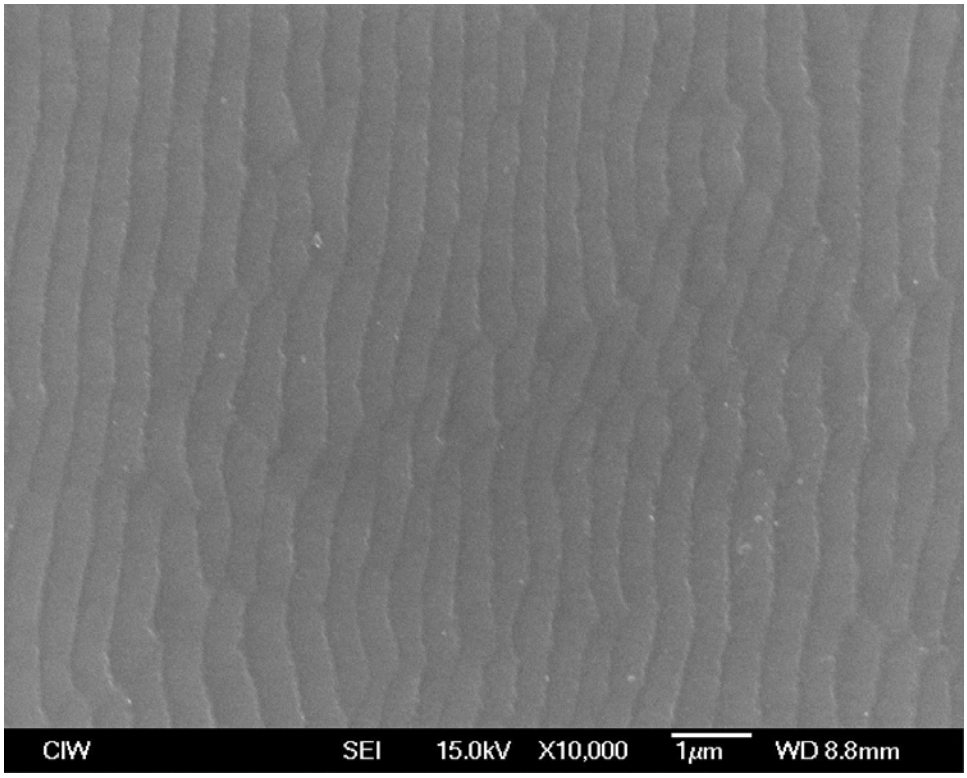

Figure 3.3: SEM image of surface morphology of as-grown CVD diamond shown previously.

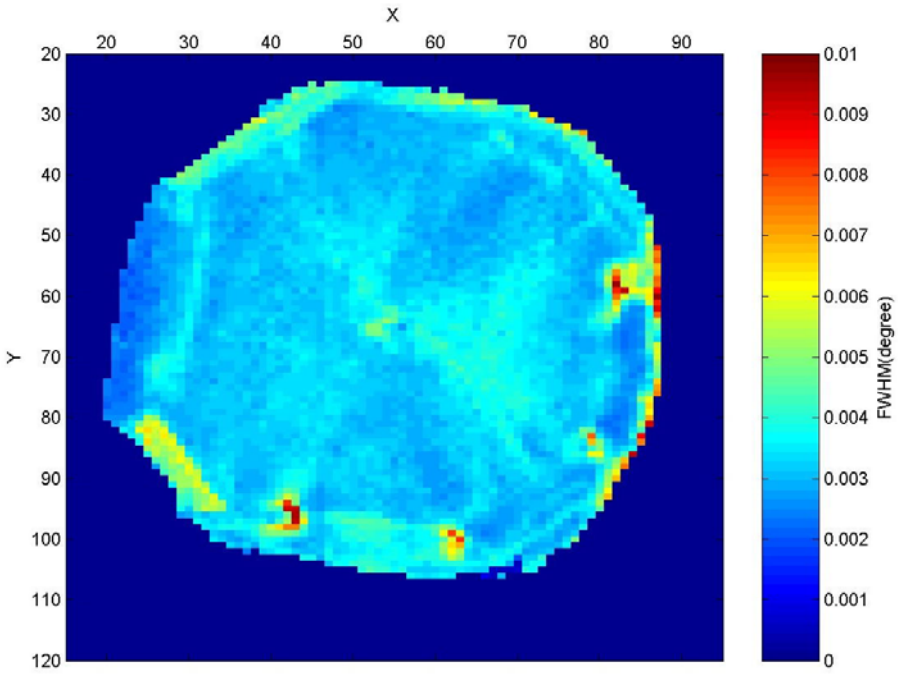

(a)

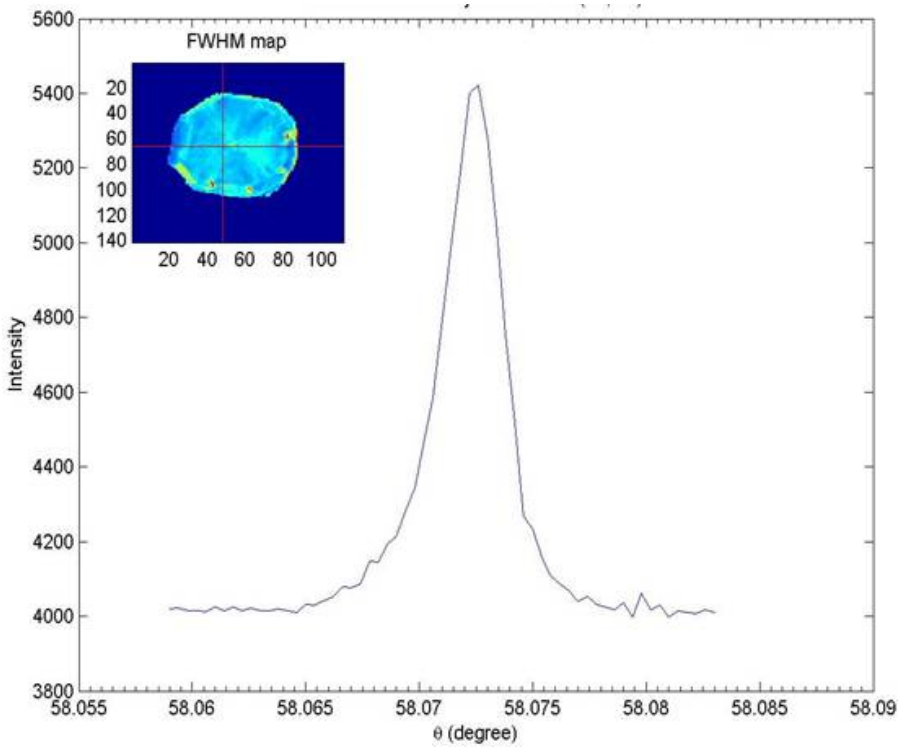

(b)

Figure 3.4: (a) Full surface mapping of HPHT seed crystal; (b) the rocking curve shows a FWHM of 0.005.

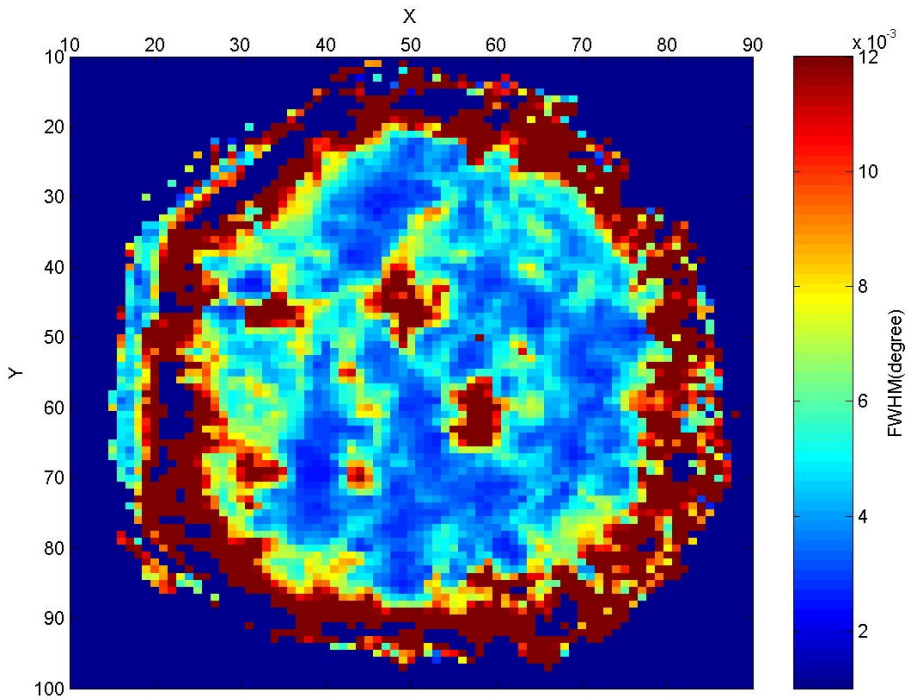

(a)

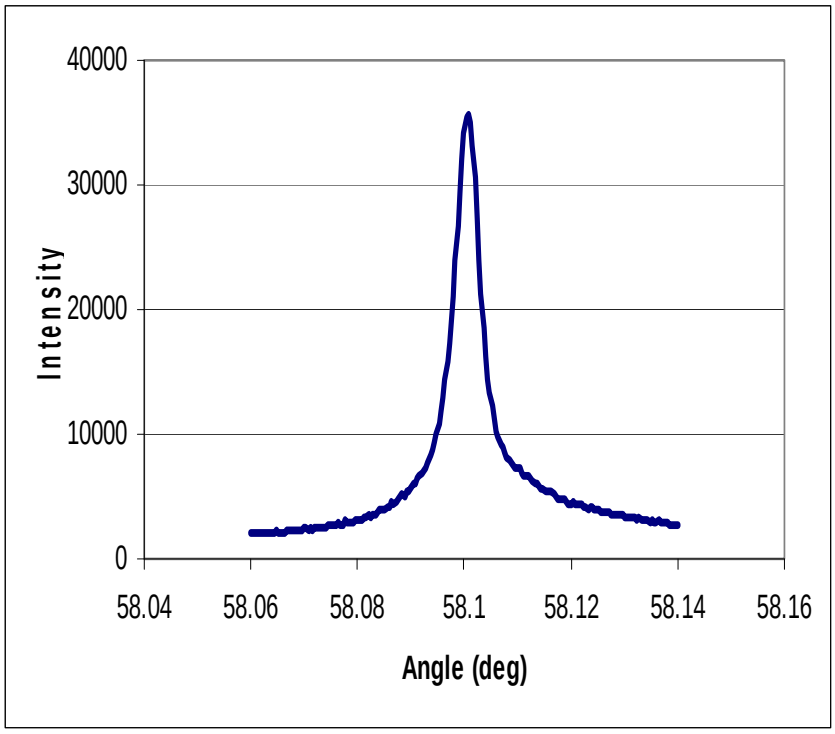

(b)

Figure 3.5: (a) Full surface mapping of CVD crystal; (b) the rocking curve shows a FWHM of 0.006.

3.5 CVD Diamond Optical Window

When the growth time was shortened, the quality of CVD films could reach the highest as the possibility for defects to occur being minimized. After removing the seed substrate by laser cutting and mechanical polishing, the CVD film could be employed as optical windows for many instruments. A CVD single crystal diamond window is shown on the left of Figure 3.6. The HPHT seed substrate was removed after CVD process. Both sides of the CVD crystal were carefully polished to a mirror-like surface.

The growth time was 5 hours and the size was measured to be $5 \times 5 \times 0.5$ mm^3 approximately [136]. Please note that the darker color of the edges was caused by polycrystalline diamond deposit that had not been previously removed. On the right hand side of the figure, a high quality natural IIA diamond window, $1.5 \times 1.5 \times 0.25$ mm^3, is shown. The suggested retail price for which was in the range of hundreds of dollars. Larger diamond windows will certainly increase the suitability for more applications. And the cost of this technique was estimated to be within the same range as the high quality natural IIA diamond, while it was almost 18 times in size.

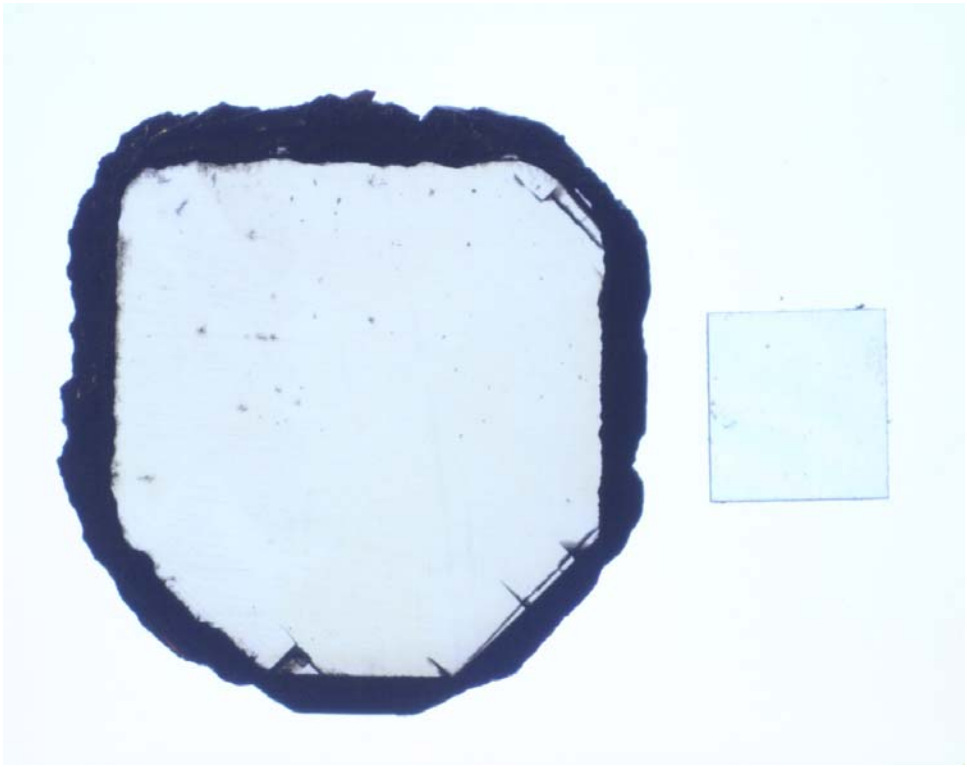

Figure 3.6: **Left**: CVD film only, HPHT seed substrate was removed. The growth time was 5 hours and the size was measured to be $5 \times 5 \times 0.5$ mm^3 [136]; **Right**: a high quality natural IIA diamond window, $1.5 \times 1.5 \times 0.25$ mm^3.

3.6 Diamond Anvils

A CVD diamond crystal being shaped as anvils is shown in Figure 3.7. The as-grown crystal originally had a larger size containing both the CVD diamond and defects. After all the defects had been removed by professional polishing, it has a height of 3.47 mm and a diameter of 5 mm at the bottom. It was estimated by weight to be 0.59 carat. The color of the CVD crystal could become more colorless by reducing the nitrogen concentration in the gas mixture that was used to promote faster growth during the CVD process. Again, the principle goal of this project was to generate large diamond single crystals for high-pressure geophysical research. Thus, the larger the tip of the anvil is, the more materials, thicker sample loads, could be applied and more studies on materials' behaviors under extremely high pressure and high temperature could be achieved without sacrificing the versatility of conventional diamond anvil cells. This crystal demonstrated the success of producing large diamond single crystal anvils by CVD techniques.

3.7 CVD Diamond Film as Substrate for CVD Growth

Since the CVD diamond film showed very similar quality and properties to the HPHT seed crystal, it then was employed as a CVD seed crystal for further CVD growth. As predicted, there was a limitation of the surface area of commercially available HPHT diamond crystals. Thus the CVD diamond surface area grown on HPHT seed substrate was also restrained. Portion A of the crystal in the Figure 3.8(a) was the original HPHT seed, and the first CVD growth was done to obtain the portion B of the CVD layer. Then the whole crystal was mechanically polished on one of the {100} faces by a diamond

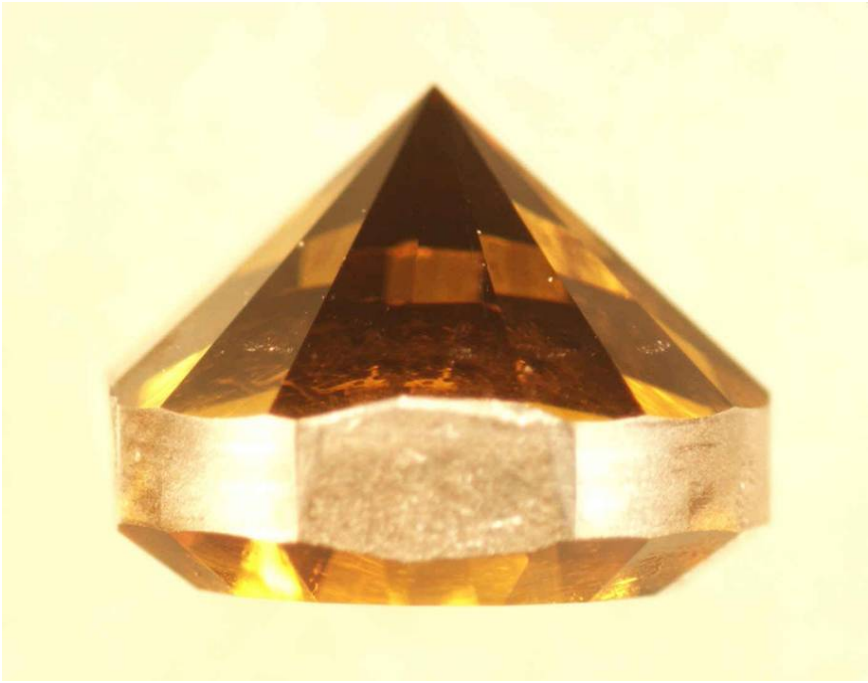

Figure 3.7: A CVD diamond crystal being shaped as anvils; the crystal had a height of 3.47mm and a diameter of 5mm. It was estimated to be 0.59 carat.

grinding wheel with diamond powder sprinkled onto the surface to rid of the polycrystalline diamond and possible defects located on the sides. The second CVD growth was done on the polished surface and the deposit was marked as portion C and D with portion C being the CVD growth on the original HPHT seed and D being the CVD growth on the first CVD layer. Portion B and portion C were expected to have very similar qualities.

Raman spectrum obtained (Figure 3.8(b)) showed that all four areas had sharp diamond peaks located at 1332 cm^{-1}. It also reveals that the diamond layers on the portions B, C, and D had pretty similar quality as the HPHT seed crystal while all CVD layers tended to have higher internal stress as the Raman curve slopes of those within the higher Raman shift region increased. No signature of sp^2 bonding was observed.

This growth technique truly increases the possibility of large size, ideally in the 100-carat range, of diamond single crystal grown by chemical vapor deposition techniques. The three-dimensional growth showed promising results and was patented by Carnegie Institution of Washington.

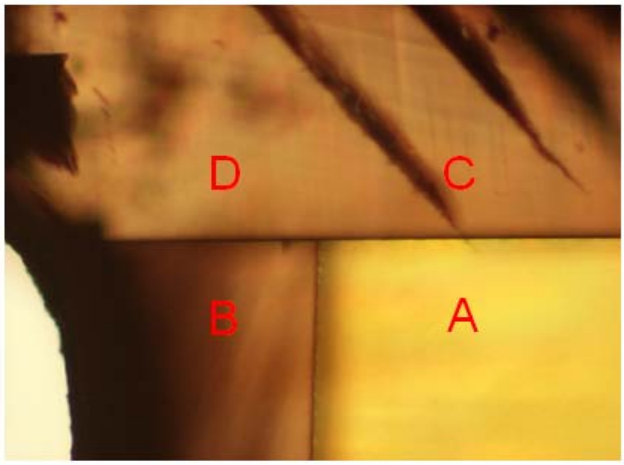

(a)

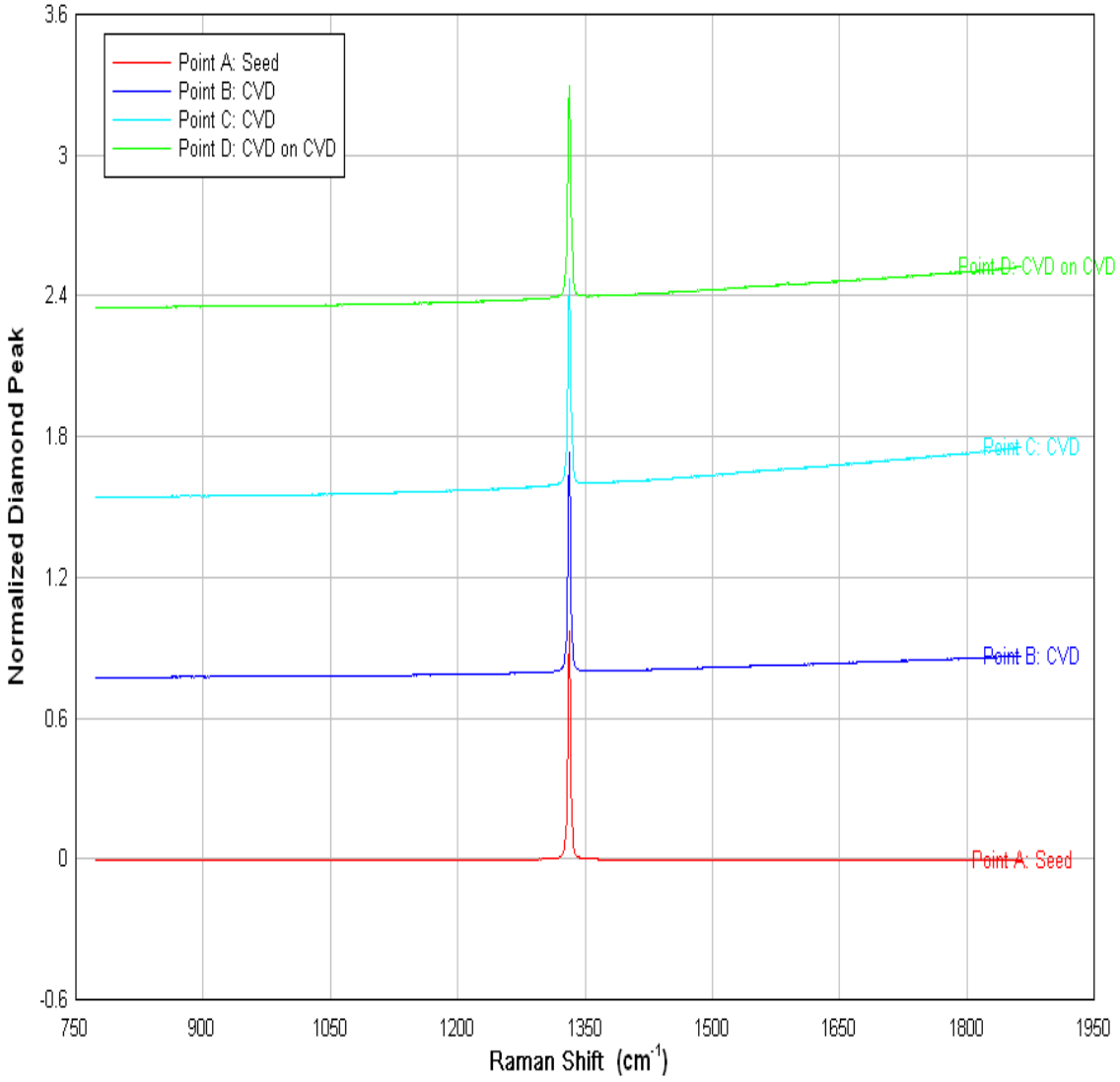

(b)

Figure 3.8: (a) Crystal A was the original HPHT seed, and the first CVD growth was done to obtain the CVD layer B. The second CVD growth was marked as C and D with C being the CVD growth on the original HPHT seed and D being the CVD growth on the first CVD layer; (b) Raman spectrum obtained showed that all four areas had sharp diamond peaks located at 1332 cm^{-1}.

3.8 Conclusion

Large CVD diamond single crystals were produced for new classes of high pressure devices, and more materials can be applied to the tips of the diamond anvils for further analysis under high pressure and high temperature environments, e.g. 200GPa, due to the large crystals in size. While mechanically polishing the crystals, it revealed that these CVD diamond single crystals actually had higher hardness and toughness than natural and HPHT diamonds. That makes these CVD diamonds become a potential candidate for high-precision cutting tools and drilling bits. While high thermal conductivity and low coefficient of thermal expansion being two of the advantages of diamond materials on electronic applications, large diamond bulks would out-perform diamond thin films.

By increasing the surface area of deposition by mosaic arrangement of array of HPHT diamond seeds in the initial run and cooperating with the rapid CVD growth method, large CVD diamond single crystals can be obtained. And the CVD layer could repeatedly serve as the seed substrate, and that will truly make many CVD diamond dreams come true.

This research was supported by the National Science Foundation, the U.S. Department of Energy through the Carnegie/DOE Alliance Center (CDAC), the W.M. Keck Foundation, and the G. Unger Vetlesen Foundation.

CHAPTER 4

CHEMICALLY VAPOR DEPOSITED DIAMOND-TIPPED ONE-DIMENSIONAL NANOSTRUCTURES AND NANODIAMOND-SILICA-NANOTUBE COMPOSITES

4.1 Introduction

Diamond's outstanding physical and chemical properties when combined with one-dimensional nanostructures may lead to hybrid nanodevices with excellent and unique functions and performance. For example, the widely used atomic force microprobe (AFM) will have much improved durability and precision when diamond AFM probes are used. When a wear resistant super-hard diamond tip is supported by a non-diamond nanorod or nanotube, the hybrid device provides scientists even broader options of probe functions and capabilities. Unique optical, electronic, chemical, and biological properties of diamond coupled with the excellent wear resistance and hardness and a wide variety of supporting nanorods or nanotubes are, therefore, highly desirable and may open up new dimensions for nanodevices based on 1-D nanostructures.

Chemical vapor deposition of diamond from carbon containing gases and compounds in the presence of atomic hydrogen has been making consistent progresses in the past twenty-some years [139 - 141]. Various energy sources including hot metal surfaces, electrical discharges, combustion flames, and laser excitation have been applied to assist in the chemical vapor deposition (CVD) of diamond on diamond seeds or nuclei

[142, 143]. Atomic hydrogen of various amounts in different CVD environments was found critical to preferentially depositing diamond phase of carbon. By enhancing the bombardment of substrates by hydrocarbon ions via a negative bias to the substrate with respect to a plasma, diamond nuclei can also be created without needing pre-synthesized diamond seeds. On the other hand, pre-synthesized diamond seeds can be placed onto selected surfaces on which further diamond growth is to be carried out. These diamond seeds can be micro-nanodiamond debris created by abrasive polishing or ultra-sonic agitation induced impact by diamond particles on substrates. Diamond particles of nanometers or tens of nanometers in sizes that are usually synthesized by means of explosive techniques followed by purification processes are also often applied by various means to adhere to substrate surfaces and serve as diamond seeds for further CVD growth of diamond. In this work, microwave plasma assisted chemical vapor deposition (MPCVD) is applied to grow diamond on diamond seeds of nanometers to tens of nanometers in sizes that are selectively adhered to the opening ends of silica nanotubes to form one-dimensional nanostructures with diamond tips. This work was presented in the 2nd International Conference on New Diamond and Nano Carbons (NDNC 2008) by author and published in the technical journal, Diamond and Related Materials [144].

4.2 Synthesis of Diamond-Tipped Nanostructures

Silica nanotubes ranging from tens of nanometers up to 140 nm in diameter and several micro-meters in length were synthesized in-house by Dr. Yeh at National Cheng-Kung University, Taiwan, and used for fabricating diamond-silica nanotube composites with diamond-tipped one-dimensional nanostructures. Detailed process for

synthesizing the silica nanotubes will appear elsewhere. Silica nanotubes of 2 mg by weight were mixed with 1 mL of distilled water. The solution was ultra-sonicated to keep silica nanotubes in a uniform suspension. Solutions that contained diamond nanoparticles of an average of 10 nm and 30 nm in size, respectively, in methanol were mixed with the silica nanotube containing solution. The mixed solutions were then ultra-sonicated for 30 min before being applied onto various substrates such as silicon, silicon dioxide at a substrate temperature of 90 °C.

Chemical vapor deposition processes for both nanocrystalline and polycrystalline diamond were applied to grow diamond on top of the diamond seeds. When the nanodiamond process was employed, a gas mixture of 1% CH_4 + 2% H_2 + 97% Ar was used while the microwave power was kept at 800 W with the gas pressure kept at 150 Torr during the growth process [145]. For the crystalline diamond deposition process, a gas mixture of 1.5% CH_4 diluted in 98.5% H_2 was used while the microwave power was kept at 1100 W with the gas pressure kept at 45 Torr throughout the whole process [146]. The growth temperature for the nanodiamond process was measured with a dual-color optical pyrometer to be approximately 600 °C, while the substrate temperature for polycrystalline diamond growth was set at approximately 700 °C. When the concentration of nanodiamond seeds that were applied to the substrate surface was high, a diamond-silica composite film was synthesized. When the concentration of nanodiamond seeds was low, individual silica nanotubes with their openings capped with diamond crystals were fabricated. After diamond deposition, samples were subjected to wet chemical etching using hydrofluoric acid solutions to etch away exposed silica nanotubes. The diamond-silica composite film became a free-standing porous diamond film with a

network of one-dimensional channels which were previously occupied by silica nanotubes. Optimized process for synthesizing porous diamond films and their properties will be reported elsewhere. In this chapter, the focus is placed on the fabrication of one-dimensional nanostructures with diamond tips and the characterization of the structures.

4.3 Polycrystalline-Diamond-Capped Silica Nanotubes

Shown in Figure 4.1 is a diamond crystal that was grown at one of the opening ends of a silica nanotube. Diamond nanoparticles of 10 nm suspending in methanol was used to place diamond seeds at the opening of silica nanotubes. Standard polycrystalline diamond growth conditions stated previously were applied to grow diamond onto the diamond seed. A well-faceted diamond crystal can be seen to cap one end of the nanotube to form a diamond-tipped nanotube. Nanodiamond particles tended to adhere more easily at the openings of the silica nanotubes than on the sidewalls likely due to mechanical lock-in effect of diamond nanoparticles by the silica nanotube openings. The small radius of curvature of the sidewall of the silica nanotube makes the effective contact area between a chemically inert diamond nanoparticle small. The curved sidewalls, therefore, allowed poor adhesion with diamond nanoparticles, especially those with well-faceted surfaces of larger sizes. The microwave plasma CVD growth increased the size of the diamond seeds and caused the tube openings to be capped. Diamond growth under the conditions intended for the growth of nanodiamond as stated previously also resulted in similar results as shown in Figure 4.2.

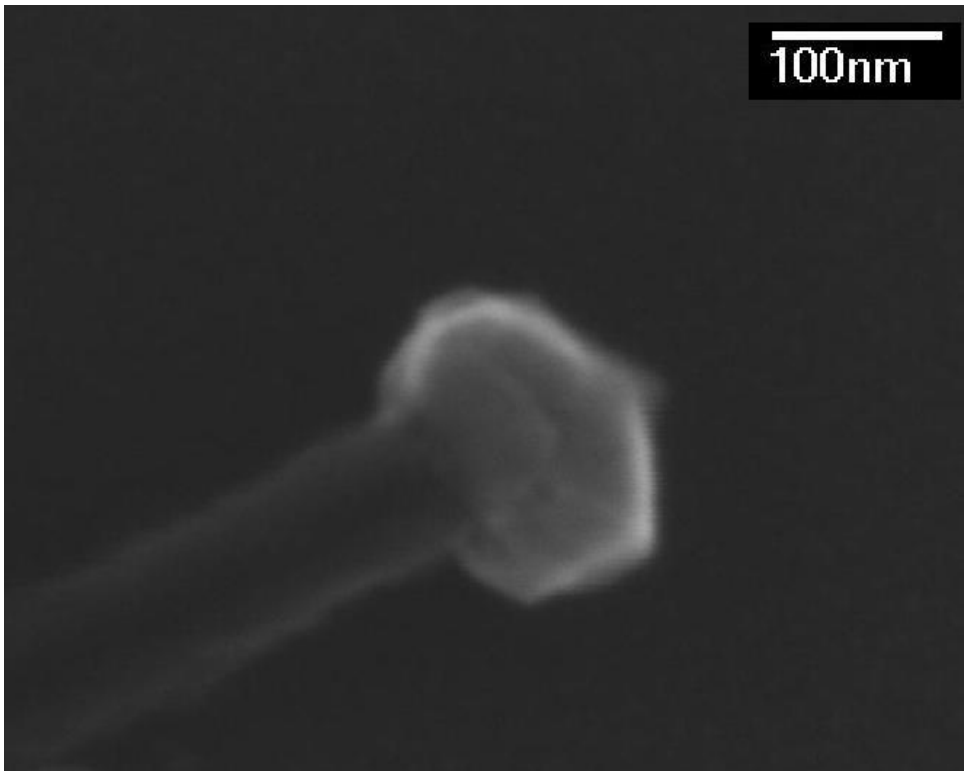

Figure 4.1: A silica nanotube with a diamond crystal capping one of the tube openings.

For the solution containing nanodiamond particles with an average of 10 nm in size, the distribution of diamond sizes was broad and contained both larger diamond clusters as well as smaller diamond nanoparticles. Diamond nanoparticles which were smaller than the radius of curvature of the silica nanotubes and those without well-faceted surfaces could more possibly adhere to the side walls of the silica nanotubes. Diamond crystals grown on sidewalls of silica nanotubes were also observed. Some smaller diamond nanoparticles could even enter the interior of the silica nanotubes. More detailed characterization of the growth process in confined space and the synthesized carbon phases inside silica nanotubes will be reported in a separate paper.

4.4 Nanocrystalline-Diamond-Capped Silica Nanotubes

Another solution containing a more uniformly distributed and suspended diamond nanoparticles of 30 nm in size was also prepared. A similar process was applied to place diamond seeds onto silica nanotubes. As expected, silica nanotubes capped with diamond were fabricated easily with little growth of diamond on sidewalls of silica nanotubes. As shown in Figure 4.2, multiple-diamond-capped silica nanotubes were seen close to each other without diamond growth on side walls of silica nanotubes. This applies to growth conditions for both nanodiamond and crystalline diamonds. The SEM photo shown in Figure 4.2 was taken from a specimen grown under nanocrystalline diamond growth conditions. As it can be seen from the diamond at the ends of silica nanotubes, these diamonds are less facetted than what is shown in Figure 4.1.

As stated in the standard processes for fabricating one-dimensional nanostructures with diamond tips, the solution that was applied to a substrate contained both

diamond-seeded silica nanotubes as well as diamond nanoparticles in suspension. When the concentration of diamond nanoparticles is adequately high, a continuous diamond film was grown to cover the silica nanotubes and the surface of the substrate. Most silica nanotubes are embedded inside the diamond film. In areas where the concentration of suspending diamond nanoparticles was low, only silica nanotubes with diamond tips could be seen as shown in Figure 4.2.

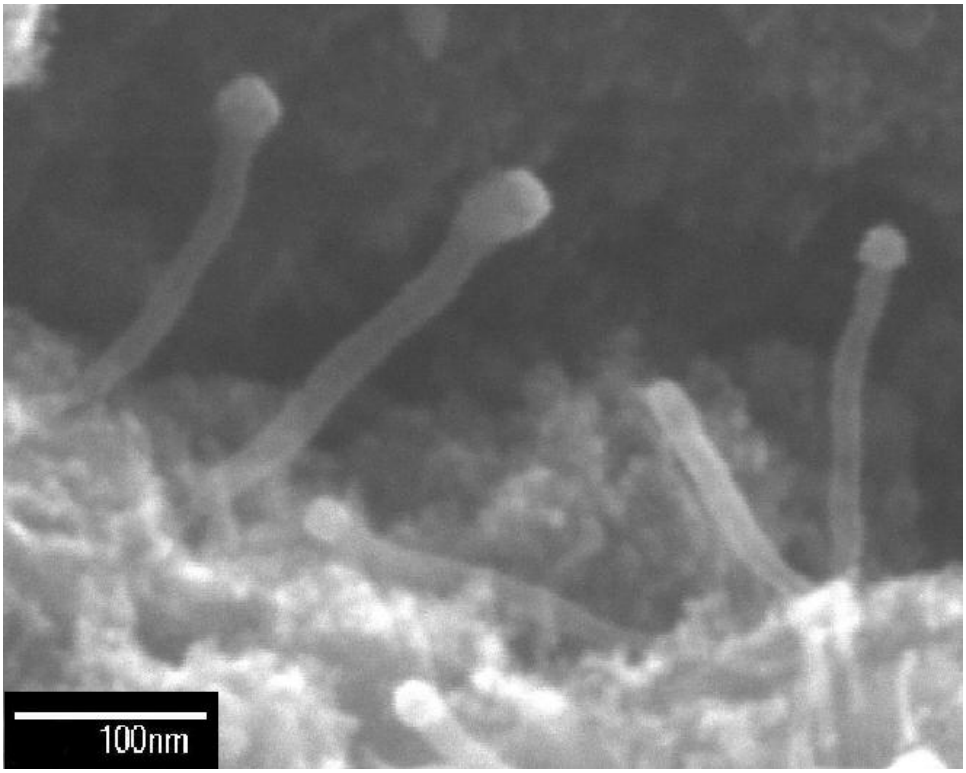

Figure 4.2: One-dimensional nanostructures formed by growing nanodiamond on diamond-seeded silica nanotubes.

4.5 Raman Spectroscopy of Nanodiamond-Silica Composite

Raman spectra were taken to analyze the synthesized nanodiamond-silica composite. One of the spectra for nanodiamond deposition is shown in Figure 4.3. The peak located at 1331 cm^{-1} is a signature of diamond crystal. The broad band around 1500 cm^{-1} that accompanies the 1150 cm^{-1} peak and often appears as the shoulder of the G mode is believed to be caused by disordered sp^3 carbon or transpolyacetylene [147 - 151]. The diamond peak appears sharper when the deposition time increases.

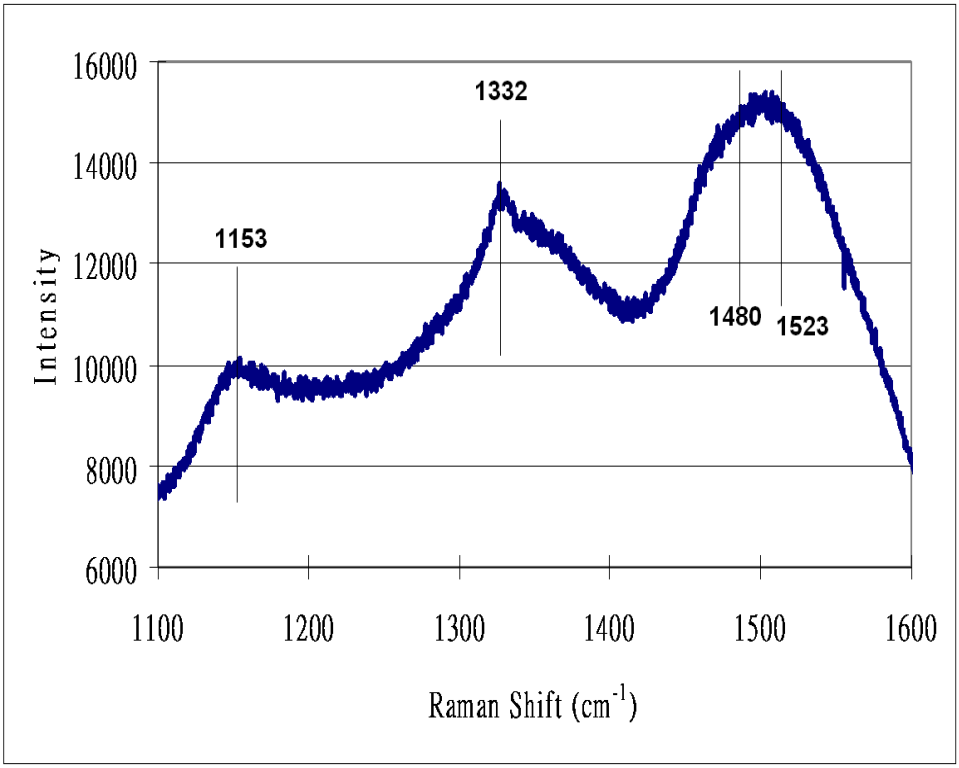

Figure 4.3: Raman spectrum taken from the samples shown in Figure 4.2, which was grown under standard nanodiamond deposition conditions

4.6 Wet Chemical Etching of Nanodiamond-Silica Composite and EDX Study

Nanodiamond-silica composite samples were chemically etched using hydrofluoric acid solution in order to dissolve exposed silica nanotubes. After the etching process, diamond capped nanotubes shown in Figure 4.2 were no longer found. Instead, needle-like nanostructures could be seen in areas where the concentration of nanodiamond seeds was low as shown in Figure 4.4. Holes could also be clearly seen scattering around the surface of the nanodiamond-silica composite film indicating that embedded silica nanotubes were etched away by the hydrofluoric acid solution. Energy dispersive X-ray (EDX) analysis was applied to analyze the diamond-silica composite film before and after etching by hydrofluoric acid. The percentage of silicon content by weight in the diamond film decreased from typically more than 18% before etching to less than 10% after. The percentage of carbon content by weight increased from originally less than 68% to 90%.Apparently, many silica nanotubes originally detectable by EDX have been etched away as expected. Some unexposed silica nanotubes were protected by the chemically inert diamond and remained intact from the wet chemical etching process.

Unlike diamond capped nanotubes shown in the Figure 1 and Figure 2, needle-like nanostructures formed after wet chemical etching did not appear like previously described nanotubes with diamond tips but instead are sharp needles with base diameter of about 20 - 30 nm that are consistent with the diameter of a number of silica nanotubes. Since silica should be etched away by hydrofluoric acid, what was left over as seen in Figure 4.4 is most likely diamond, non-diamond carbon phase, or silicon carbide originally grown inside silica nanotubes. Although the EDX used has a focus spot of 5 -

10 nm in diameter, background noise caused by the electron scattering after it hits the the specimen could have an as high as 100% reading for the content of carbon. The signal coming from silicon substrate has been eclipsed.

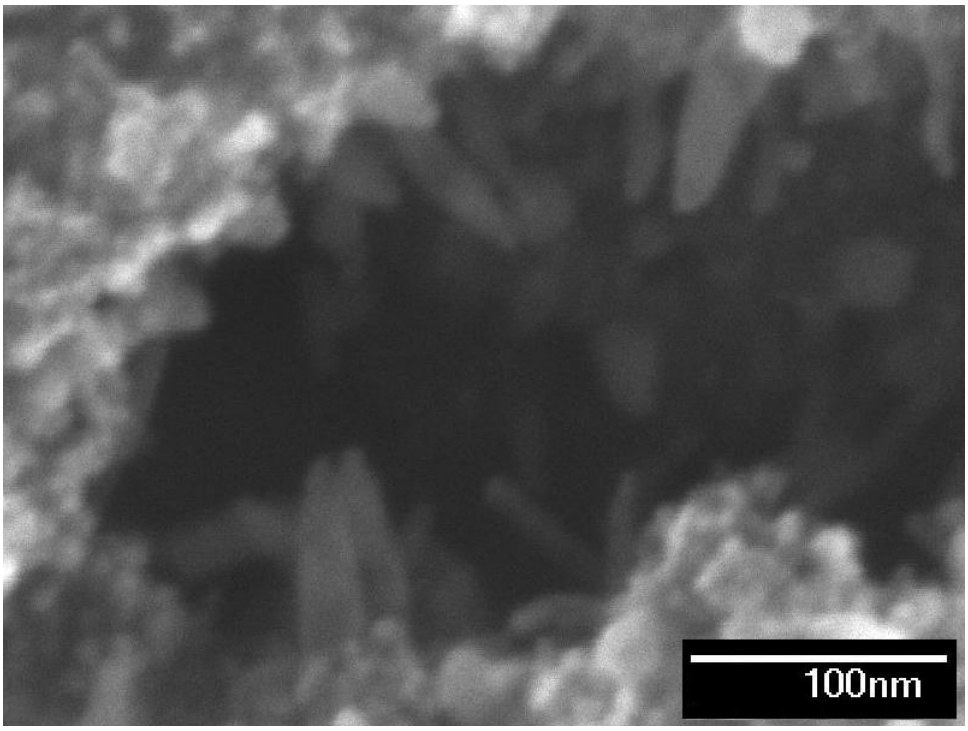

Figure 4.4: Needle-shaped nanostructures formed after wet chemical etching by hydrofluoric acid in grown areas with low concentration of excessive nanodiamond seeds besides diamond seeded silica nanotubes.

4.7 Room-Temperature Photoluminescence (PL) Spectra Study

Room-temperature photoluminescence (PL) spectra were taken using excitation of 325 nm light from a He-Cd laser. The collecting time was 3000 ms. Because of non-uniform silica nanotube distribution, the intensities taken from the measurements are not as high as those reported by other groups. The background photoluminescence was taken into considerations in order to minimize its effects. The top PL spectrum shows the emissions from the as-grown specimen (top curve in Figure 4.6). Four characteristic emission peaks and bands are present, i.e., 426 nm, 460 nm, 512 nm, and 555 nm. The luminescence peak around 2.23 eV (555 nm) is from the self-trapped excitons. It is likely caused by the structural defects suggesting that the self-trapped exciton is confined to a SiO4 tetrahedron [152, 153]. The peak at the wavelength of 512 nm, corresponding to 2.42 eV, could be attributed to defect centers associated with oxygen deficiencies in the silica nanotubes [154, 155]. The band at 2.70 eV (460 nm) is ascribed to the neutral oxygen vacancy (≡Si–Si≡) [152, 155 - 157] and the band at 2.91 eV (426 nm) is due to some intrinsic diamagnetic defect centers, such as a two-fold coordinated silicon lone-pair center (O–Si–O) [152, 153, 155, 158, 159].

In this study, these bands caused by various defects of silica nanotubes were used to determine the presence of the silica nanotubes. After wet chemical etching using hydrofluoric acid solution, the intensities of these three peaks were reduced but not completely minimized (bottom curve in Figure 4.5). Some embedded silica nanotubes that could not be etched away by hydrofluoric acid solution still contribute to some extent to the light emission detected by PL.

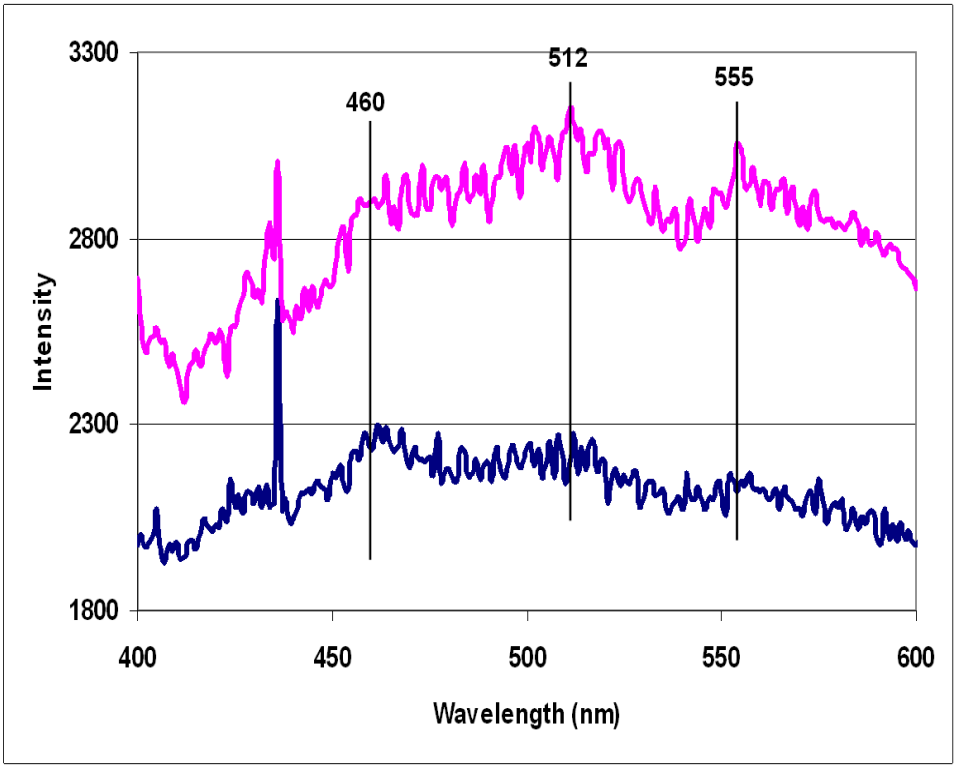

Figure 4.5: Photoluminescence spectra of the samples before (top) and after (bottom) being subjected to HF wet chemical etching.

4.8 Conclusion

Fabrication of one-dimensional nanostructures with diamond tips has been successfully achieved. Diamond nanoparticles adhere to openings of silica nanotubes by means of mechanical locking and encapsulate the openings after chemical vapor deposition of diamond. The selective seeding technique can be applied to nanotubes of materials other than silica. By etching away silica in the diamond-silica composite films using hydrofluoric acid solution, porous diamond nanostructures with one-dimensional nanochannels could be obtained. One-dimensional nanostructures with diamond tips, porous diamond films, diamond with nanochannels, and needle-shaped carbon-based nanostructures are among many possible nanostructures observed from the reported process according to SEM examination. Studies of diamond growth in confined space inside nanotubes of silica and composites employed other materials could be interesting and worth pursuing. Fabrication of polycrystalline diamond nanotubes is possible if the buffer nanotube material could be removed easily, although when that is really achieved, high-power transmission electron microscopy (TEM) or other verifying methods should be employed.

CHAPTER 5

INKJET PRINTING OF NANODIAMOND SUSPENSIONS IN ETHYLENE GLYCOL FOR CVD GROWTH OF PATTERNED DIAMOND STRUCTURES AND PRACTICAL APPLICATIONS

5.1 Introduction

Synthetic diamond fabricated using chemical vapor deposition methods has been studied extensively and has become a promising material for various potential applications due to its outstanding physical, mechanical, chemical, and biological compatibility properties [21, 27, 111]. Among various diamond deposition methods, including hot filaments, combustion flames, plasmas and others, microwave plasma assisted chemical vapor deposition (MPCVD) has the greatest advantage of being reproducible and possessing precious in-process control for the growth of diamond [145, 148, 160 - 162]. In the present work, MPCVD was used to deposit nanocrystalline diamond on patterns that were seeded with nanodiamond by inkjet printing using inks containing nanodiamond powder.

Desired diamond patterns with different dimensions for various applications can be achieved by either pre-growth selective seeding/nucleation or post-growth etching of diamond [163 - 169]. Pre-growth selective seeding is a relatively cost-effective method. Inkjet printing is a mature and useful technique for direct writing and printing for the printing industry. In the reference [169], water based ink was used for a regular inkjet

printer to print diamond seeds on paper-mounted substrates. The number density of printed diamond seeds was low and subsequent diamond CVD for as long as twenty some hours was needed to form polycrystalline diamond films of patterns showing many scattered diamond particles surrounding the patterns due to the splashing of ink. Commercial inkjet printers designed for printing special inks such as those containing carbon and silver nanoparticles for direct printing of conductive micro-patterns [170] are available in the market. Nanometer-sized diamond powder mixed with commercially available conductive ink for the selective nucleation process for polycrystalline and nanocrystalline diamond deposition has been demonstrated by author and published in a form of technical paper [171]. When the inkjet printing technique is further improved and employed for pre-growth selective nucleation of diamond, nanometer-sized nanodiamond powder is mixed into a solvent with the desired viscosity and used as the ink, which is then used for direct printing of patterns. Expensive lithographic and etching facilities for post-growth patterning for pattern dimensions within the capability of inkjet printing could be replaced with commercially available and relatively inexpensive image software for pre-growth selective seeding.

For large scale production of diamond films with a high demand of precision patterning, the cost of diamond seeding can be further reduced by selectively printing diamond seeds only on patterns that are pre-formed by lithographic processes instead of seeding the whole sample surface. This process yields an easy technique for forming possible 1-D, 2-D. and 3-D nanodiamond structures. In this chapter, details on this process and progress in implementing it will be reported, and potential applications will be discussed.

5.2 Dimatix Materials Inkjet Printer DMC-11610

Dimatix Materials inkjet printer and Dimatix DMC-11610 cartridges by FUJIFILM were employed for the selective printing of diamond seeds (Figure 5.1). This particular printer was originally designed for printing structural patterns with special materials such as carbon and silver. Ink with nanodiamond suspensions was custom-made for our research by International Research Center (ITC) in North Carolina, USA. For this ink, 12 g of 40 - 50 nm of aggregates with 4 - 5 nm primary nanodiamond particles was suspended in every 1 Liter of ethylene glycol. The stability is due to the following factors: (i) additional high purification of the initial nanodiamond; (ii) surface groups dissociating in the solvent resulting in high surface charge (so that inter-particle repulsion prevents

Figure 5.1: Dimatix materials inkjet printer [172]

agglomeration); and (iii) small size of the nanodiamond particles, that prevent undesirable sedimentation. Diamond particles were well-dispersed in the ethylene glycol to form a solution with desirable viscosity and would not precipitate to the bottom for an extended period of time. As a comparison, the cited reference [169] reported the use of water based inks, which didn't provide as high density and uniformly distributed diamond seeds as what is being demonstrated in this work. Besides, water is an unfriendly material for vacuum systems where diamond CVD is done.

The printing process was performed with both the cartridge head and the substrate kept at room temperature in order to minimize premature vaporization of the solvent during the printing process. Fine patterning was achieved by means of optimizing the drop spacing and firing distance. In this study, drop spacing ranging from 12 μm to25 μm was examined. Each cartridge reservoir had 16 nozzles linearly spaced at 254 μm for individually controlled printing. For this set of experiments for printing micro-patterns, only a few of these nozzles were used. Furthermore, the effective size of the nozzle opening was 21 μm, which was much larger than the size of the diamond powder.

5.3 Chemical Vapor Deposition on the Printed Patterns

Nanocrystalline diamond films were deposited in gas mixtures of 1% CH_4 + 2% H_2 + 97% Ar with 800Wof microwave power while the gas pressure was kept at 150 Torr and growth temperature was approximately 570 - 620 °C [145, 146]. Because of the excellent nanodiamond suspension, very high surface number density of fine nanodiamond seeds was able to form an almost continuous film on the substrate even before diamond CVD was done. The sizes of nanodiamond seeds were of a narrow

distribution which allowed a very smooth diamond film to be grown on the printed seeds. This is in contrast to the large-grained polycrystalline films that were reported by the cited reference [169]. With the uniformly suspended diamond powder in the solution, it took as short as 15 to 20 min of microwave plasma CVD to grow diamond on the diamond nanoparticles to form pinhole-free nanodiamond films of desired patterns with few scattered diamond particles around the printed areas usually due to splashing of inferior inks.

Silicon substrates with a 5000 Å thick silicon dioxide layer were utilized as the pre-patterned substrates for the combined selective printing/lift-off process. Patterns and printing sites were designed to ensure that the diamond seeds were only printed on desired areas so that a minimum amount of diamond seeding ink was used. After a short period of growth time, typically less than 10 min, a lift-off process was performed using HF solution that removed the silicon dioxide layer along with diamond on it from the undesired areas outside of the pre-formed pattern. The substrate was subsequently subjected to further diamond growth to realize continuous films. Unlike conventional seeding processes, this technique allows users to economize the use of diamond powder and also obtain sharp pattern edges. The specimens were characterized by means of scanning electron microscopy (SEM) for surface morphologies, and Raman spectroscopy for crystallinity and defects of diamond or diamond containing films.

5.4 SEM Inspections on the Specimen

Key requirements for high-performance inkjet printing of diamond seeds are, for example, (i) Nano-scaled diamond seeds remain suspended instead of forming large

aggregates; (ii) Printed ink remains in the pre-designed printed fine areas on the substrates without splash or unwanted re-flow of the ink; (iii) Diamond seeds don't clog the orifice of the inkjet; and (iv) Multiple printing on the same spot with variable quantity of ink and ink-covered areas can be precisely done. A practical and useful inkjet printing technique for the growth of diamond fine patterns is presented in this chapter. Figure 5.2 is an optical image of a printed pattern on silicon. The silicon substrate was cleaned by HF solution to remove residual silicon dioxide on the surface, with no other cleaning or preparation performed. This pattern is an array (6 × 6) of 36 squares in the dimensions of 200 μm × 200 μm. After inkjet printing, the actual dimensions became 220 μm × 220 μm. The ink utilized for this experiment was a solution with nanodiamond powder suspending in ethylene glycol to achieve a desired viscosity. The solvent used in the ink, i.e., ethylene glycol, is an excellent feedstock for the growth of diamond as well and would not adversely affect the quality of CVD diamond. The splash problem was minimized by optimizing the solution concentration and viscosity, as well as other printing parameters.

Undesired diamond seeding in areas surrounding the desired seeded pattern was minimized. The hydrophobic silicon substrate surface caused some blurry edges of the printed patterns. Further work is processed in controlling the wetting of the substrates to improve the quality of printed diamond seeds.

Figure 5.3(a) shows the SEM image of the sample shown in Figure 5.2 after it was subjected to a brief (20 min) diamond growth. With the uniformly suspended diamond powder in the ink, the required time for obtaining continuous diamond films was significantly reduced. The patterned diamond films had a uniform thickness of 450 nm and good adhesion to the substrate surface as tested by a tape-and-peeling process.

Continuous diamond films across the pattern and the surface morphology were shown in Figure 5.3(b) and (c), respectively.

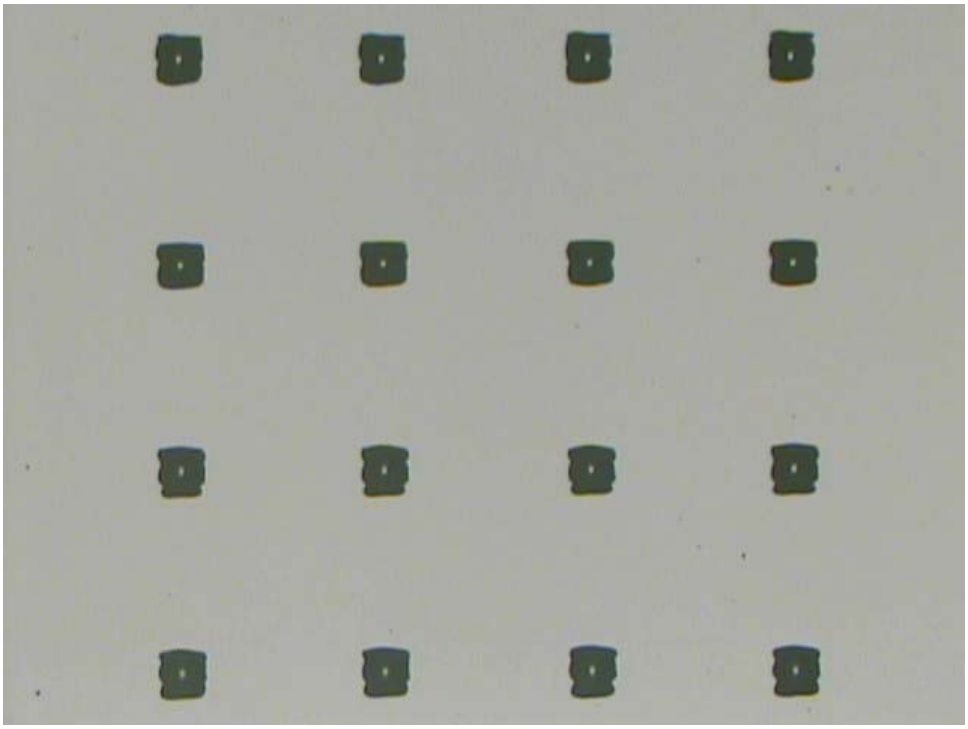

Figure 5.2: An inkjet printed array (6 × 6) of 36 squares of 200 μm × 200 μm in dimensions.

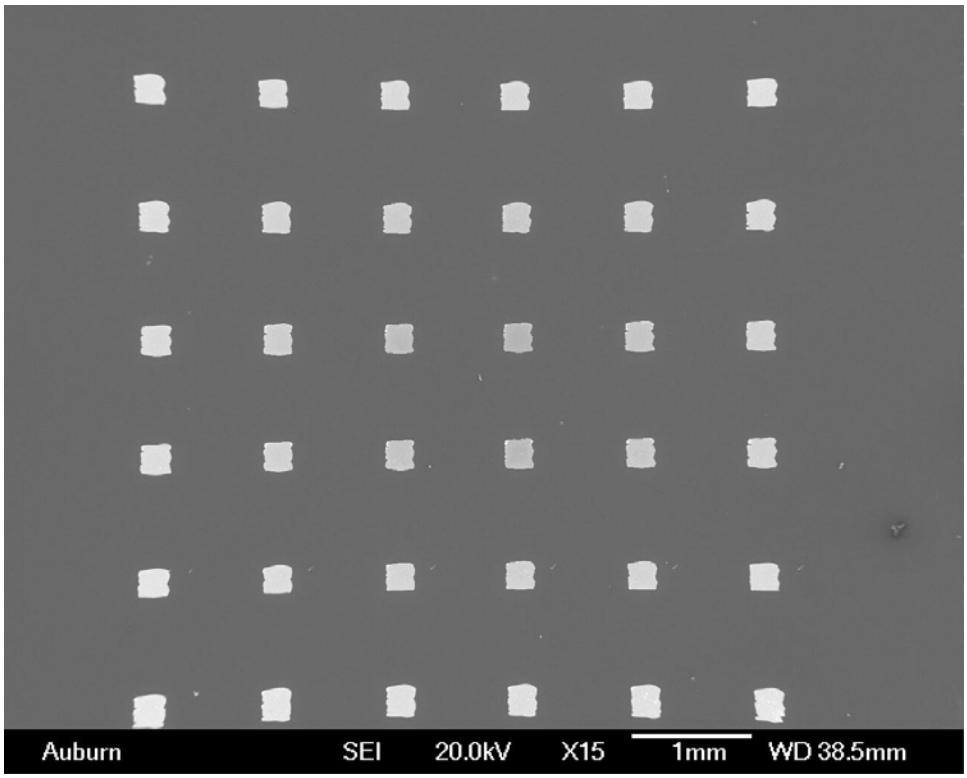
Auburn SEI 20.0kV X15 1mm WD 38.5mm

(a)

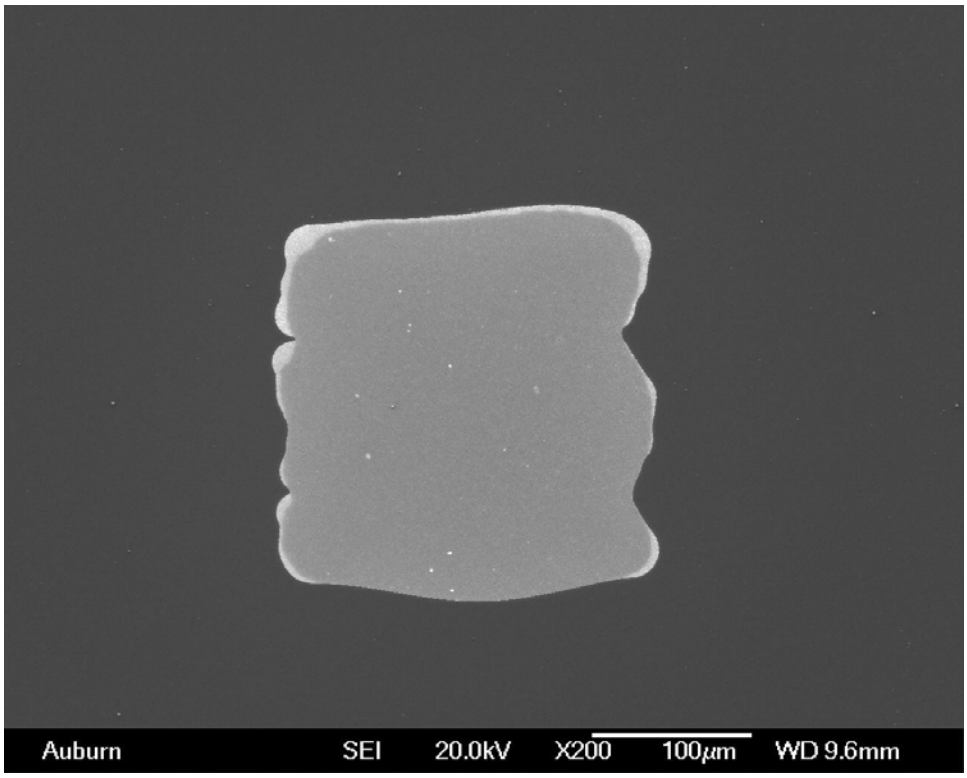
Auburn SEI 20.0kV X200 100μm WD 9.6mm

(b)

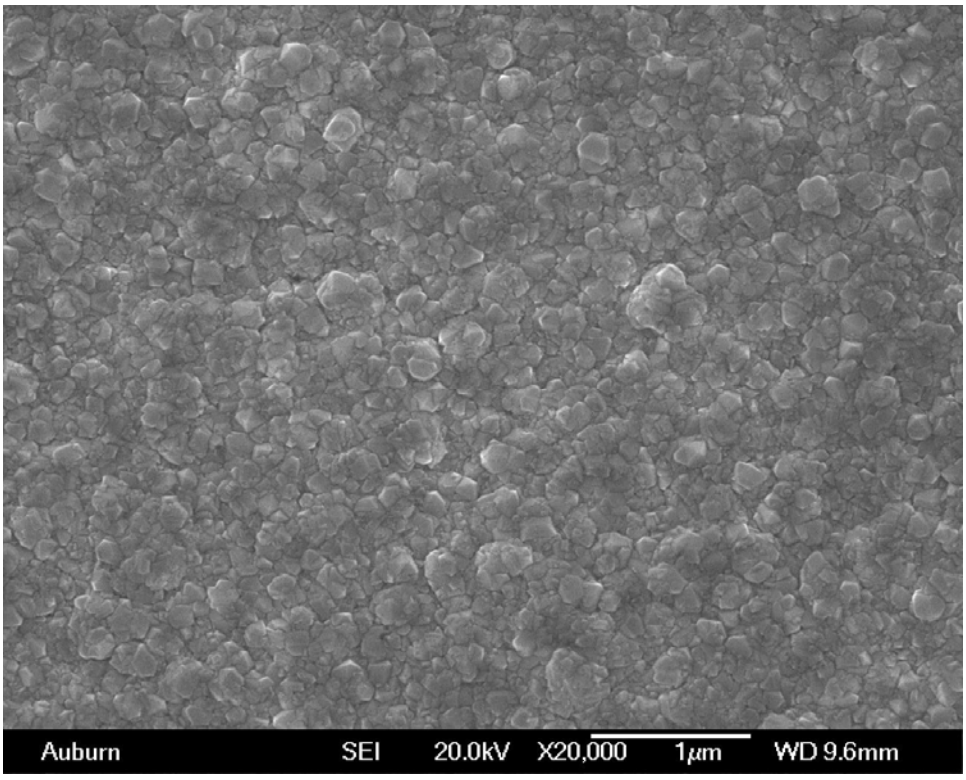

(c)

Figure 5.3 SEM images of a printed sample, as shown in Fig. 1, after 20 min of diamond growth (a) an array of squares; (b) a continuous film obtained after 20 min of deposition; (c) surface morphology of a deposited diamond film.

5.5 Raman Spectroscpy and Electron Field Emission Measurement

Raman spectrum obtained from one of the square patterns after diamond deposition shows the sharp diamond peak, 1334 cm^{-1} (Figure 5.4). Other features of the Raman spectrum including the peaks located at 1154 cm^{-1} and around the graphite band, 1489 and 1510 cm^{-1} are commonly seen on nanodiamond films [149 - 151, 162, 173, 174]. With the addition of ethylene glycol as the carrier, SEM and Raman spectrum on printed samples showed no significant differences from nanodiamond films grown without the solvent under similar conditions. Electron field emission measurement of the sample was also carried out. Electron field emission of an as-grown sample started at 7 V/μm is shown in Figure 5.4(b) [15, 175].

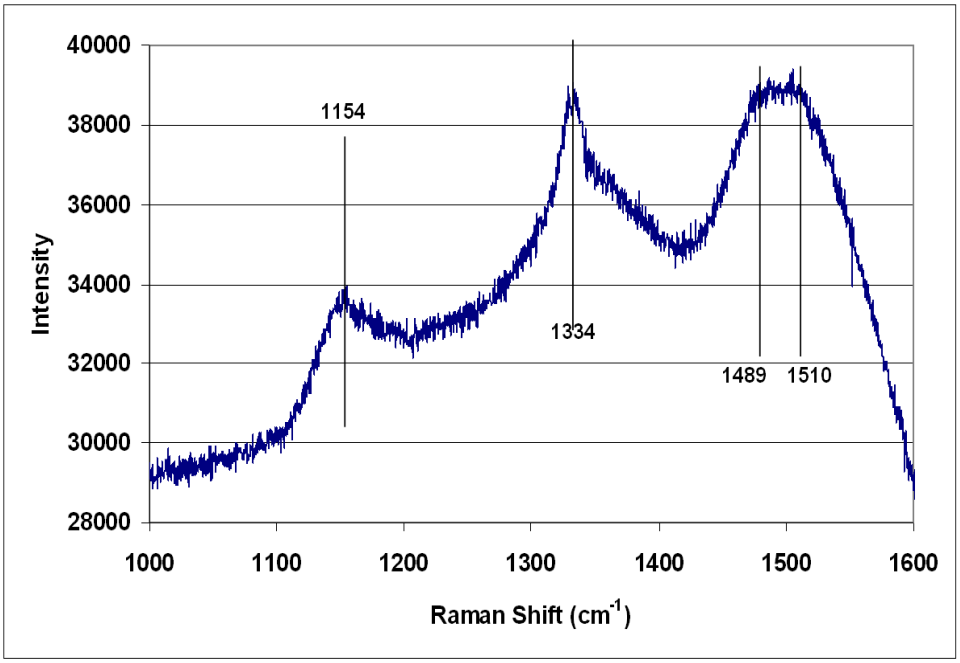

(a)

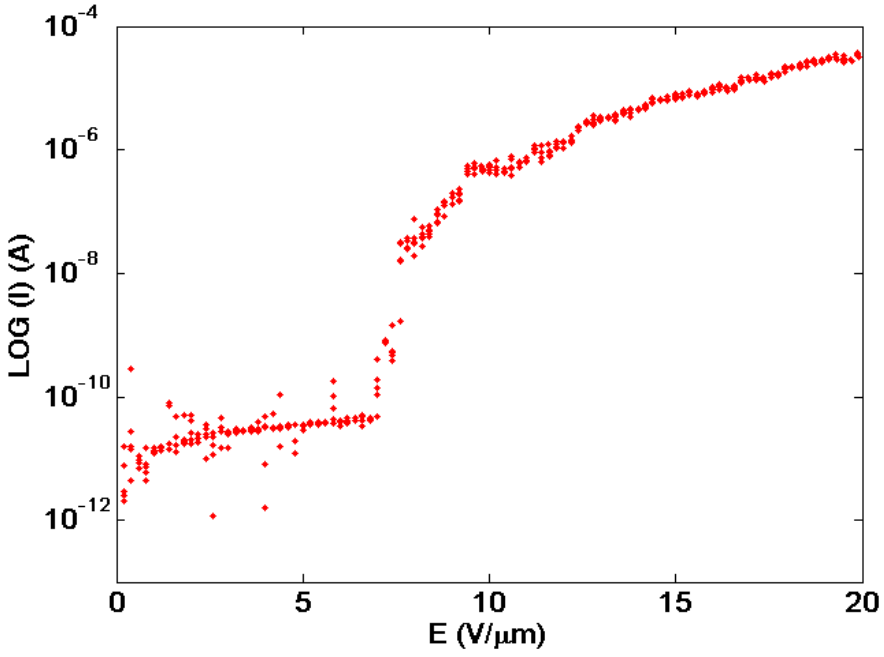

(b)

Figure 5.4 (a) Raman spectra from the printed square pattern after 20 min of diamond deposition; (b) Electron field emission measurement shows that the sample starts to conduct electron field emission at 7 V/μm.

5.6 Inkjet Seeding Technique Applied onto Pre-Formed Patterns

Nanodiamond-containing ink was accurately and selectively jetted onto the patterns, where silicon was exposed, pre-formed in the silicon dioxide layer on a silicon wafer. The optical image shown in Figure 5.5 demonstrates the step by step process. By conventional lithography processing, patterns in shapes of “trenches” were defined. In Figure 5.5(a), silicon dioxide was patterned on the silicon substrate prior to the inkjet seeding. The jetting sites were precisely designed so that only desired areas would be seeded and jetted ink would be directed to the bottom of the “trench” to fill it up to avoid waste of diamond materials. The top pattern of Figure 5.5(b) demonstrates a well-aligned printing of diamond seeding within the pattern. The unwanted structures caused by ink deposited outside the pattern were lifted off by buffer oxide etchant (BOE) after 10 min of CVD growth for the diamond seeds to be desirous to adhere to the exposed silicon areas. After the lift-off, the substrates were subjected to further CVD diamond growth to ensure that continuous films with good adhesion could be obtained. Thus patterns with well-defined edges were formed (Figure 5.5(c)). The thickness of the silicon dioxide layer is believed to be a factor in the sharpness of the edges. When it is thicker, the seeding pattern tends to have a larger gap between the seeding within the pattern and outside the pattern, ensuring the performance of the lift-off process.

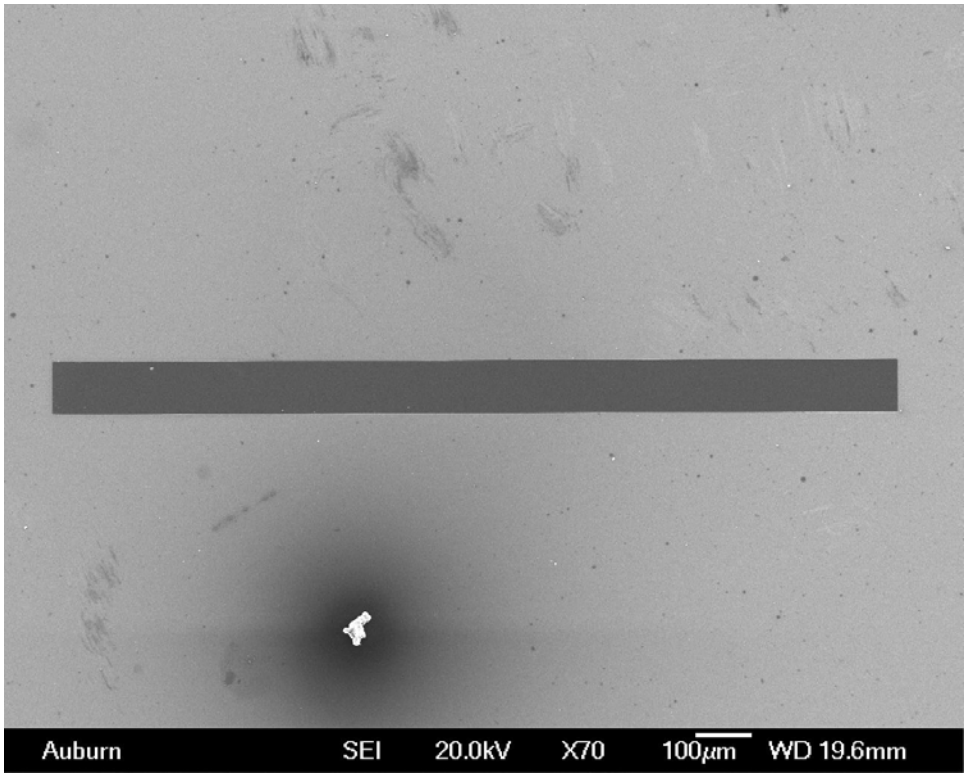

(a)

(b)

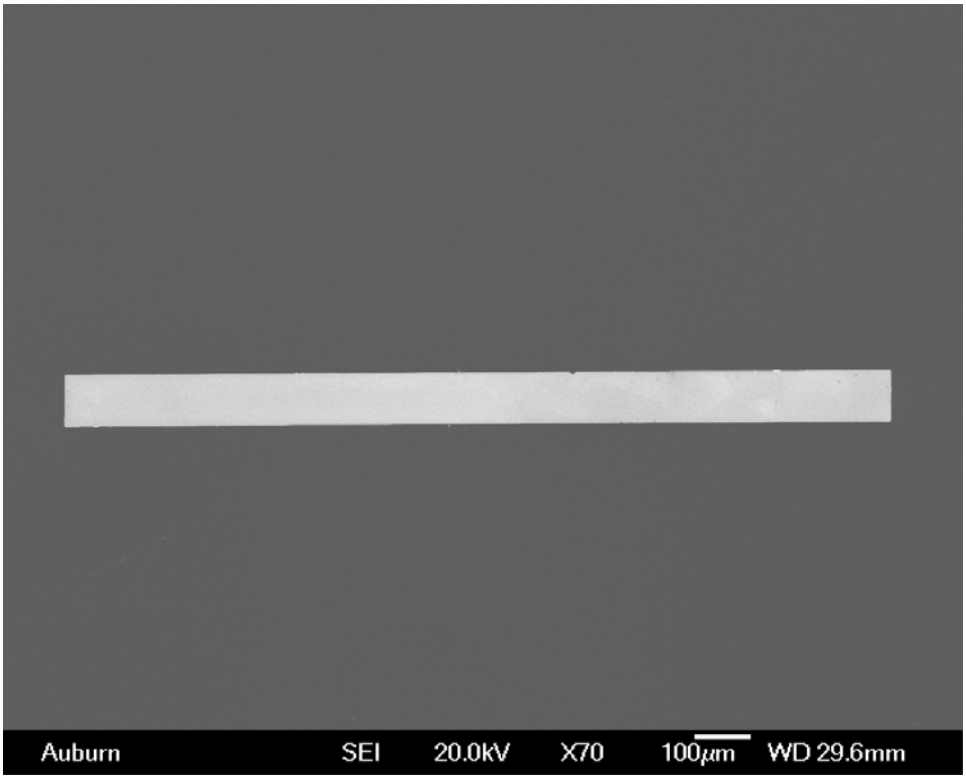

(c)

Figure 5.5: Sequential steps of the process: (a) a square pattern on silicon dioxide on a silicon substrate is fabricated; (b) selective printing of nanodiamond seeds into the pattern; (c) After diamond pre-deposition, lift-off, and deposition, nanodiamond line pattern is fabricated.

5.7 Raman Spectroscopy of the Specimen

Raman spectroscopy was also employed for the quality inspection of the specimens (Figure 5.6). The peak located at 1156 cm^{-1} is common in CVD nanodiamond films. The pronounced sp^3 diamond peak located at 1335 cm^{-1} was observed. There appeared to be a broad line within the range of 1480 - 1507 cm^{-1}, usually accompanying the 1156 cm^{-1} peak, indicating the existence of trans-polyacetylene [149 - 151, 162, 173, 174].

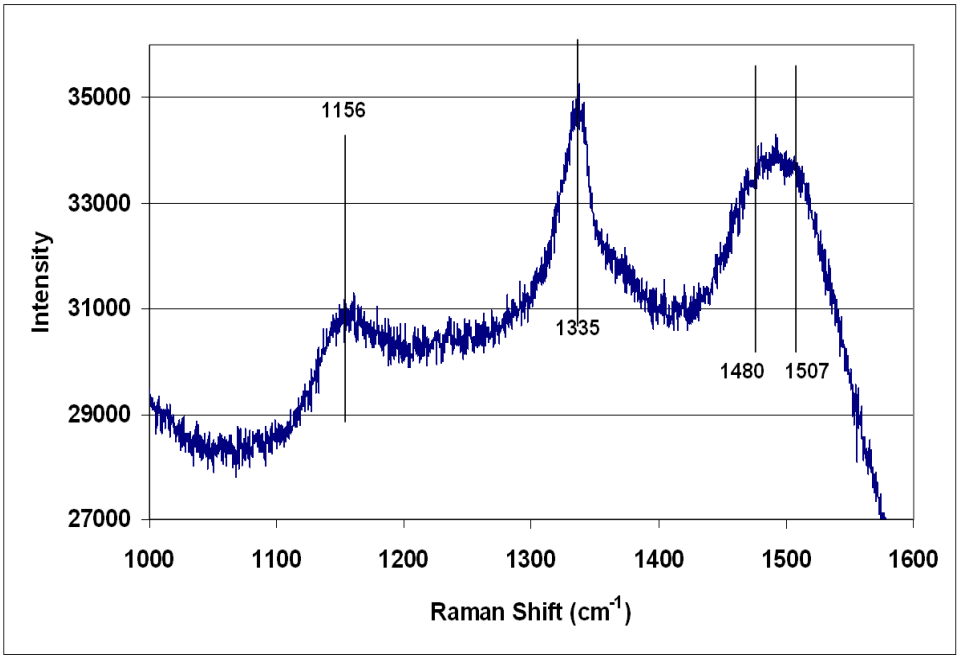

Figure 5.6: Raman spectra for films grown on printed diamond seeds after the sequential seed printing, growth, lift-off, and growth procedure.

5.8 Conclusion

This chapter demonstrates a significant progress towards a number of new practical applications of inexpensive and rapid patterning of thin and/or smooth nanodiamond films. By utilizing the inkjet printing technique with an ink containing nanodiamond powder in ethylene glycol, selective-area and patterned diamond seeding has been successfully demonstrated. Continuous diamond films of desired patterns are formed on printed diamond seeds following a brief MPCVD diamond growth process. Selective patterning of polycrystalline diamond films can also be obtained by similar process but different growth conditions [171]. Fabrication of patterned diamond films is further improved by combining a conventional lithographic process with inkjet printing assisted diamond seeding. Minimum diamond growth time for obtaining continuous diamond films is adjusted and improved by varying the amount of applied ink and the concentration of diamond powder of the size of 40 - 50 nm uniformly suspended in the ink. This technique allows a cost-effective method for selective seeding and patterning of diamond coatings. Future applications employing 3-D diamond structures can be obtained by sequential and repeated printing and deposition. This work was presented in the conference, 2nd International Conference on New Diamond and Nano Carbons (NDNC 2008), and published in the journal, Diamond and Related Materials [176] while it attracted ardent discussion.

CHAPTER 6

SUMMARY

Applications of CVD diamond derive from its unique hardness, toughness, electrical properties, thermal conductivity, among others. While applications based on new single crystal CVD techniques are emerging, products that employ polycrystalline CVD diamond have become available for years. With the developments and intensive studies on CVD techniques, the cost of diamond films and crystals is expected to decrease, and CVD diamond materials appear to be on their way to replace natural diamonds for many industrial applications. Nanocrystalline diamond's unique electrical and mechanical properties also attract much attention. Applications including, for example, diamond-based transistors and MEM devices are currently on a fast track of being developed.

Three different crystallites of CVD diamond, including single crystal diamond, polycrystalline diamond, and nanocrystalline diamond, were studied. Different compositions of gas mixtures and working pressures in various kinds of CVD chambers were examined. The focus of this research is not only on the growth of specimen, but also on the practical and promising applications. A demonstration for each category has been made.

Large CVD diamond single crystals grown at a high rate and of good quality were obtained. All these crystals are classified as Type IIa with nitrogen content of less than 20

ppm and have a high hardness and toughness. This CVD technique has overcome the size and cost constraints of the traditional HPHT method and reduces the potential danger from using high pressure presses for large diamond synthesis. These crystals have been used as diamond anvils for new classes of high pressure devices in a higher P-T condition. With the capability of producing larger, harder, and tougher diamond single crystals, applications in high-precision cutting tools, far-infrared and high-power microwave windows are becoming more and more important. Other applications include large electron field emission sources, surface acoustic wave devices, and high performance semiconductor devices. In addition, while high thermal conductivity and low coefficient of thermal expansion are two of the most significant advantages of diamond materials for electronic applications, micro-trenches could even be created in diamond bulks with a size large enough to allow fluids to flow through to conduct better thermal managements than conventional diamond heat sinks/spreads.

Fabrication of one-dimensional nanostructures with diamond tips has been successfully achieved. Diamond nanoparticles could be applied to the openings of silica nanotubes by means of mechanical locking and to encapsulate the openings after both polycrystalline and nanocrystalline CVD diamond growth processes. This technique of coating specific areas with diamond crystals can be applied to nanostructures, namely nanotubes, of materials other than silica, such as carbon nanotubes. The tip of the Atomic Force Microscope (AFM) probe made of carbon nanotubes generally starts to wear out after a few times of probing sequences under contact mode. By applying a diamond crystal at the tip of the nanotube, it not only increases the durability of the probe, but also takes advantage of diamond's chemically inertness to further broaden types of hazardous

materials that could be inspected by AFM.

Porous diamond nanostructures with one-dimensional nano-channels could be obtained by wet chemical etching of silica in the diamond-silica composite films after carbon deposition. Various structures, including one-dimensional nanostructures with diamond tips, porous diamond films, diamond with nano-channels, and needle-shaped carbon-based nanostructures are among many possible nanostructures observed from the reported process according to SEM examination.Fabrication of polycrystalline diamond nanotubes is possible if the buffer nanotube material could be completely removed afterwards.

A significant progress was also delivered towards a number of new practical applications of inexpensive and rapid patterning of thin and/or smooth polycrystalline/nanocrystalline diamond films. Continuous diamond films of desired patterns were formed on printed areas of diamond seeds followed by a brief MPCVD diamond growth process. Because of the fine distribution of diamond nanoparticles in the printed solution, the time required for obtaining continuous films is greatly reduced, from more than 20 hours reported by other groups down to less than 20 minutes conducted here at Auburn. Fabrication process of patterned diamond films was further improved to have sharper edges and finer shapes by combining a conventional lithographic process with inkjet diamond-printing technique. This demonstrated technique avoids the long and complicated traditional fabrication processes and allows a cost-effective method for selective seeding and patterning of diamond coatings. Three-dimensional diamond structures can be obtained by sequential and repeated printing and deposition.

In conclusion, with the rapid progress in the development of CVD diamond,

especially advances in single crystal diamond growth during the last few years, and growing understanding of the CVD mechanism and techniques, the full potential of CVD diamond in a broad range of applications may be finally realized. The diamond age has finally arrived.

BIBLIOGRAPHY

[1] A. S. Barnard, "The diamond formula", Butterworth Heinemann, Oxford, 2000

[2] F. P. Bundy, H. T. Hall, H. M. Strong, and R. H. Wentorf Jr., *Nature*, 176, 51 (1955)

[3] J. E. Field, "The properties of natural and synthetic diamond", Academic Press, London, 1992

[4] H. T. Hall, *Proceeding of the 1957 Conference on Carbon*, 75 (1957)

[5] R. M. Hazen, "The new alchemists: Breaking through the barriers of high pressure", Random House, Time Books, 1993

[6] International Diamond Lab., http://www.diamondlab.org/80-hpht_synthesis.htm

[7] H. Liu and D. S. Dandy, "Diamond chemical vapor deposition", Noyes, New Jersey, 1995

[8] B. V. Spitsyn, L. L. Bouilov, and B. V. Derjaguin, *J. Cryst. Growth*, 52, 219 (1981)

[9] M. Kamo, Y. Sato, S. Matsumoto, and N. Setaka, *J. Cryst. Growth*, 62, 642 (1983)

[10] S. Matsumoto, Y. Sato, M. Kamo, and N. Setaka, *Jpn. J. Appl. Phys*., 21, L183 (1982)

[11] S. Matsumoto, Y. Sato, M. Tsutsumi, and N. Setaka, *J. Mater. Sci*., 17, 3106 (1982)

[12] M. Kamo, *The Rigaku Journal*, 7, 22 (1990)

[13] T. R. Anthony and J. F. Fleischer, Patient 5,110,579, United States, 1992

[14] Z. H. Shen, P. Hess, J. P. Huang, Y. C. Lin, K. H. Chen, L. C. Chen, and S. T. Lin, *J. Appl. Phys*., 99, 124302 (2006)

[15] Y. C. Yu, J. H. Huang, and I. N. Lin, *J. Vac, Sci. Technol*., B, 19, 975 (2001)

[16] F. Bénédic, M. B. Assouar, F. Mohasseb, O. Elmazria, P. Alnot, and A. Gicquel,

Diamond Relat. Mater., 13, 347 (2004)

[17] F. Mubarok, J. M. Carrapichano, F. A. Almeida, A. J. S. Fernandes, and R. F. Silva, *Diamond Relat. Mater.*, 17, 1132 (2008)

[18] C. E. Nebel, B. Rezek, D. Shin, H. Uetsuka, and N. Yang, *J. Phys. D: Appl. Phys*., 40, 6443 (2007)

[19] A. Kaiser, D. Kueck, P. Benkart, A. Munding, G. M. Prinz, A. Heittmann, H. Huebner, R. Sauer, and E. Kohn, *Diamond Relat. Mater.*, 15, 1967 (2006)

[20] P. K. Ang, K. P. Loh, T. Wohland, M. Nesladek, and E. Van Hove, *Adv. Funct. Mater.*, 19, 109 (2009)

[21] K. E. Spear and J. P. Dismukes, editor, "Synthesis diamond: emerging CVD science and technology", John Wiley & Sons, Inc., 1997

[22] Amethyst Galleries, Inc., http://www.galleries.com/

[23] Wikipedia, http://en.wikipedia.org/wiki/Material_properties_of_diamond

[24] University of Bristol, Physical and Theoretical Chemistry, Jeremy Harvey
http://www.chm.bris.ac.uk/pt/harvey/gcse/covalent.html

[25] University of Exeter, School of Physics, Steve Sque,
http://newton.ex.ac.uk/research/qsystems/people/sque/diamond/

[26] Electronics Cooling Online, http://www.electronics-cooling.com/

[27] R. F. Davis, editor, "Diamond films and coatings", Noyes Publication, 1993

[28] S. T. Lee, Z. Lin, and X. Jiang, *Mater. Sci. Eng., A*, 25, 123 (1999)

[29] L. R. Radovic, P. M. Walker, and P. A. Thrower, "Chemistry and physics of carbon: a series of advances", Marcel Dekker, New York, 1965

[30] Wikipedia, http://en.wikipedia.org/wiki/Diamond

[31] R. C. Eden, *Diamond Relat. Mater.*, 25, 1051 (1993)

[32] Q. Su, Y. Xia, L. Wang, J. Liu, and W. Shi, *Appl. Surf. Sci.*, 252, 8239 (2006)

[33] T. Teraji, M. Hamada, H. Wada, M. Yamamoto, K. Arima, and T. Ito, *Diamond Relat. Mater.*, 14, 255 (2005)

[34] J. E. Field, "The properties of diamond", Academic Press, Oxford, 1979

[35] F. J. Himpsel, J. A. Knapp, J. A. Van Yechten, and D. E. Eastman, *Phys. Rev. B,* 20, 624 (1979)

[36] J. Singh, "Physics of semiconductors and their heterostructures", McGraw-Hill, New York, 1993

[37] S. M. Sze, "Physics of Semiconductor Devices", 2nd Edition, John Wiley & Sons, New York, 1981

[38] V. V. Zhirnov, G. J. Wojak, W. B. Choi, J. J. Cuomo, and J. J. Hren, *J. Vac. Sci. Technol., A,* 15, 1733 (1997)

[39] J. B. Cui, J. Ristein, and L. Ley, *Phys. Rev. Lett.,* 81, 429 (1998)

[40] R. Kalish, *J. Phys. D: Appl. Phys.*, 40, 6467 (2007)

[41] J. Butler, Short course, ADC/FCT, 2001

[42] M. Komori, T. Maki, T. Kim, G. Hou, Y. Sakaguchi, K. Sakuta, T. Kobayashi, *Appl. Phys. Lett.*, 62, 582 (1993)

[43] P. J. Kung, Y. Tzeng, *J. Appl. Phys.*, 66, 4676 (1989)

[44] J. B. Posthill, D. P. Malta, T. P. Humphreys, G. C. Hudson, R. E. Thomas, *J. Appl. Phys.*, 79, 2722 (1996)

[45] C. Chang, D. L. Flamm, D. E. Ibbotson, and J. A. Mycha *J. Appl. Phys*., 63, 1744 (1988)

[46] S. Matsumoto, *J. Mater. Sci. Lett.*, 4, 600 (1985)

[47] K. Suzuki, A. Sawabe, H. Yasuda, T. Inuzuka, *Appl. Phys. Lett.*, 50, 728 (1987)

[48] M. Breiter, C. Doppleb, K. H. Weib, and G. Nutsch, *Diamond Relat. Mater.,* 9, 333 (2000)

[49] University of Bristol, School of Chemistry, http://www.bris.ac.uk/Depts/Chemistry/MOTM/diamond/diamond.htm

[50] X. J. Guo, S. L. Sung, J. C. Lin, F. R. Chen, and H. C. Shih, *Diamond Relat. Mater.,* 9, 1840 (2000)

[51] T. Teraji, S. Mitani, C. Wang, and T. Ito, *J. Cryst. Growth*, 235, 287 (2002)

[52] J. P. Vitton, J. J. Garenne, S. Truchet, *Diamond Relat. Mater.,* 2, 713 (1993)

[53] T. Tachibana, Y. Ando, A. Watanabe, Y. Nishibayashi, K. Kobashi, T. Hirao, and K. Oura, *Diamond Relat. Mater.*, 10, 1569 (2001)

[54] T. Bacci, E. Borchi, M. Bruzzi, M. Santoro, and S. Sciortino, *Mater. Sci. Eng.*, B, 47, 54 (1997)

[55] J. Wei, and Y. Tzeng, *J. Cryst. Growth*, 128, 413 (1993)

[56] Y. Ando, S. Tobe, T. Saito, J. Sakurai, H. Tahara, and T. Yoshikawa, *Thin Solid Films*, 457, 217 (2004)

[57] K. A. Snail and L. M. Hanssen *J. Cryst. Growth,* 112, 651 (1991)

[58] F. Akatsuka, Y. Hirose, and K. Komaki, *Jpn. J. Appl. Phys., Part 2,* 27, 1600 (1988)

[59] K. A. Snail, J. Macia, S. Kellog, J. E. Butler, and L. M. Hanssen, *Carbon*, 28, 794 (1990)

[60] T. Kobayashi and S. Ono, *J. Ceram. Soc. Jpn.*, 99, 119 (1991)

[61] K. Doverspike, V. A. Shamamian, J. A. Freitas, *Mater. Res. Soc. Symp. Proc.,* 339, 313 (1994)

[62] P. K. Bachmann, D. Leers, and H. Lydtin, *Diamond Relat. Mater.,* 1, 1 (1991)

[63] Y. Nishibayashi, H. Saito, T. Imai, and N. Fujimori, *Diamond Relat. Mater.,* 9, 290 (2000)

[64] H. Okushi, *Diamond Relat. Mater.,* 10, 281 (2001)

[65] O. A. Williams, and R. B. Jackman, *Diamond Relat. Mater.,* 13, 557 (2004)

[66] Y. Tzeng, J. Wei, J. T. Woo, and W. Landford (1993) *Appl. Phys. Lett.*, 63, 2216 (1993)

[67] P. Doering and R. Linares, *Proc. Appl. Diamond Conference/Frontier Carbon Technol.*, 32 (1999)

[68] J. Isberg, J. Hammersberg, E. Johansson, T. Wikstrom, D. J. Twitchen, A. J. Whitehead, S. E. Coe, and G. A. Scarsbrook, *Science*, 297, 1670 (2002)

[69] W. Wang, T. Moses, R. C. Linares, J. E. Shigley, M. Hall, and J. E. Bulter, *Gem & Gemology*, 39, 268 (2003)

[70] J. C. Angus, M. Sunkara, S. R. Sahaida, and J. T. Glass, *J. Mater. Res.,* 7, 3001

(1992)
[71] M. A. Tamor and M. P. Everson, *J. Mater. Res.,* 9, 1839 (1994)

[72] C. S. Yan and Y. K. Vohra, *Diamond Relat. Mater.,* 8, 2022 (1999)

[73] C. S. Yan, "Multiple twinning and nitrogen defect center in chemical vapor deposited homoepitaxial diamond", Ph.D. Dissertation, 1999

[74] C. S. Yan, Y. K. Vohra, H. K. Mao, and R. J. Hemley, *Proc. Nat. Acad. Sci. U.S.A.,* 99, R25 (2002)

[75] C. S. Yan, H. K. Mao, W. Li, J. Qian, Y. Zhao, and R. J. Hemley, *Phys. Status Solidi A,* 201, R24 (2004)

[76] R. Locher, C. Wild, N. Herres, D. Behr, and P. Koidl, *Appl. Phys. Lett.*, 65, 34 (1994)

[77] W. Muller-Sebert, E. Worner, F. Fuchs, C. Wild, and P. Koidl, *Appl. Phys. Lett.*, 68, 759 (1996)

[78] Y. Tzeng and J. Wei, "High temperature nucleation and growth of polycrystalline diamond by high-power-density microwave plasmas", 4th International Conference on New Diamond Science and Technology, Kobe, Japan, 1994

[79] Y. Tzeng, "Diamond Deposition in High Power-density CH_4/H_2 Microwave Plasmas", invited paper, APS meeting, Pittsburg, PA., 1994; also invited speaker in Workshop on Processing and Applications of Diamond, SRRC, Taiwan, 1994

[80] T. H. Chein, J. Wei, and Y. Tzeng, *Diamond Relat. Mater.,* 8, 1686 (1999)

[81] T. Kondo, Y. Einaga, B. V. Sarada, T. N. Rao, D. A. Tryk, and A. Fujishima, *J. Electrochem. Soc.* 149, E179 (2002)

[82] K. Kobashi, Y. Nishibayashi, Y. Yokota, Y. Ando, T. Tachibana, N. Kawakami, K. Hayashi, K. Inoue, K. Meguro, H. Imai, H. Furuta, T. Hirao, K. Oura, Y. Gotoh, H. Nakahara, H. Tsuji, J. Ishikawa, F. A. Koeck, R. J. Nemanich, T. Sakai, N. Sakuma, and H. Yoshida, *Diamond Relat. Mater.*, 12, 233 (2003)

[83] K. Ohtsuka, H. Fukuda, K. Suzuki, A. Sawabe, *Jpn. J. Appl. Phys., Part 2, Letters* 36, L1214 (1997)

[84] T. Tachibana, Y. Yokota, K. Miyata, K. Kobashi, and Y. Shintani, *Diamond Relat. Mater.*, 6, 266 (1997)

[85] T. Tsubota, M. Ohta, K. Kusakabe, S. Morooka, M. Watanabe, and H. Maeda, *Diamond Relat. Mater.,* 9, 1380 (2000)

[86] C. Bednarski, Z. Dai, A. P. Li, and B. Golding, *Diamond Relat. Mater.,* 12, 241 (2003)

[87] K. V. Ravi, *J. Mater. Res.,* 7, 384 (1992)

[88] S. Buhlmann, E. Blank, R. Haubner, and B. Lux, *Diamond Relat. Mater.,* 8, 194 (1999)

[89] S. Delclos, D. Dorignac, F. Phillipp, F. Silva, and A. Gicquel, *Diamond Relat. Mater.,* 7, 222 (1998)

[90] A. Mainwood, *Phys. Status Solidi. A,* 172, 25 (1999)

[91] J. Narayan, A. S. Nandedkar, G. Matera, M. Lango, A. Rengan, and S. M. Kanetkar, *Carbon*, 28, 775 (1990)

[92] L. H. Robins, E. N. Farabaugh, A. Feldman, and L. Cook, *Carbon*, 28, 792 (1990)

[93] D. M. Gruen, *Annu. Rev. Mater. Sci.*, 29, 211 (1999)

[94] O. A. Williams, M. Nesladek, M. Daenen, s. Michaelson, A. Hoffman, E. Osawa, K. Haenen, and R. B. Jackman, *Diamond Relat. Mater.*, 17, 1080 (2008)

[95] F. Jansen, M.A. Machonkin, and D.E. Kuhman, *J. Vac. Sci. Technol. A*, 8, 3785 (1990)

[96] K. Mitsuda, Y. Kojima, T. Toshida, and K. Akashi, *J. Mater. Sci.*, 22, 1557 (1987)

[97] P. K. Bachmann, W. Drawl, D. Knight, R. Weimer, and R. F. Messier, *Mater. Res. Soc.,* EA-15, 99 (1988)

[98] B. Singh, Y. Arie, A. W. Levine, and O. R. Mesker, *Appl. Phys. Lett.*, 526, 451 (1988)

[99] S. Mitura, *J. Cryst. Growth,* 80, 417 (1987)

[100] S. T. Lee, Y. W. Lam, Z. Lin, Y. Chen, and Q. Chen, *Phys. Rev. B.*, 5524, 15937 (1997)

[101] Sh. Michaelson, and A. Hoffman, *Diamond Relat. Mater.,* 14, 470 (2006)

[102] P. O. Joffreau, R. Bichler, R. Haubner, and B. Lux, *Int. J. Refract. Hard Metals.,* 7, 92 (1988)

[103] J. C. Arnault, L. Demuynck, C. Speisser, and F. Le Normanda, *Eur. Phys. J. B,* 11, 327 (1999)

[104] SEM image courtesy of International Technology Center, Raleigh, NC.

[105] J. J. Lander, and J. Morrison, *Surf. Sci.,* 4, 241 (1966)

[106] J. C. Angus, H. A. Will, and W. S. Stanko, *J. Appl. Phys.,* 39, 2915 (1968)

[107] B. B. Pate, *Surf. Sci.,* 165, 83 (1986)

[108] A. V. Hamza, G. D. Kubiak, and R. H. Stulen, *Surf. Sci.,* 206, 833 (1988)

[109] K. Larsson, and S. Lunell, *J. Phys. Chem. A,* 101, 76 (1997)

[110] T.R. Anthony, *Vacuum*, 41, 1356 (1990)

[111] F. G. Celii and J. E. Butler, *A. Rev. Phys. Chem.,* 42, 643 (1991)

[112] C. Liu, "Diamond and carbon nanotube coated cold cathodes for vacuum electronic applications", Ph.D. Dissertation, 2004

[113] K. Ishibashi and S. Furukawa, *Jpn. J. Appl. Phys,.* 24, 912 (1985)

[114] X. Jiang, W. J. Zhang, M. Paul, and C. P. Klages, *Appl. Phys. Lett.*, 68, 1927 (1996)

[115] B. Sun, X. Zhang, and Z. Lin, *Phys. Rev. B.*, 47, 15, 9816 (1993)

[116] B. J. Waclawski, D. T. Pierce, N. Swanson, and R. J. Celotta, *J. Vac. Sci. Technol.,* 21, 368 (1982)

[117] M. Frenklach and H. Wang, *Phys. Rev. B,* 43, 1520 (1991)

[118] W. Zhu, G. P. Kochanski, S. Jin, and L. Seibles, *J. Appl. Phys.,* 78, 2707 (1995)

[119] A. A. Talin, L. S. Pan, K. F. McCarty, H. J. Doerr, and R. F. Bunshah, *Appl. Phys. Lett.,* 69, 3842 (1996)

[120] J. Robertson, *J. Vac. Sci. Technol. B*, 17, 659 (1999)

[121] J. Robertson, *Diamond Relat. Mater.,* 5, 797 (1996)

[122] J. Rutter and J. Robertson, *Phys. Rev. B,* 57, 9241 (1998)

[123] Y. C. Chen, A. J. Cheng, M. Clark, Y. K. Liu, and Y. Tzeng, *Diamond Relat. Mater.,* 15, 440 (2006)

[124] I. N. Lin, Y. H. Chen, and H. F. Cheng, *Diamond Relat. Mater.,* 9, 1574 (2001)

[125] D. Hong, and D. Aslam, *IEEE Trans. Electron Devices*, 45, 977 (1998)

[126] N. S. Xu, J. C. She, S. E. Huq, J. Chen, S. Z. Deng, and J. Chen, *Ultramicroscopy*, 89, 111 (2001)

[127] Y. Show, T. Matsukawa, M. Iwase, and T. Izumi, *Mater. Chem. Phys.,* 72, 201 (2001)

[128] K. H. Park, S. Lee, K. -H. Song, J. Park II, K. J. Park, S. -Y. Han, S. J. Na, N. -Y. Lee, and K. H. Koh, *J. Vac. Sic. Technol., B,* 16, 724 (1998)

[129] W. P. Kang, A. Wisitsora-at, J. L. Davidson, D. V. Kerns, Q. Li, J. F. Xu, and C. K. Kim, *J. Vac. Sci. Technol. B*, 16, 684 (1998)

[130] P. J. Fallon and L. M. Brown, *Diamond Relat. Mater.,* 2, 1004 (1993)

[131] M. W. Geis, J. C. Twichell, J. Macaulay, and K. Okano, *Appl. Phys. Lett.,* 67, 1328 (1995)

[132] K. Okano, S. Koizumi, S. R. P. Silva, and G. A. J. Amaratunga, *Nature*, 381, 140 (1996)

[133] R. M. Chrenko, *Phys. Rev.,* B7, 4560 (1973)

[134] J. F. H. Custers, *Physica,* 18, 489 (1952)

[135] P. R. W. Hudson and I. S. T. Tsong, *J. Mater. Sci,* 12, 2389 (1977)

[136] R. J. Hemley, Y. C. Chen, and C. S. Yan, *Elements*, 1, 105 (2005)

[137] C. S. Yan, Y. C. Chen, S. S. Ho, H. K. Mao, and R. J. Hemley, "Large single crystal CVD diamonds at rapid growth rates", Oral presentation, Applied Diamond Conference NanoCarbon, Argonne Illinois, 2005

[138] Y. C. Chen, C. S. Yan, H. K. Mao, R. J. Hemley, M. Origlieri, S. Krasnicki, and Y. Tzeng, "Characterization of single-crystal diamonds grown by high-growth-rate chemical vapor deposition methods", Poster presentation, Applied diamond Conference NanoCarbon, Argonne Illinois, 2005

[139] P. W. May, *Phil. Trans. R. Soc. Lond. A*, 358, 473 (2000)

[140] P. W. May, *Science*, 319, 1490 (2008)

[141] P. Strobel, M. Riedel, J. Ristein and L. Ley, *Nature*, 430, 439 (2004)

[142] D. Zhou, D. M. Gruen, L. C. Qin, T. G. McCauley, and A. R. Krauss, *J. Appl. Phys.,* 83, 540 (1998)

[143] D. M. Gruen and I. Buckley-Golder, *MRS Bulletin*, 23, 16 (1998)

[144] Y. Tzeng, Y. C. Chen, A. J. Cheng, Y. T. Hung, C. S. Yeh, M. Park, and B. M. Wilamowski, *Diamond Relat. Mater.,* 18, 173 (2009)

[145] Y. Liu, C. Liu, Y. Chen, Y. Tzeng, P. Tso, and I. Lin, *Diamond Relat. Mater.,* 13, 671 (2004)

[146] Y. Tzeng and Y. K. Liu, *Diamond Relat. Mater.,* 14, 261 (2005)

[147] L. C. Nistor, J. Van Landuyt, V. G. Ralchenko, E. D. Obrazsova, and A. A. Smolin, *Diamond Relat. Mater.,* 6, 159 (1997)

[148] S. Lee, S. -Y. Han, and S. -G. Oh, *Thin Solid Films*, 353, 45 (1999)

[149] Z. Sun, J. R. Shi, B. K. Tay, and S. P. Lau, *Diamond Relat. Mater.,* 9, 1979 (2000)

[150] H. Kuzmany, R. Pfeiffer, N. Salk, and B. Günther, *Carbon*, 42, 911 (2004)

[151] D. Zhang and R. Q. Zhang*, J. Phys. Chem. B*, 109, 9006 (2005)

[152] K. -H. Lee, C. Lofton, K. Kim, W. -S. Seo, Y. Lee, M. -H. Lee, and W. Sigmund, *Solid State Commun.,* 131, 687 (2004)

[153] C. Itoh, T. Suzuki, and N. Itoh, *Phys. Rev. B,* 41, 3794 (1990)

[154] Q. Wei, G. Meng, X. An, Y. Hao, an L. Zhang, *Solid State Commun.*, 138, 325 (2006)

[155] G. W. Meng, X. S. Peng, Y. W. Wang, C. Z. Wang, X. F. Wang and L. D. Zhang, *Appl. Phys. A,* 76, 119 (2003)

[156] H. Nishikawa, T. Shiroyama, R. Nakamura, Y. Phki, K. Nagasawa, and Y. Hama, *Phys. Rev. B,* 45, 586 (1992)

[157] L. -S. Liao, X. -M. Bao, X. -Q. Zheng, N. -S. Li, and N. -B. Min, *Appl. Phys. Lett.*, 68, 850 (1996)

[158] R. Tohmon, H. Mizuno, Y. Ohki, K. Sasagane, K. Nagasawa, and Y. Hama, *Phys. Rev. B,* 39, 1337 (1989)

[159] S. Kar and S. Chaudhuri, Solid *Solid State Commun.,* 133, 151 (2005)

[160] D. M. Gruen, *MRS Bulletin*, 23, 32 (1998)

[161] A. R. Krauss, D. M. Gruen, D. Zhou, T. G. McCauley, L. C. Qin, T. Corrigan, O. Auciello, and R. P. H. Chang, *Mater. Res. Soc. Symp. Proc.*, 495, 299 (1998)

[162] T. Sharda, M. Umeno, T. Soga, and T. Jimbo, *Appl. Phys. Lett.*, 77, 4304 (2000)

[163] K. Hirabayashi, Y. Taniguchi, O. Takamatsu, T. Ikeda, K. Ikoma, and N. Iwasaki-Kurihara, *Appl. Phys. Lett.*, 53, 1815 (1988)

[164] R. Ramesham, T. Roppel, C. Ellis, D. A. Jaworske, and W. Baugh, *J. Mater. Res.*, 6, 1278 (1991)

[165] J. L. Valdes, J. W. Mitchel, J. A. Mucha, L. Seibles, and H. Huggins, *J. Electrochem. Soc.*, 138, 635 (1991)

[166] S. J. Lin, S. L. Lee, J. Hwang, and T. S. Lin, *J. Electrochem. Soc.*, 139, 3255 (1992)

[167] N. Xu, Z. Zheng, Z. Sun, X. Zhang, C. Xu, P. Wan, and P. Xin, *Surf. Coat. Technol.* 63, 159 (1994)

[168] R. Ramesham, W. Welch, W. C. Neely, M. F. Rose, and R. F. Askew, *Thin Solid Films*, 304, 245 (1997)

[169] N. A. Fox, M. J. Youh, W. N. Wang, J. W. Steeds, H. -F. Cheng, I -N. Lin, *Diamond Relat. Mater.*, 9, 1263 (2000)

[170] J. Perelaer, B. -J. de Gans, U. S. Schubert, *Adv. Mater.*, 18, 2101 (2006)

[171] Y. C. Chen, Y. Tzeng, A. Davray, A. Cheng, R. Ramadoss, M. Park, *Diamond Relat. Mater.*, 17, 722 (2008)

[172] FUJIFILM Dimatix, Inc. 2009, http://www.dimatix.com/

[173] Y. Lifshitz, C. H. Lee, Y. Wu, W. J. Zhang, I. Bello, and S. T. Lee, *Appl. Phys. Lett.*, 88, 243114 (2006)

[174] E. Perevedentseva, A. Karmenyan, P. -H. Chung, Y. -T. He, and C. -L. Cheng, *Surf. Sci.*, 600, 3723 (2006)

[175] C. Gu, X. Jiang, Z. Jin, W. Wang, *J. Vac. Sci. Technol. B*, 19, 962 (2001)

[176] Y. C. Chen, Y. Tzeng, A. J. Cheng, R. Dean, M. Park, and B. M. Wilamowski, *Diamond Relat. Mater.*, 18, 146 (2009)